Mapping class groups of 4-manifolds via barbell diffeomorphisms, Budney–Gabai invariants and handle structures

Weizhe Niu

Submitted in fulfilment of the requirements for the

Degree of Doctor of Philosophy

School of Mathematics and Statistics

College of Science and Engineering

University of Glasgow

September 2024

Contents

List of Figures

Acknowledgements

I would like to express my deepest gratitude to my primary supervisor, Brendan Owens, for his patient guidance, invaluable advice on mathematics, and unwavering support in non-academic matters throughout the entirety of my PhD journey. His mentorship has been instrumental in both my academic and personal growth. I am equally grateful to my second supervisor, Mark Powell, for the numerous enlightening discussions and the many inspiring ideas he has generously shared. His insights have profoundly shaped my research. My time as a student and researcher at the University of Glasgow, particularly within the School of Mathematics and Statistics, has been a privilege. I greatly appreciate the excellent facilities and opportunities for collaboration that the university has provided, all of which have contributed significantly to my development. I would also like to extend my heartfelt thanks to Ryan Budney. His work has been a significant influence on this thesis, and our many valuable discussions during my two-month visit (June-August 2023) to Victoria have been both enriching and inspiring.

On a personal note, I am eternally grateful to my wife, Jiamei Mu, for her love, trust, and constant encouragement, especially during the most challenging times. Her support has been a source of strength. I also wish to thank my parents for their unwavering support throughout this journey. Without their belief in me, none of this would have been possible.

Declaration

I declare that, except where explicit reference is made to the contribution of others, this thesis is my own work and has not been submitted for any other degree at the University of Glasgow or any other institution.

Chapter 1

Introduction

The overarching topic of this thesis is **mapping class groups of 4-manifolds**. More precisely, the main objects we are interested in are the smooth mapping class groups of smooth, compact, and oriented 4-manifolds. In this thesis, unless otherwise stated, all manifolds fall into the above class.

Let X be an n-manifold, and let A be a submanifold of X (A can be empty). Two self-diffeomorphisms Φ_0 and Φ_1 of X are called *isotopic* (or *isotopic relative to* A) if there is a smooth map $F\colon I \times X \to X$ such that $F_0 = \Phi_0$, $F_1 = \Phi_1$, and F_t is a diffeomorphism (or a diffeomorphism that fixes A pointwise) for all $t \in I$. Unless otherwise stated, we use $\mathrm{Diff}(X, A)$ to denote the group of orientation-preserving self-diffeomorphisms of X fixing A pointwise. When $A = \emptyset$, we just write $\mathrm{Diff}(X)$. Also, following the convention as in [3], we use $\mathrm{Diff}_0(X, A)$ (or just $\mathrm{Diff}_0(X)$ when $A = \emptyset$) to denote the subgroup of diffeomorphisms that are *homotopic* to the identity relative to A. Note that this convention may be non-standard for some readers, but we stick to it for better comparison with [3, 4].

We call the group $\pi_0\mathrm{Diff}(X)$ the *mapping class group of* X, and the group $\pi_0\mathrm{Diff}(X, \partial X)$ the *mapping class group of* X *relative to the boundary*. We equip them with the Whitney C^∞ topology (see Section 4.4 of [26] for background reading). These are groups of isotopy classes of diffeomorphisms of X, and are related by the long exact sequence of homotopy

groups induced from the fibration

$$\mathrm{Diff}(X, \partial X) \to \mathrm{Diff}(X) \to \mathrm{Diff}(\partial X)$$

given by the restriction of diffeomorphisms to the boundary ∂X. These groups capture the information of symmetries of X. In this thesis, we will focus on the case when the dimension of X is 4.

The thesis is structured as follows. Chapter 2 introduces two classes of 4-manifold diffeomorphisms, namely barbell diffeomorphisms [3, 4] and Montesinos twin twists [9, 11], and explores the relationship between them. The main result of Chapter 2 is Theorem 2.11 which roughly says that barbell diffeomorphisms are special cases of Montesinos twin twists. This is achieved by realizing both classes as compositions of levelwise Dehn twists.

Theorem. *(Theorem 2.11) Let M be a 4-manifold, and let $\mathcal{B}$ be an embedded thickened model barbell in M that induces a barbell diffeomorphism $\Phi_{\mathcal{B}} \in \mathrm{Diff}(M, \partial)$. Then there exists a Montesinos twin W in M such that the corresponding Montesinos twin twist Φ_W is isotopic to $\Phi_{\mathcal{B}}$. Further, W can be constructed from $\mathcal{B}$.*

Chapter 3 describes an approach to understanding diffeomorphisms of manifolds (more precisely, handlebodies) via representing isotopy classes of diffeomorphisms by handle moves, and gives examples of such representations. These include examples that are covered in Chapter 2. In Section 3.1, we discuss how *handle slides*, *level-preserving isotopies* and *adding/removing cancelling pairs* of n-dimensional handlebodies give rise to isotopy classes of diffeomorphisms of handlebodies, which we call *handle animation diffeomorphisms*. We then discuss the case when $n = 4$ in Section 3.2. Finally, low dimensional examples are given in Section 3.3. These include Dehn twists on orientable surfaces, the boundary Dehn twist of $S^1 \times D^2$, Montesinos twin twists and barbell diffeomorphisms.

Theorem. *(Theorem 3.6) For an oriented, compact, smooth 4-manifold X with a preferred handle structure σ, consider any finite sequence $\mathcal{S}$*

$$(D_1, \phi_1) \to (D_2, \phi_2) \to \cdots \to (D_m, \phi_m)$$

of Kirby diagrams D_i together with attaching maps $\phi_i\colon \#_r S^1 \times S^2 \to \partial X^2_{D_i}$ of 3- and 4-handles, connected by handle moves, where D_1 and D_m are identical as diagrams representing σ, along with identical attaching maps $\phi_1 = \phi_m$ of 3- and 4-handles. Here r is the number of 3-handles.

In this scenario, there exists a ***handle animation*** *self-diffeomorphism Φ induced from $\mathcal{S}$ as a composition of induced diffeomorphisms from each handle move in the sequence, which is well-defined up to isotopy. If X has less than or equal to one 3-handle ($r \leq 1$), then we do not need to keep track of the attaching maps of 3- and 4-handles.*

We conjecture that mapping classes of manifolds in all dimensions are handle animation diffeomorphisms. The following theorem proves that this is true in dimension 2.

Theorem. *(Theorem 3.10) Let S be an orientable surface (with or without boundary). Then there exists a handle structure of S such that for any embedded simple closed curve l in S, the Dehn twist T_l along l can be factored as a sequence of 1-handle slides starting and ending with isomorphic handle structures. Thus $\pi_0\mathrm{Diff}(S, \partial)$ are handle animation diffeomorphisms.*

Theorem. *(Theorem 3.16) For any element in the subgroup $\mathcal{M}_0$ of $\pi_0\mathrm{Diff}(S^4)$ generated by half-unknotted Montesinos twin twists, there exists a handle structure σ of S^4 such that this element is realized by a sequence of Kirby diagrams starting and ending with the same diagram representing σ, connected by handle moves. In other words, Montesinos twin twists are handle animation diffeomorphisms.*

Moreover, the same is true for the subgroup $\mathcal{B}_0$ generated by half-unknotted barbell diffeomorphisms.

Chapter 4 is centered on the detection of barbell diffeomorphisms of $S^1 \times D^3$ by an invariant called W_3 defined by [3,4]. We review the W_3 invariant for $\pi_0\mathrm{Diff}(S^1 \times D^3, \partial)$ and present some new results. In [3] and [4], Budney–Gabai proved that there exist infinitely many linearly independent barbell diffeomorphisms δ_k for $k \geq 4$ in $\pi_0\mathrm{Diff}(S^1 \times D^3, \partial)$ using this invariant W_3. We present more linearly independent barbell diffeomorphisms in addition to δ_k. We extend the calculations of W_3 in [4] in Theorem 3.5 using the

approach presented in [4]. We also outline the ideas of calculating the invariant W_3 of any diffeomorphism induced from an unknotted barbell in $S^1 \times D^3$ (see Lemma 4.26). Our main results in Chapter 4 are

Theorem. *(Lemma 4.19 and Theorem 4.23) The barbells $\theta_k(e_i, e_j)$ with $j > k - i$ and $k \geq 3$ satisfy*

$$\begin{aligned}
&W_3(\theta_k(e_i, e_j)) = \\
&(k-i-1)(-t_1^j t_3^i - t_1^i t_3^j + t_1^{-i} t_3^{j-i} + t_1^{j-i} t_3^{-i}) + \\
&(-k+j+i-1)(-t_1^{-j} t_3^{i-j} + t_1^{-i} t_3^{j-i} + t_1^{j-i} t_3^{-i} - t_1^{i-j} t_3^{-j}) + \\
&(k-j-1)(-t_1^{-j} t_3^{-i} - t_1^{-i} t_3^{-j} - t_1^{-j} t_3^{i-j} + t_1^{-i} t_3^{j-i} + t_1^i t_3^{i-j} + t_1^{i-j} t_3^i + t_1^{j-i} t_3^{-i} - t_1^{i-j} t_3^{-j}).
\end{aligned}$$

Theorem. *(Theorem 4.28) The elements $\theta_k(e_{k-1}, e_{k-3})$ for $k \geq 6$ of $\pi_0\mathrm{Diff}(S^1 \times D^3, \partial)$ are linearly independent. Further, these elements are linearly independent to*

$$\delta_k = \theta_k(e_{k-1}, e_{k-2}) = \theta_k((0, \ldots, 0, 1), (0, \ldots, 0, 1, 0))$$

for $k \geq 4$.

More generally, there exist linearly independent elements $\theta_k(e_{k-1}, e_{k-m})$ of $\pi_0\mathrm{Diff}(S^1 \times D^3, \partial)$ for $m \in \{3, 4, \ldots, [(k-1)/2] - 1\}$ with $k \geq 2m - 1$. Here $[(k-1)/2]$ is the integer part of $(k-1)/2$.

Chapter 5 is part of an ongoing but unfinished project aimed at finding isotopically non-trivial splitting 3-spheres of the 2-dimensional unlink in S^4. In this chapter, we define a version of the W_3 invariant for $\pi_0\mathrm{Diff}(\natural_m S^1 \times D^3)$ with $m \geq 2$ where $\natural_m S^1 \times D^3$ denotes the boundary connected sum of m copies of $S^1 \times D^3$. We then focus on the $m = 2$ case, and study the mapping class group $\pi_0\mathrm{Diff}(\natural_2 S^1 \times D^3)$. In particular, we prove the following.

Theorem. *(Theorem 5.15) The group $\pi_0\mathrm{Diff}(S^1 \times D^3 \natural S^1 \times D^3, \partial) / \prod_2 \pi_0\mathrm{Diff}(S^1 \times D^3, \partial)$ has an infinitely generated subgroup. Moreover, there exist infinitely many properly embedded separating 3-balls in $S^1 \times D^3 \natural S^1 \times D^3$ with common boundary that are not isotopic relative to the boundary.*

Finally, in Section 5.4, we describe an unfinished program about how the above can be used to construct knotted splitting 3-spheres of the 2-dimensional unlink in S^4.

Chapter 2

Barbell diffeomorphisms and twin twists

In this chapter, we talk about examples of 4-manifold diffeomorphisms. We review the notion of barbell diffeomorphism defined by Ryan Budney and David Gabai [3, 4], and the notion of Montesinos twin twist defined by David Gay [9], inspired by Montesinos [22], in Sections 2.1 and 2.2. We then explore their relationship in Sections 2.3 and 2.4. Roughly speaking, we show that barbell diffeomorphisms are special cases of Montesinos twin twists. Definitions and results in this chapter will be needed in the following chapters.

2.1 Barbell diffeomorphisms

Ryan Budney and David Gabai proved that the mapping class group $\pi_0\mathrm{Diff}(S^1 \times D^3, \partial)$ is infinitely generated. They proposed a method for creating diffeomorphisms of a 4-manifold by embedding a "barbell manifold" inside of it and performing a construction similar to the "point-pushing" map on surfaces. The resulting diffeomorphism is referred as the associated *barbell diffeomorphism*. They then exhibit (isotopically) non-trivial barbell diffeomorphisms in $S^1 \times D^3$. Here we recall their construction.

The *model barbell* in $\mathbb{R}^3 \subset \mathbb{R}^4$ is the union of two 2-spheres of radius 1 centered at $(0, 0, -2)$ and $(0, 0, 2)$ in $\mathbb{R}^3$ with the interval $[-1, 1] \times (0, 0) \subset \mathbb{R} \times \mathbb{R}^2$ connecting the two 2-spheres. The two 2-spheres are called the *cuff spheres*, and the interval is called the *bar*. See Figure 2.1. The *thickened model barbell* $\mathcal{B}$ is a closed neighbourhood of

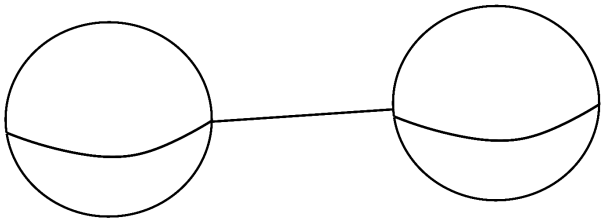

Figure 2.1: The standard model barbell.

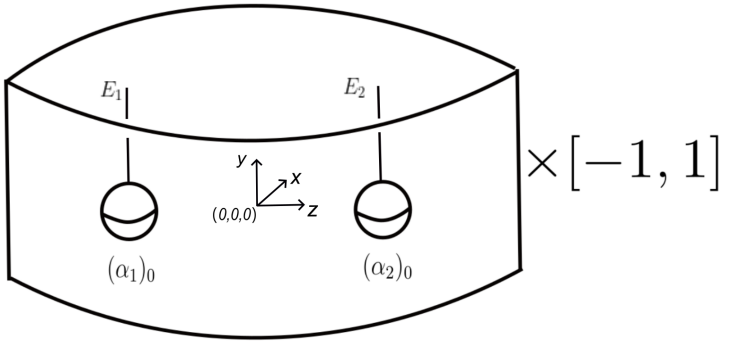

Figure 2.2: The thickened barbell manifold.

the model barbell in $\mathbb{R}^4$. It can be identified with the boundary connected sum of two trivial D^2-bundles over S^2, i.e. $S^2 \times D^2 \natural S^2 \times D^2$. which is also naturally isomorphic to $S^2 \times B^1 \times I \natural S^2 \times B^1 \times I$, and we denote the I-coordinate by t. In other words, this can be obtained by taking a tubular neighbourhood of the model barbell in $\mathbb{R}^3$ and taking the product with I. See Figure 2.2. We call the vertical direction the y direction.

We will now define an element in $\pi_0\text{Diff}(\mathcal{B}, \partial)$ that will be called the barbell diffeomorphism. Denote the two complementary 4-balls of the thickened model barbell $\mathcal{B}$ by α_1 and α_2, both are parameterized by $I \times B^3$. Let $(\alpha_i)_t$ for $t \in [-1, 1]$ denote the intersection between α_i and the t-slice $\mathcal{B}_t$ of $\mathcal{B}$. The two slices $(\alpha_1)_0$ and $(\alpha_2)_0$ are shown in Figure 2.2 The two 2-disks E_1 and E_2 represent two properly embedded orthogonal 2-disks to the 2-spheres $\partial(\alpha_1)_0$ and $\partial(\alpha_2)_0$. More precisely, if we give $\mathcal{B}$ a standard handle structure (cf. Section 3.1 for discussion of handle structures) with one 0-handle and two 2-handles, then they can be viewed as the cocores of the two handles. At the $t = 0$ slice of $\mathcal{B}$, push the 3-ball $(\alpha_1)_0$ along a closed loop around $(\alpha_2)_0$, but not touching $(\alpha_2)_0$, as in Figure 2.3. This leads to a path of embedded 3-balls in $(\mathcal{B})_0 \cup (\alpha_1)_0 \cup (\alpha_2)_0$. As t approaches ± 1, swing the path to the upward/downward direction, tracing out two hemispheres, until it

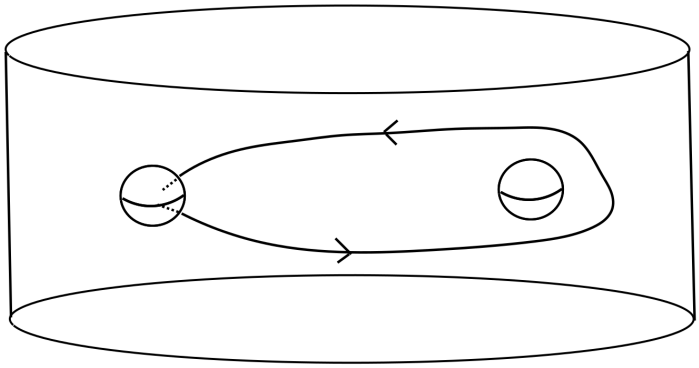

Figure 2.3: The model barbell and the $t = 0$ slice of the thickened barbell manifold.

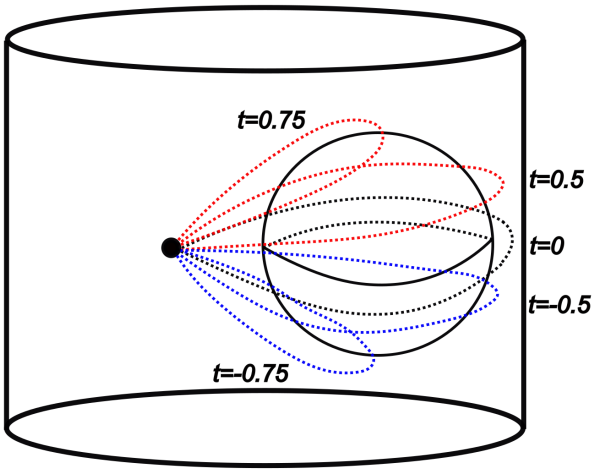

Figure 2.4: The time-dependent path in the barbell that defines the barbell diffeomorphism via isotopy extension.

reaches the trivial arc orthogonal to α_1 (parallel to the normal 2-disk E_1 to the 2-sphere $\partial(\alpha_1)_0$). See Figure 2.4 for the loops when $t = \pm 0.5$ and $t = \pm 0.75$. Note that we draw the left 2-sphere (and the complementary 3-ball $(\alpha_1)_0$) it bounds) as a black dot just to make it easier to visualise. The above defines a loop of embedded 4-balls, or more precisely, a loop of string links (i.e. a loop of embeddings of $I \times D^3$), in $\mathcal{B} \cup \alpha_1$ based at α_1 that is t-level-preserving. We also arrange so that it is away from the boundary of $\mathcal{B}$.

Now, applying the isotopy extension theorem to this loop in the manifold $\mathcal{B} \cup \alpha_1$ gives rise to a well-defined isotopy class of diffeomorphisms of $\mathcal{B}$, which only depends on the isotopy class of this t-level preserving path by the uniqueness of the isotopy extension theorem. This is called the *barbell diffeomorphism*. Since the barbell diffeomorphism fixes the boundary pointwise, we can make the following definition.

Definition 2.1. Let X be a 4-manifold. Let $\mathcal{B}$ be an embedded barbell in X. The induced barbell diffeomorphism $\Phi_{\mathcal{B}} \in \mathrm{Diff}(X, \partial)$ is defined by extending the barbell diffeomorphism using the identity map to the rest of the ambient manifold X, and it gives rise to an element $[\Phi_{\mathcal{B}}] \in \pi_0\mathrm{Diff}(X, \partial)$. This is called a *barbell implantation*.

Since we always assume that X is orientable which implies that embedded 2-spheres admit unique framings, such an embedding is determined by the embedding of two disjoint 2-spheres together with a framed embedded bar connecting them. As argued in Remark 5.12 in [3], different framings of the bar give rise to different barbell implantations that are related by full right-hand twists of the x-y plane as one travels along the bar. Such twists preserve isotopy classes of barbell implantations since they fix the union of E_1 and its image under the barbell diffeomorphism setwise (see Remark 5.4 of [3]) for details).

Therefore, when talking about barbell implantations, we usually do not distinguish between an embedded barbell and an embedded thickened model barbell. We sometimes omit the word embedded as well.

We set up some more terminology. A barbell in X is called *unknotted* if its two cuff spheres are both isotopically unknotted. By an isotopically unknotted 2-sphere in X we mean an embedded 2-sphere that bounds a D^3. Similarly, a barbell in X is called *half-unknotted* if at least one of the two cuffs spheres is isotopically unknotted.

We consider the case when $X = S^1 \times D^3$. An unknotted barbell in $S^1 \times D^3$ is determined by the relative isotopy class of the bar. Namely, if we choose two embedded unknotted spheres B and R in X, together with two fixed points b_0 on B and r_0 on R, then the space of unknotted barbells is determined by isotopy classes of embeddings

$$\pi_0\mathrm{Emb}(I, X; b_0, r_0)$$

which can be described by a word in the free group F_3 with 3 generators: the meridians ν_R and ν_B of the two spheres, and the circle factor t of $S^1 \times D^3$. We orient the bar by saying that it starts from B and ends at R. In other words, the induced barbell diffeomorphism is obtained by looping B around R. In fact, the opposite orientation gives the inverse of

the barbell diffeomorphism, which can be seen by directly tracking the definitions.

If the bar links the sphere B before looping around the S^1-factor at all, or links the sphere R just before reaching R in the end, then these linkings can be eliminated by an isotopy that directly drags the spheres B and R out of the parts of the bar near the two ends. Therefore, such barbells are completely determined by the double coset

$$\langle \nu_B \rangle \backslash \langle \nu_B, \nu_r, t \rangle / \langle \nu_R \rangle.$$

In other words, we do not need to consider words that start with ν_B or end with ν_R.

Example 2.2. There is a subclass of such barbells studied by Budney and Gabai, which will play an important role in the coming sections and chapters. For $k \in \mathbb{Z}^+$ and $(v)_i, (w)_i \in \mathbb{Z}^{k-1}$ where $i = 1, 2, \ldots, k-1$, let $\theta_k(v, w)$ denote the following barbell in $S^1 \times D^3$: choose two disjoint, parallel embedded 2-spheres $B \subset \{s_2\} \times D^3 \subset S^1 \times D^3$, R in $\{s_1\} \times D^3 \subset S^1 \times D^3$ with $s_1 \neq s_2$. We specify a bar connecting them. The integer $k-1$ indicates the number of times the bar moves around the S^1 factor in total, and we require the bar to go in the negative S^1 direction (we give the product orientation to $S^1 \times D^3$) only throughout. If we cut the bar with a 3-ball $\{s_0\} \times D^3 \subset S^1 \times D^3$ with $s_0 \notin \{s_1, s_2\}$ such that the order of the triple (s_0, s_1, s_2) agrees with the orientation of S^1, then there are $k-1$ intersection points between the bar and $\{s_0\} \times D^3$. We arrange these intersection points to lie on the same line in $\{s_0\} \times D^3$ and give them indices $\{1, 2, \ldots, k-1\}$ as shown in Figure 2.5 for $\theta_{10}((0, \ldots, 0, 1, 0), (0, \ldots, 0, 1, 0))$. Note that for better compatibility with Budney–Gabai's work, we follow the convention used in [4] that we label the strands in opposite directions at the top and bottom. So, the journey of the bar from B to R leads to $k-1$ vertical (i.e. parallel to the circle direction) strands with indices and R can link each of these strands. We use each entry of the vector $(v)_i$ with $i \geq 1$ to indicate the signed number of times the i-th vertical strand of the bar wraps around the sphere R, counting from left to right at the bottom of Figure 2.5. We fix the convention such that a vertical strand going through a cuff sphere from top to bottom (i.e. pointing to the negative S^1 direction) is positive. Similarly, for the blue cuff B, following the convention as in [4], we

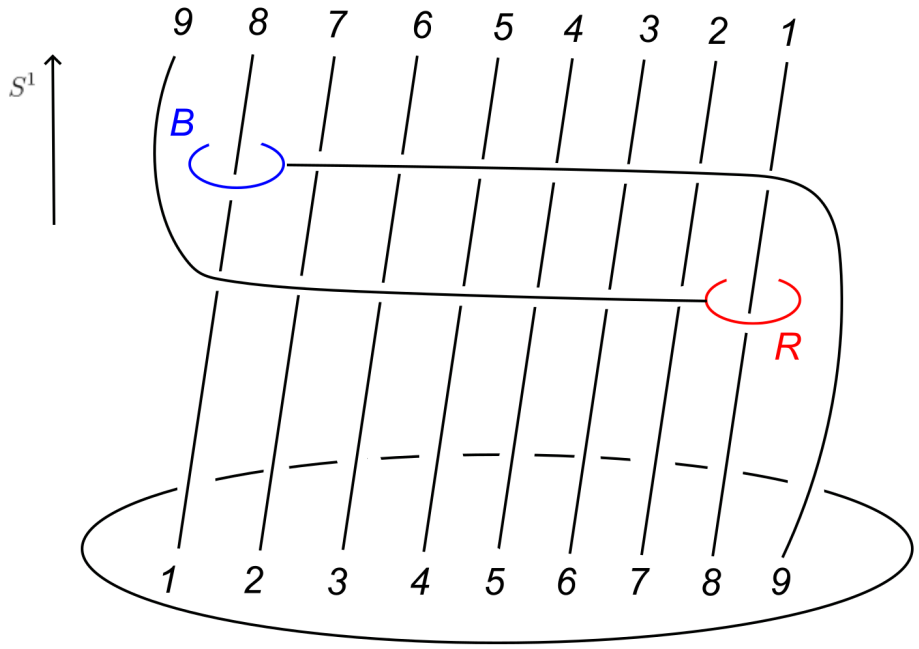

Figure 2.5: The embedded barbell $\theta_{10}((0,\dots,0,1,0),(0,\dots,0,1,0))$. Strand number k on the top is glued to strand number $10-k$ on the bottom.

give indices to the same strands, but with reversed order. These are shown in Figure 2.5 on the top. Each vector entry $(w)_i$ with $i \geq 1$ indicates the signed number of times the i-th vertical strand of the bar wraps around the sphere B counting from right to left on the top. When both B and R link the same strand, we only consider the barbell such that such a strand first links B, and then links R. Note that we always keep B in $\{s_2\} \times D^3$ and R in $\{s_1\} \times D^3$.

In the language of free group words, $\theta_k(v,w)$ corresponds to the word

$$\nu_R^{v_{k-1}} t^{-1} \nu_B^{w_1} \nu_R^{v_{k-2}} t^{-1} \dots t^{-1} \nu_B^{w_{k-2}} \nu_R^{v_1} t^{-1} \nu_B^{w_{k-1}}.$$

Example 2.3. Fix a point $x_0 \in S^3$. Let S_0^1 denote the circle $S^1 \times \{x_0\} \subset S^1 \times S^3$ and $N(S_0^1)$ denote a neighbourhood of S_0^1. Consider the fibration

$$\mathrm{Diff}_0(S^1 \times S^3, N(S_0^1)) \to \mathrm{Diff}_0(S^1 \times S^3) \to \mathrm{Emb}_0(S^1 \times D^3, S^1 \times S^3)$$

given by restricting a diffeomorphism of $S^1 \times S^3$ to a neighbourhood of S_0^1. The fiber is homotopy equivalent to $\mathrm{Diff}_0(S^1 \times D^3, \partial)$, the subgroup of diffeomorphisms homotopic

to the identity. The base space $\mathrm{Emb}_0(S^1 \times D^3, S^1 \times S^3)$ is the component that contains $N(S^1_0)$ and is homotopy equivalent to $\mathrm{Emb}_0(S^1, S^1 \times S^3)$.

We justify that this fibration map is well-defined. For $\Phi \in \mathrm{Diff}_0(S^1 \times S^3)$, the image $\Phi(N(S^1_0))$, after composing with a homotopy equivalence, lives in $\mathrm{Emb}(S^1, S^1 \times S^3)$, and is homotopic to S^1_0 thruogh an induced homotopy from a choice of a homotopy between Φ and $\mathrm{Id}_{S^1 \times S^3}$. For embedding of 1-manifolds in a 4-manifold, homotopy implies isotopy. Hence $\mathrm{Emb}_0(S^1, S^1 \times S^3)$ is the correct base space.

A detailed discussion of this fibration can be found in Section 3 of [3]. The final part of the long exact sequence of homotopy groups is as follows:

$$\cdots \to \pi_1 \mathrm{Emb}_0(S^1, S^1 \times S^3; S^1_0) \to \pi_0 \mathrm{Diff}_0(S^1 \times D^3, \partial) \to \pi_0 \mathrm{Diff}_0(S^1 \times S^3) \to 0$$

where the first map is given by isotopy extension and the second map is induced by inclusion and extension by the identity map. The following proposition is implicitly discussed and used in [3].

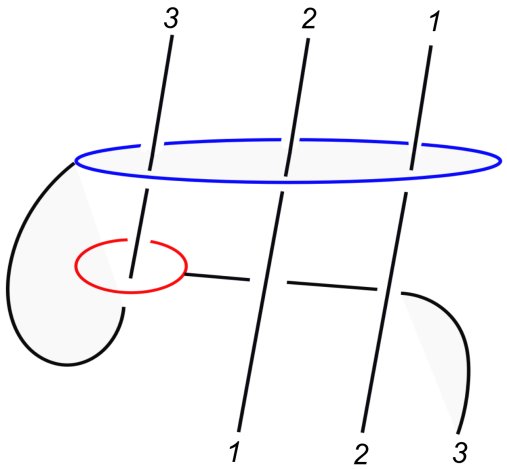

Figure 2.6: The barbell in $S^1 \times D^3$ induced by α_3. The strand i on the top is glued to the strand $4 - i$ on the bottom for $i = 1, 2, 3$.

Proposition 2.4 ([3]). *The image of $\pi_1 \mathrm{Emb}_0(S^1, S^1 \times S^3; S^1_0)$ is generated by a set of barbells denoted by α_i ($i \geq 1$). Figure 2.6 shows the case when $i = 3$. The barbell α_i is given by taking two 2-spheres B and R in $S^1 \times D^3$ and letting the bar start from B, go through R once negatively and go through B negatively for i times as it goes along the*

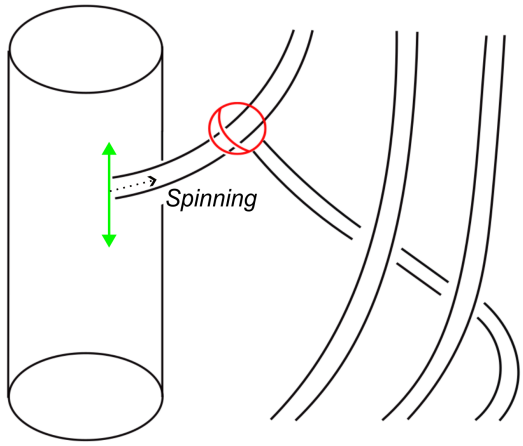

Figure 2.7: The generator α_3 in $\pi_1\mathrm{Emb}_0(S^1, S^1 \times S^3; S^1_0)$

positive S^1 factor for i times and finally gets to R.

In fact, as discussed in [3], the group $\pi_1\mathrm{Emb}_0(S^1, S^1 \times S^3; S^1_0)$ has a generating set given by a sequence of embedded tori $\alpha_i \colon S^1 \times S^1 \to S^1 \times S^3$. Each torus α_i is defined as follows: fix the embedded torus $S^1_0 \times S^1 \subset S^1 \times D^2 \subset S^1 \times D^3$ and add an arm to the boundary of this torus that first loops i times positively around the S^1-factor, and then links itself. Figure 2.7 shows α_3 where the vertical cylinder is part of the torus with the top and bottom identified. Using Construction 5.25 of [3], we pick a short vertical subarc of S^1_0 in the cylinder part of Figure 2.7 (drawn as a double-arrow arc) near where the arm is attached, and we perform a spinning of this arc around the red sphere following the arm. This gives rise to an embedded barbell in $S^1 \times S^3$ as shown in Figure 2.8 by the isotopy extension theorem. Details about spinning can be found in Section 4 of [3]. Alternatively, one can apply Proposition 2.1 in Section 2 of [4] to deduce the barbell in Figure 2.8 by resolving the double point near the red sphere (sphere R). The dashed line in Figure 2.8 indicates S^1_0. Drilling out a neighbourhood of S^1_0 gives rise to the barbell in Figure 2.6.

To end this section, we give some insights of the barbell diffeomorphism as a generalization of Dehn twists in dimension 2. Since the barbell diffeomorphism preserves the t-levels by construction, we can consider each t-slice separately. We will describe the barbell diffeomorphism as a composition of levelwise (we will explain the meaning of this in a second) Dehn twists.

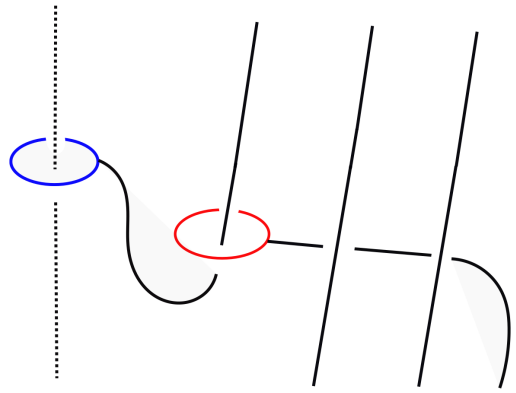

Figure 2.8: The initial barbell induced from α_3 in $S^1 \times S^3$.

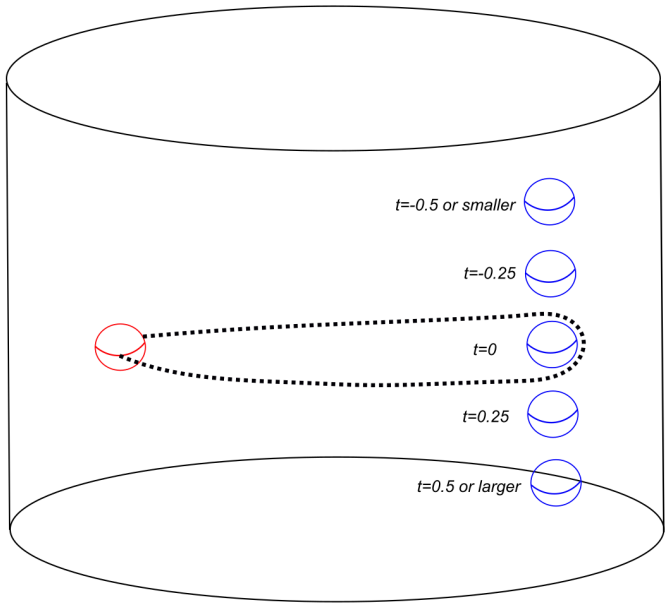

Figure 2.9: An alternative model of the barbell diffeomorphism.

To simplify our argument, we make use of an equivalent but slightly different model of the barbell manifold and the barbell diffeomorphism. We construct a bundle over $[-1, 1]$ as in Figure 2.9. Each fibre is diffeomorphic to a cylinderical 3-ball with two 3-balls removed, leaving two 2-sphere boundaries which we draw as red and blue in Figure 2.9. They form a bundle in the following way. For $t \geq 0.5$, the blue sphere is located in the lower half near the bottom of the cylinder, and for $t \leq -0.5$, the blue sphere is located in the upper half near the top. During $[-0.5, 0.5]$, the blue sphere moves down from the top to the bottom, and when $t = 0$, it is located at the middle horizontal plane (at the same level of the red sphere). Throughout, the red sphere stays in the same position. To define the barbell

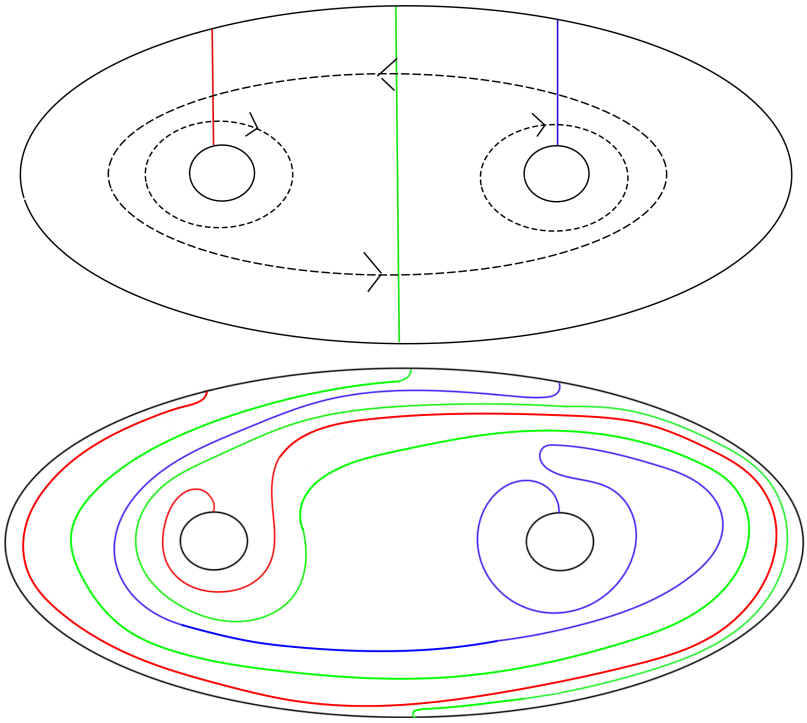

Figure 2.10: The $t = 0, y = 0$ slice of the barbell diffeomorphism as three Dehn twists.

diffeomorphism in this setting, we specify a fiberwise path (of embedded 3-balls based at the red sphere R) as follows. For $t \in [-0.5, 0.5]$, the path stays in the $y = 0$ plane as in Figure 2.9. For $t \geq 0.5$ and $t \leq -0.5$, we apply a *planar* null-homotopy of this path to contract it to the trivial path based at the centre of the left inner 3-ball (with boundary the red sphere). The barbell diffeomorphism is then defined in each fiber as the result of isotopy extension applied to this path.

This alternative description has the advantage that the barbell diffeomorphism now becomes both t- and y-level preserving (recall that we use the vertical direction as the y-direction as in Figure 2.2).

With this definition, we can now analyze each t- and y-level separately. We start by looking at the $t = 0$, $y = 0$ slice as a surface. The restriction of the barbell diffeomorphism to this twice punctured disk is shown in Figure 2.10 as a **point-pushing** map:

Definition 2.5. Let S be a surface with a fixed point $x \in \mathrm{Int}S$. Let $\gamma\colon [0, 1] \to S$ be a loop in S based at x as an isotopy of points. The point-pushing map of X along γ, denoted by $\mathrm{push}(x, \gamma)$ is the mapping class obtained from applying the isotopy extension

theorem to γ.

This mapping class is determined by looking at where the three colored arcs in Figure 2.10 go. From this we deduce that the restriction of the barbell diffeomorphism to the $t = 0$, $y = 0$ slice is isotopic to a composition of three Dehn twists drawn in the upper picture of Figure 2.10 as circles with arrows. Fix $t = 0$. When y goes positive or negative, these three Dehn twists remain, but the core circles of the Dehn twists gradually become null-homotopic as the two punctures become smaller and finally disappear completely. This means that the Dehn twists become twists along curves bounding disks, thus can be null isotoped to the identity map as y approaches ± 1.

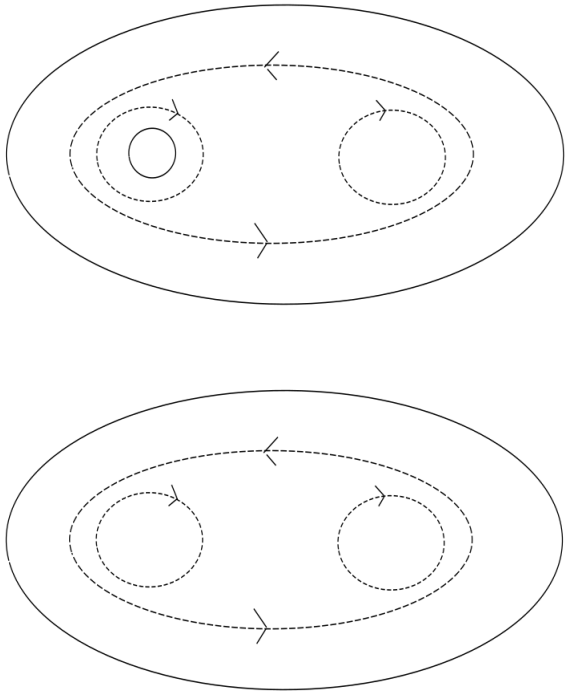

Figure 2.11: The barbell diffeomorphism for $t = 0.125$ and $y = 0.125$ (a) and for $t = 0.125$ and $y = 0.5$ (b).

Next, we analyze the situation for t being positive. Figure 2.11 shows the situation when $t = 0.125$ and y being positive. When t goes positive, the blue sphere moves down. This implies that for $y = 0$, the restriction of the barbell diffeomorphism will change gradually from the composition of three to only two Dehn twists, since the right puncture disappears as t increases. Also, for a fixed t-positive level, the behaviour in the y-levels is

as follows: as y goes positive, the core circles of the Dehn twists (two or three, depending on the exact value of t) becomes smaller in order. Namely, the right one disappears first, followed by the disappearance of the left one. See Figure 2.11. Similarly, as y goes negative, the left core circle disappears first, followed by the right one.

When t goes negative, the blue sphere moves up. Therefore, the opposite of the previous paragraph happens. We summarize these in the following proposition.

Proposition 2.6. *The thickened model barbell $\mathcal{B}$ can be parameterized in the way as in Figure 2.9 such that the barbell diffeomorphism is both t- and y-level preserving. Furthermore, in each slice $t = a$, $y = b$ where $a, b \in [-1, 1]$, the restriction of the barbell diffeomorphism is given by a composition of up to three Dehn twists along disjoint core curves as in the first picture of Figure 2.10. As t or y approaches ± 1, all of the three Dehn twists become trivial.*

2.2 Montesinos twin twists

In this section, we summarize the concept of Montesinos twin twist of 4-manifolds due to [9], which was inspired by [22].

Definition 2.7. A *Montesinos twin* (or just a twin) in a 4-manifold X is a pair $W = (R, S)$ of embedded 2-spheres which intersect each other at 2 points transversely.

A basic example is to take the two standard perpendicular 2-planes in $\mathbb{R}^4$ and view them as a pair of 2-spheres in S^4 that intersect at the origin and the point at infinity.

The local picture of a Montesinos twin is described in the following two lemmas. Details can be found in Section 3 of [22].

Lemma 2.8 ([22])**.** *Let $W = (R, S)$ be a twin in a 4-manifold X, and let $N(W)$ be a closed regular neighbourhood of W. Then $N(W)$ can be parameterized by the space*

$$E^4 = \{(x_1, x_2, x_3, x_4) \in \mathbb{R}^4 \colon x_1^2 + x_2^2 \leq 1 \text{ or } x_3^2 + x_4^2 \leq 1\} \cup \{\infty\} \subset \mathbb{R}^4 \cup \{\infty\} \cong S^4$$

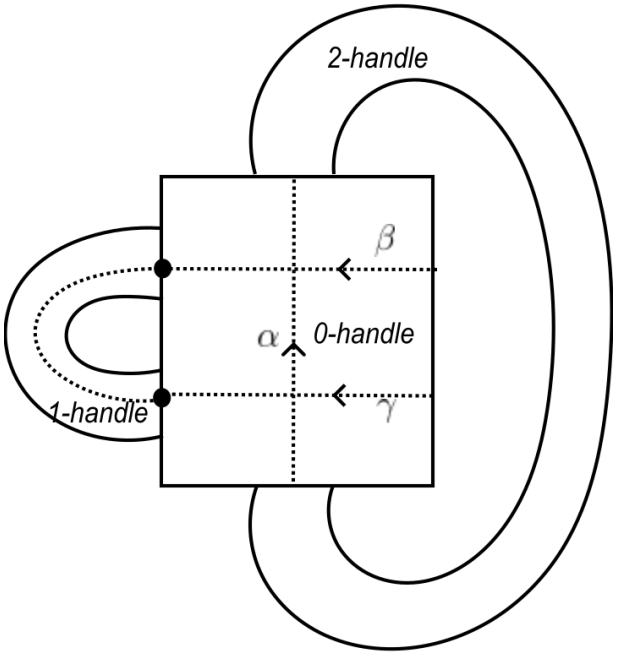

Figure 2.12: A handle structure of E^4 that consists of one 0-handle, one 1-handle and two 2-handles.

sitting in the one-point compactification of $\mathbb{R}^4$*. The 2-spheres* R *and* S *are parametrized by the (compactified) coordinate planes:*

$$R \cong \mathbb{R}^2 \times \{0\} \cup \{\infty\},\ S \cong \{0\} \times \mathbb{R}^2 \cup \{\infty\}$$

that intersect transversely at the origin and $\{\infty\}$*.*

Moreover, if we parametrize R *and* S *using the longitude-latitude coordinate systems* (t, g) *and* (t, h) *with* g *and* h *being the longitude angle coordinates, and* $t \in [0, 1]$ *being the latitude coordinate, then the boundary* ∂E^4 *can be understood as the quotient*

$$\bigsqcup_2 [0,1] \times S^1 \times S^1 / ((0, g, h) \sim (0, h, g), (1, g, h) \sim (1, h, g))$$

which is diffeomorphic to the 3-torus $S^1_l \times S^1_r \times S^1_s$ *where* S^1_l *corresponds to the* t*-coordinate.*

We describe a handle structure of E^4 as shown in Figure 2.12 following an approach due to Montesinos. See Section 3 of [22] for details.

Lemma 2.9 ([22])**.** *The space E^4 has a handle structure that can be built through the following steps. See Figure 2.12 which is meant to be a 2-dimensional slice of E^4.*

- *Take a neighbourhood of an arc in S that connects the two intersection points as a 0-handle.*
- *Choose three (oriented) curves α, β and γ on the boundary of the 0-handle as shown in Figure 2.12.*
- *Attach a 0-framed 2-handle along a neighbourhood of α to complete a regular neighbourhood of S.*
- *Attach a 1-handle to connect β and γ, along a neighbourhood of the pair of black dots as shown in Figure 2.12.*
- *Attach a 2-handle along a neighbourhood of the curve, drawn as horizontal dashed in Figure 2.12, consisting of parts of β, γ together with two parallel curves along the core of the newly attached 1-handle to complete a regular neighbourhood of R.*

A Kirby diagram of E^4 is given by Figure 2.13. The additional green arc represents the coordinate-t circle S^1_l. Equivalently, it is the Borromean rings with one circle dotted and the other two 0-framed. See Figure 2.14. The three circles of the boundary torus can be seen in the diagram as three merdians of the Borromean rings, with S^1_l corresponding to a meridian of the dotted circle.

Definition 2.10. Let X be a 4-manifold and let W be a twin embedded in the interior of X with $N(W)$ parameterized by E^4. Choose a closed collar neighbourhood of $\partial N(W)$ in $N(W)$ which is parameterized by $[0,1] \times S^1_r \times S^1_s \times S^1_l$ as discussed in Lemma 2.8 and Lemma 2.9. Define a self-diffeomorphism of this collar by taking the product of a Dehn twist along $[-1,1] \times S^1_l$ with the identity map on the other two circles. In other words, we take the map

$$\Phi'_W \colon [-1,1] \times S^1_l \times S^1_r \times S^1_s \to [-1,1] \times S^1_l \times S^1_r \times S^1_s$$

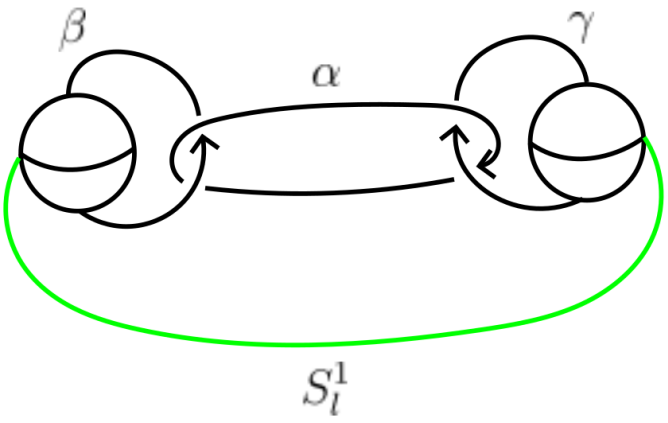

Figure 2.13: A Kirby diagram of E^4 with an additional green arc representing S^1_l.

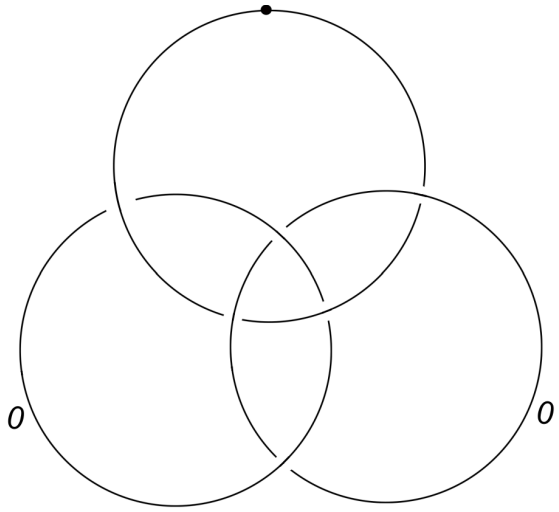

Figure 2.14: A Kirby diagram of E^4 in dotted circle notation.

given by

$$(\theta, t, g, h) \to (\theta, te^{2\pi i\theta}, g, h).$$

The *Montesinos twin twist* Φ_W of X induced from W is given by

$$\Phi_W = \begin{cases} \Phi'_W & \text{on } [-1,1] \times \partial N(W) \\ \text{Id} & \text{Otherwise} \end{cases}.$$

A twin embedded in X *unknotted* or *half-unknotted* if two or at least one of the two spheres is isotopically unknotted respectively.

Remark. We describe a standard way of constructing Montesinos twins in S^4 proposed by [9, 11]. By [3], the fundamental group of the space of embeddings $\pi_1\text{Emb}(S^1, S^1 \times S^3; S^1_0)$ is generated by embedded tori $S^1 \times S^1 \hookrightarrow S^1 \times S^3$ (see also Proposition 2.4). If we pick such an embedded torus and perform a surgery to the pair $(S^1 \times S^3, S^1 \times S^1)$ along the base circle $\{p\} \times S^1$ (drawn in red in Figure 2.15) that replaces $D^3 \times S^1$ by $S^2 \times D^2$. Then the torus becomes a 2-sphere that intersects the dual sphere of the circle $\{p\} \times S^1$ at two transverse points. This gives a Montesinos twin in S^4. Any unknotted or half-unknotted Montesinos twin embedded in S^4 can be described in this way. To see this, observe that we can do the reversed surgery to an unknotted twin on an unknotted sphere to get an embedded torus out of it.

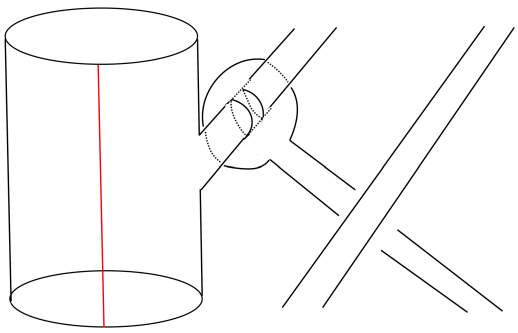

Figure 2.15: A Montesinos twin represented by an embedded torus in $S^1 \times S^3$.

2.3 Relationship between barbell diffeomorphisms and Montesinos twin twists

In this section, we describe the relationship between barbell diffeomorphisms and Montesinos twin twists. We start by summarizing the setup so far. Let M be a 4-manifold. An embedding of the thickened model barbell $\mathcal{B}$ in (the interior of) M induces an element $[\Phi_{\mathcal{B}}]$ in $\pi_0\text{Diff}(M, \partial)$. We would like to construct a corresponding embedded twin W in M such that the induced twin twist Φ_W is isotopic to Φ_B in $\text{Diff}(M, \partial)$. In other words, the twin twist induced from W of this embedded barbell lies in the same isotopy class as the barbell diffeomorphism induced from $\mathcal{B}$.

More precisely, we have the following theorem.

Theorem 2.11. *Let M be a 4-manifold, and let $\mathcal{B}$ be an embedded thickened model barbell in M that induces a barbell diffeomorphism $\Phi_{\mathcal{B}} \in \text{Diff}(M, \partial)$. Then there exists a Montesinos twin W in M such that the corresponding Montesinos twin twist Φ_W is isotopic to $\Phi_{\mathcal{B}}$. Further, W can be constructed from $\mathcal{B}$.*

Proof. The idea is roughly as follows. Pushing a finger from one of the two cuff spheres of $\mathcal{B}$ along the bar and performing a finger move near the other cuff sphere creates a pair of transverse intersection points and thus alters the two cuff spheres into a twin.

We now describe such an induced twin in detail. We use the alternative description of the barbell diffeomorphism as in Figure 2.9. We would like to describe a twin in this picture. Imagine that the model barbell is sitting in the $t = 0$ slice of the thickened model barbell (drawn as dotted) as two 2-spheres with each 2-sphere looping around one of the two complementary 3-balls, and the bar is the straight arc connecting them as in Figure 2.16. Figure 2.17 shows an induced twin W. For the $t = 0$ slice, draw a bigger sphere around the left-hand side inner 3-ball, representing one of the 2-spheres of the twin which we denote by R_W. In other words, we take the left hand side sphere of the embedded model barbell in Figure 2.16 as one sphere of our twin. To describe the other sphere B_W, we draw a circle (drawn as a blue solid circle in Figure 2.17) in the $t = 0, y = 0$ plane

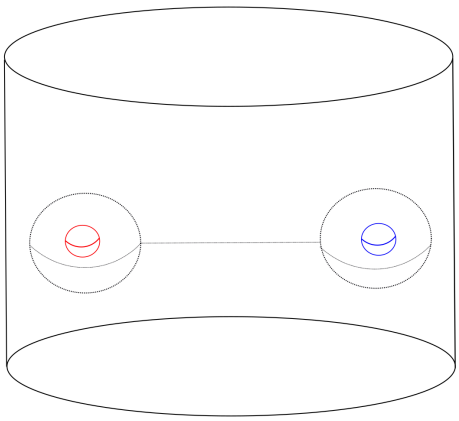

Figure 2.16: The $t = 0$ slice of the thickened model barbell with the model barbell sitting inside.

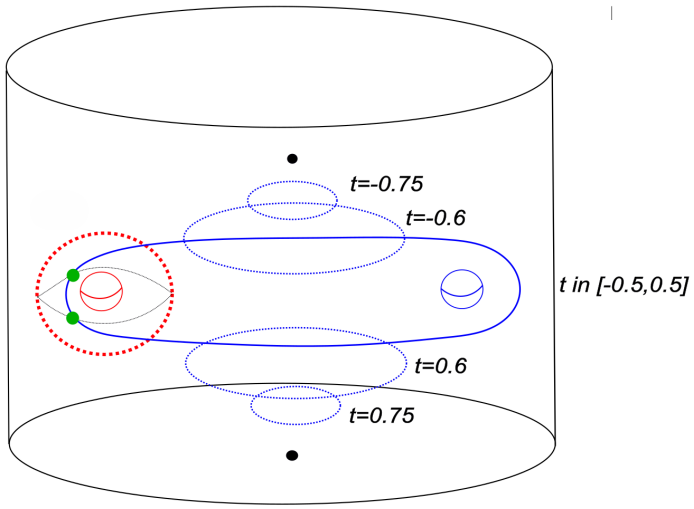

Figure 2.17: A Montesinos twin inherited from the barbell manifold.

intersecting R at two points. When t goes positive, the blue inner 3-ball moves downwards, so we draw the dotted blue circles as in Figure 2.17 that initially move downwards with size unchanged until $t = 0.5$, then continue moving down and get smaller until converging to a single point as t approaches 1. This forms a hemisphere of B_W. Similarly, when t goes negative, the dotted blue circles that converge to a single point in the upper half of the thickened model barbell form the other half of B_W. Combining both hemispheres gives rise to the second sphere B. Then the pair $W = (B_W, R_W)$ is a twin embedded in the thickened model barbell.

Figure 2.18 shows the $t = 0$ slice of a neighbourhood of W, i.e. the intersection of $N(W)$ with the $t = 0$ level of the thickened model barbell. It is diffeomorphic to a space

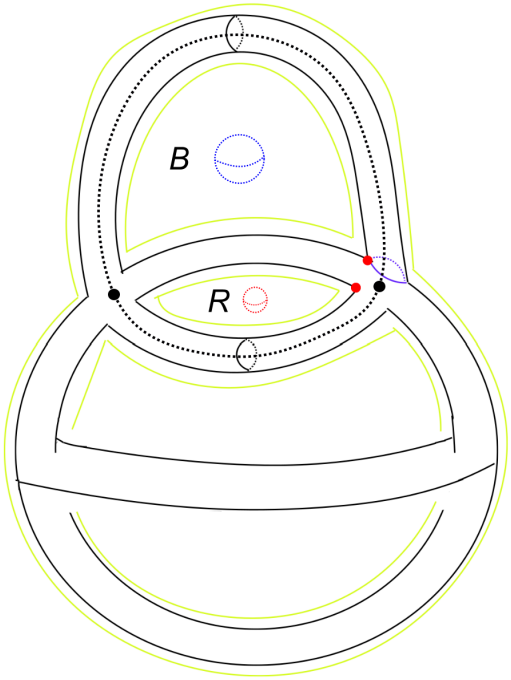

Figure 2.18: The local picture of a neighbourhood of $R_W \cup S_W$ at $t = 0$.

that is obtained by attaching two 1-handles to $S^2 \times I$ to the two boundary components respectively. The two black dots indicate the pair of intersection point of the twin. By imagining the paper to be the $y = 0$ plane, we can also observe the $t = 0$, $y = 0$ slice from the same figure as a 2-disk with three punctures, each of which is indicated by an inner yellow circle. The boundary 2-spheres of the two inner 3-balls of the thickened model barbell, which we denote using the notations B and R, are drawn as blue and red dotted spheres contained in the two upper punctures respectively. Note that they are different from the notation we use for the twin $W = (B_W, R_W)$.

The t-slices of $N(W)$ with $t \neq 0$ can be obtained from Figure 2.18 as follows. When t change from 0 to 1, Figure 2.18 gradually becomes a disjoint union of a thickened sphere with a solid torus, i.e. the two 1-handles gradually merge into a solid torus as they get away from the neighbourhood of R by moving into the page. This solid torus then converges to a point and disappears, with the thickened 2-sphere stays still. The same thing happens when t becomes negative with the two 1-handles moving out of the page, merging into a solid torus and disappearing.

To locate the three circles of the 3-torus boundary of $N(W)$, we look a bit closer at

the local neighbourhood of $R \cup S$ at various values of t. At $t = 0$, as shown in Figure 2.18, we have a thickened 2-sphere with two 1-handles attached, one from the inside and one from the outside. The boundary is a disjoint union of two tori. In Figure 2.18, S^1_r is drawn in blue as a meridian of the black dotted line and S^1_s is drawn as two red dots which trace out a red circle when varying t. The $t = 0, y = 0$ slice has 4 boundary circles, all of which are copies of S^1_l drawn in yellow in Figure 2.18. As y changes, the biggest yellow circle and the upper inner yellow circle trace out a torus boundary and the two lower inner ones trace out another torus boundary. Dehn twists are performed along each of these circles. They can be drawn as in the upper picture of Figure 2.10 with one more trivial Dehn twist along a null homotopic loop added between the outer Dehn twist and the left-hand side inner Dehn twist. This shows that the restriction of Φ_W to the $t = 0$, $y = 0$ slice of the thickened model barbell is isotopic to the restriction of $\Phi_{\mathcal{B}}$ to the same slice. In particular, on the $t = 0, y = 0$ slice, only three of the four Dehn twists on this twice-punctured disk are non-trivial. This matches with the fact that on this slice the barbell diffeomorphism recovers the **point-pushing** map which is a composition of three Dehn twists as discussed in Section 2.1.

When y goes to the positive direction, the core circles of the four Dehn twists become smaller and diverge to points and disappear. This is exactly what happens to $\Phi_{\mathcal{B}}$ except for the existence of a trivial Dehn twist. Therefore, this tells us $\Phi_{\mathcal{B}}$ and Φ_W are isotopic on the $t = 0$ slice.

When t changes from 0 to ± 0.5, the dotted blue sphere B moves down or up as in Figure 2.9. As we already discussed, the t-slice $(W)_t$ of the twin remains essentially the same shape as for $t = 0$, but the two 1-handles move down or up from the $y = 0$ plane. When t continues to increase or decrease to ± 1, $(W)_t$ firstly becomes a solid torus (the neighbourhood of R disappears) and then converges to a point and disappears. Therefore, for $y = 0$, and as t goes from 0 to ± 0.5, the Dehn twist around the dotted blue sphere B gradually becomes trivial. And when t continues increasing to ± 1, the four Dehn twists gradually become two Dehn twists around the $y = 0$ slice of the dotted red sphere R with opposite directions, and finally disappear completely. All of this behaviour is consistent

with $\Phi_{\mathcal{B}}$ up to null-isotoping trivial Dehn twists, and up to replacing the planar null-homotopy used in defining $\Phi_{\mathcal{B}}$ in Figure 2.9 by the process of a neighbourhood of R_W getting thinner and disappearing (and hence two Dehn twists around the $y = 0$ slice of a neighbourhood of R disappear in the end as t goes to ± 1).

In fact, for a fixed t, one can similarly analyze the behaviour of Φ_W when varying y, and verify that $\Phi_{\mathcal{B}}$ and Φ_W are isotopic on all t- and y-levels, because W and $\mathcal{B}$ share the red sphere, i.e. R_W is isotopic to R. Moreover, one can choose such t- and y-levelwise isotopies, by varying the size of R_W and B_W in an appropriate way if necessary, such that they assemble into a continuous t- and y-parameter families of isotopies. Thus, we conclude that $[\Phi_{\mathcal{B}}] = [\Phi_W] \in \pi_0\mathrm{Diff}(M, \partial)$. So we have proven Theorem 2.11. □

From a personal communication with David Gay [10], the author understands this is obtained independently by David Gay as well.

Remark. Conversely, given a Montesinos twin W in M, if there exists an appropriate Whitney disk such that then one can resolve the pair of intersections, then this gives rise to an embedded barbell $\mathcal{B}$. In this case, one can argue that $\Phi_{\mathcal{B}}$ is isotopic to Φ_W. However, we do not expect this to be always possible in general.

2.4 Half-unknotted barbells and Montesinos twins

Recall that we call a barbell, or a Montesinos twin, *half-unknotted* if at least one of the cuff spheres, or one of the embedded 2-spheres of the twin, is unknotted.

Let $\mathcal{M}_0$ denote the subgroup of $\pi_0\mathrm{Diff}(S^4)$ generated by half-unknotted twin twists and let $\mathcal{B}_0$ denote the subgroup of $\pi_0\mathrm{Diff}(S^4)$ generated by half-unknotted barbell diffeomorphisms. Gay–Hartman [11] showed that every twin twist in the 4-sphere that arises from a half-unknotted twin is isotopic to a twin twist arises from an unknotted twin. More precisely, they give a set of generators of $\mathcal{M}_0$ called $W(i)$, $i \geq 1$, which are unknotted. Figure 2.19 shows $W(3)$. It is isotopic to Figure 2.20 which is deduced from Figure 2.6 by viewing it in S^4.

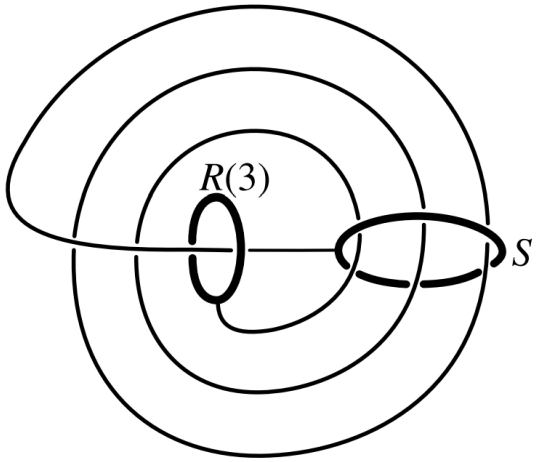

Figure 2.19: Gay's twin $W(3)$ (the original picture used as Figure 2 in [11]).

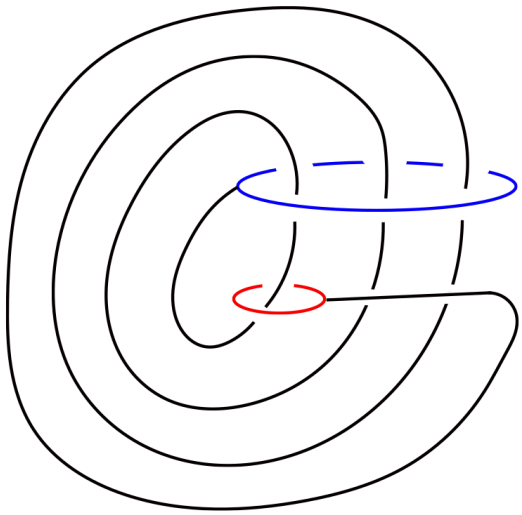

Figure 2.20: The barbell α_i viewed as a Montesinos twin $W(\alpha_i)$ in S^4.

Theorem 2.12. *([9, 11]) The group $\mathcal{M}_0$ is generated by the twin twists $\Phi_{W(i)}$ from twins $W(i)$. Moreover, $W(i)$ is isotopic to $W(\alpha_i)$ where $W(\alpha_i)$ is the induced twin from α_i (see Figure 2.20, for the case $i = 3$) viewed as a barbell in S^4.*

As an application of Theorem 2.11 and Theorem 2.12, we prove the following result.

Theorem 2.13. *There is an isomorphism from $\mathcal{B}_0$ to $\mathcal{M}_0$ given by taking the induced twin of a barbell. In particular, half-unknotted barbell diffeomorphisms of S^4 can be understood through unknotted barbells in S^4.*

Proof. By Theorem 2.11, we have $\mathcal{B}_0 \subset \mathcal{M}_0$. We define an inverse. By Theorem 2.12, it suffices to consider the twins $W(i)$. As discussed in Section 3 of [11] (and in particular Figure 5 and Figure 6 of [11]), after reversing surgeries as discussed in the end of Section 2.2, $W(i)$ can be represented by an unknotted embedded torus with an arm that goes around the S^1 factor i times and links the arm itself. For example, see Figure 2.15 when $i = 2$ and Figure 2.7 when $i = 3$.

Such a torus induces a barbell $B(\alpha_i)$ as discussed in Section 2.1 (see Figures 2.6, 2.7 and 2.8). One can recover the twin $W(i)$ from $B(\alpha_i)$ via a finger move as in Section 2.3 and in the proof of Theorem 2.11. Therefore, the corresponding induced barbell diffeomorphism $\Phi_B(\alpha_i)$ is isotopic to the twin twist $\Phi_{W(\alpha_i)}$ by Theorem 2.11. □

Chapter 3

Representing diffeomorphisms by handle moves

In this chapter, we discuss an approach to understanding diffeomorphisms of manifolds through handlebody decompositions and handle moves. We give necessary definitions and construction in Section 3.1, followed by a discussion for dimension 4 in Section 3.2. Finally, low-dimensional examples are given in Sections 3.3.

3.1 Definitions and construction

We start by giving a definition of handlebodies and handle decompositions of manifolds. The reader can refer to [12] for a detailed discussion of handle structure of smooth manifolds, and see [21] for a treatment of Morse theory. Here, we first recall some terminology of the theory of handle decomposition of smooth manifolds that we will use in this thesis. For $0 \leq k \leq n$, an n-dimensional *index k-handle*, or just a *k-handle*, is a copy of $D^k \times D^{n-k}$. The disk $D^k \times \{0\}$ is called the *core*, the disk $\{0\} \times D^{n-k}$ is called the *cocore*, $\partial D^k \times D^{n-k}$ is called the *attaching region*, $\partial D^k \times 0$ is called the *attaching sphere* and $\{0\} \times \partial D^{n-k}$ is called the *belt sphere*. We define an n-dimensional handlebody as follows.

Definition 3.1. An n-dimensional *handlebody* consists of

- for each $0 \leq k \leq n$, a collection of n-dimensional k-handles $\{h_i^k\}$

- for each $0 < k \leq n$, a collection of embeddings $g_i^k \colon (\partial D^k \times D^{n-k} \subset \partial h_i^k) \to \partial X^{k-1}$ called *gluing maps*, where X^{k-1} is recursively defined as $X^0 = \bigsqcup h_i^0$ and $X^l = (X^{l-1} \cup \bigsqcup h_i^l)/(x \sim g_i^l(x))$ for $l \geq 1$.

There is a canonical way of smoothing corners by replacing an angular boundary by a smooth corner. Thus an n-dimensional handlebody can be interpreted as a smooth n-manifold. A *handle decomposition* of an n-manifold X is an identification of X with an n-dimensional handlebody. A k-handlebody is a handlebody consisting of handles of index at most k.

Let X be a connected n-manifold. Choose a Morse function $f_0 \colon X \to \mathbb{R}$ together with a gradient-like vector field v_0 on X. In other words, we fix a triple (X, f_0, v_0). With some additional auxiliary data, this induces a handle decomposition of X. There are three kinds of elementary handle moves that preserve the diffeomorphism type, namely level-preserving isotopies, creating/cancelling $(i/i+1)$-pairs and handle slides. The key idea behind the results in this section is that these moves induce diffeomorphisms that are well defined up to isotopy. We shall now discuss these moves separately in detail. We begin with a notion of isomorphism of handlebodies.

Definition 3.2. Let X and X' be n-dimensional handlebodies. Denote the handles of X and X' by $\{h_i^k\}$ and $\{h_i^{k'}\}$ respectively, and denote the gluing maps of X and X' by $\{g_i^k\}$ and $\{g_i^{k'}\}$ respectively (cf. Definition 3.1). Then X and X' are called *isomorphic* handlebodies if there is an *isomorphism of handlebodies* between X and X' which consists of

- for each k, a bijection $\{h_i^k\} \to \{h_i^{k'}\}$ giving rise to a canonical diffeomorphism $\psi_k \colon \bigsqcup_i h_i^k \to \bigsqcup_i h_i^{k'}$ where $h_i^{k'}$ are handles of X' attached via $\{g_i^{k'}\}$.

- for each k, a diffeomorphism $\Psi_k \colon X^k \to X'^k$ recursively defined using the bijection with $\Psi_0 = \psi_0$ satisfying $g_i^{k'} = \Psi_{k-1} \circ g_i^k \colon \partial D^k \times D^{n-k} \to X^{k-1'}$.

In other words, such an isomorphism gives rise to a handle by handle identification between X and X'

$$\Phi \coloneqq \Phi_n \colon X = X^n \to X' = X^{n'}.$$

that is intertwined with the attaching maps of handles.

With the above definition, we now describe diffeomorphisms induced from elementary moves. Assume that the Morse function f_0 has critical points with distinct critical values, and satisfies the condition that the critical points with higher indices have larger critical values. Then it produces a handle decomposition of X with all handles attached in increasing index order.

A **level-preserving isotopy** ϕ_t of index k with respect to the Morse function f_0 is an isotopy (of attaching regions of index k handles) that moves the attaching regions of index k handles and keeps them disjoint. Such an isotopy ϕ_t induces a diffeomorphism Φ_1 from X^{k-1} to the $\{k-1\}$-skeleton $X^{k-1'}$ of a handlebody X' by the isotopy extension theorem applied to the $\{k-1\}$-skeleton of X. Here, the handlebody X' is defined as $X^{k-1} \cup_{\Phi_1 \circ g} C$ where C is the union of handles of X with indices k or higher, and $g\colon \partial C \to \partial X^{k-1}$ is the union of the gluing maps of X with indices k or higher. Extending Φ_1 to the higher index handles by dragging the attaching maps of the higher dimensional handles along and extending using the identity map, we get the induced diffeomorphism Φ is defined by

$$\Phi = \begin{cases} \Phi_1 & \text{on } X^{k-1} \\ \mathrm{Id} & \text{on the } k\text{-handles with attaching regions removed.} \\ \mathrm{Id} & \text{on the higher dimensional handles with attaching regions removed.} \end{cases}.$$

Note that the handle structure of X' can be obtained from the pair $(f_0 \circ \Phi^{-1}, \Phi_*(v_0))$. If the handle structures of X and X' are isomorphic in the sense of Definition 3.2, then using Definition 3.2, we can view Φ as a **self-diffeomorphism** of the handlebody X. In low dimensions, one often relies on pictures and diagrams to naturally identify handlebodies. However, one needs to be careful that choices are involved in such identifications.

Example 3.3. The standard handle decomposition of $D^2 \times S^2 \natural D^2 \times S^2$, the boundary connected sum of two D^2-bundles over S^2 has a Kirby diagram which contains an unlink with framing numbers 0. An isotopy that drags one of the unknots through the other one and then comes back to its original position gives rise to a self-diffeomorphism by the

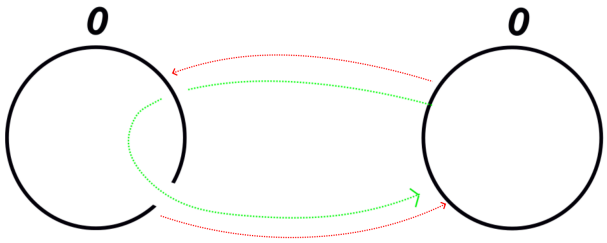

Figure 3.1: An example of a level-preserving isotopy in a 4-manifold with one 0-handle and two 0-framed 2-handles.

isotopy extension theorem. This diffeomorphism acts trivially on homology. See Figure 3.1 for a picture. The dashed light green path indicates this isotopy. However, it is not clear to the author whether this diffeomorphism is isotopic to the identity.

Another example of a non-trivial diffeomorphism can be constructed by exchanging the locations of the two unknots in Figure 3.1 following the dashed red lines. The resulting handlebody is isomorphic to the original one. The induced diffeomorphism acts non-trivially on homology, namely, it exchanges the two generators of the second homology. Therefore, it can not be isotopic to the identity.

More generally, for any 4-dimensional 2-handlebody M, there is a homomorphism from the fundamental group of the embedding space of L (the link which specifies M) in S^3, which is denoted by $\pi_1\mathrm{Emb}(L, S^3)$, to $\pi_0\mathrm{Diff}(M)$.

Suppose h_1^k and h_2^k are k-handles of X whose attaching maps have codomain ∂X^{k-1}. A **handle slide** of h_1^k over $h_2^k \cong D^k \times D^{n-k}$ is defined by an isotopy

$$\phi_t \colon S^{k-1} = \partial D^k \times \{0\} \to \partial(h_2 \cup X^{k-1})$$

of the attaching sphere of h_1^k that drags it along a k-disk $D^k \times \{*\}$ inside h_2^k and returns it to ∂X^{k-1}. This move induces an isotopy class of a diffeomorphism Φ_1 from X to the handlebody $X' = X^{k-1} \cup_{\Phi_1 \circ g} C$ by the isotopy extension theorem. Here C denotes the union of all handles with indices k or higher except h_1^k and h_2^k, and

$$g \colon C \to \partial(h_2^k \cup X^{k-1} \cup h_1^k)$$

is the union of the gluing maps of X with indices k or higher except h_1^k and h_2^k. In particular, we define a diffeomorphism Φ of X in a similar way as for level-preserving isotopies:

$$\Phi = \begin{cases} \Phi_1 & \text{on } X^k \setminus (h_1^k \setminus S^{k-1}) \\ \text{Id} & \text{on } h_1^k \text{ with the attaching sphere removed.} \\ \text{Id} & \text{on the higher dimensional handles with attaching regions removed.} \end{cases}$$

Here Φ_1 is the result of isotopy extension applied to ϕ_t. Again, higher-dimensional handles get dragged along the way, i.e. they are attached by the compositions of their original attaching maps with Φ. Thus, we have a diffeomorphism from X to X'. Note that Φ_1 is isotopic to the identity as a diffeomorphism of $X^k \setminus (h_1^k \setminus S^{k-1})$, but this is not necessarily the case when we add the remaining part of h_1. Handles slides can be viewed as isotopies that **do not** preserve levels, i.e. isotopies that do not keep the attaching regions of index k handles disjoint. This means that during a handle slide of index k, handles of index k can not be attached at the same time, i.e. not all index k handles belong to the same attachment level anymore.

We have now described how handle slides and level-preserving isotopies induce diffeomorphisms. We now turn to the last type of handle move. We denote a **cancelling** $(i/i+1)$**-pair** by (h^i, h^{i+1}, p) where h^i is an index i handle, h^{i+1} is an index $i+1$ handle, and p is the unique intersection point between the belt sphere of h_i and the attaching sphere of h^{i+1}. Such a cancellation can be described by a perturbation of the Morse function f_0 to a new Morse function f_0' with 2 fewer critical points. The corresponding perturbed new gradient-like vector field is distinct from the old one only in a small neighbourhood of the integral curve between the two critical points that define h^i and h^{i+1} that passes through p. The manifold $X \cup h^i \cup h^{i+1}$ is diffeomorphic to X through a natural choice of diffeomorphism (which we shall describe now) that is supported in a neighbourhood N of $h^i \cup h^{i+1}$ in $X \cup h^i \cup h^{i+1}$.

For all n and $0 < i < n$, we fix two standard decompositions of the n-ball D^n as a

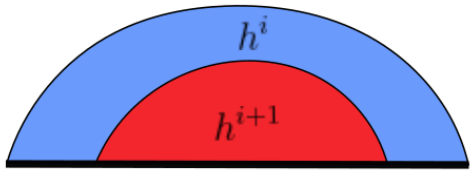

Figure 3.2: A standard decomposition of the n-ball into a cancelling pair.

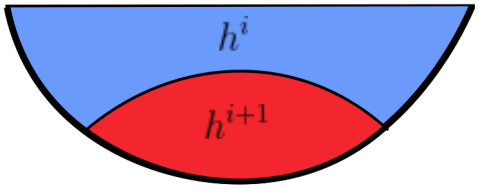

Figure 3.3: Another standard decomposition of the n-ball into a cancelling pair.

union of two handles $h^i = D^i \times D^{n-i}$ and $h^{i+1} = D^{i+1} \times D^{n-i-1}$ as shown in Figures 3.2 and 3.3 (for dimension 2, with higher dimensions obtained by taking a suspension with standard parameterized intervals). The attaching regions are thickened in black, and we will denote them by ∂D^n_-. The rest of the boundary is denoted by ∂D^n_+. Up to smoothing the corners, we will use these standard models as our models for cancelling pairs.

We now define a diffeomorphism from $X \cup h^i \cup h^{i+1}$ to X in the following way. We first map $X^{i-1} \cup h^i \cup h^{i+1}$ to X^{i-1} through a diffeomorphism Φ. Namely, take an n-ball collar neighbourhood B of the attaching region of $h^i \cup h^{i+1}$ in X^{i-1}. It is drawn in green

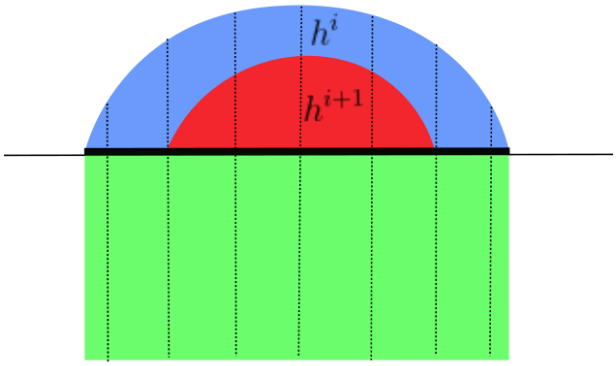

Figure 3.4: The domain $X^{i-1} \cup h^i \cup h^{i+1}$ of the induced diffeomorphism Φ from a cancelling pair.

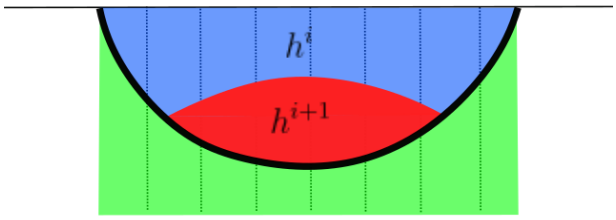

Figure 3.5: The image $\Phi(X^{i-1} \cup h^i \cup h^{i+1})$ of the induced diffeomorphism Φ from a cancelling pair.

in Figure 3.4. The union $B \cup h^i \cup h^{i+1}$ is also an n-ball. It admits an interval fibering: for $n = 2$, the fibering is drawn in Figure 3.4, and for $n > 2$, we take the product with I^{n-2}. We define a fiberwise diffeomorphism using this fibering. For each interval fiber of $B \cup h^i \cup h^{i+1}$, we use a diffeomorphism that contracts this interval to the corresponding shorter interval in B. Intuitively, we "push" the cancelling pair into the interior of X^{i-1}. Note that the attaching region is mapped to the interior.

Figures 3.4 and 3.5 illustrate the domain and image of Φ for $n = 2$ respectively. The boundary of X^{i-1} is drawn as a black line in Figure 3.4. Note that the parts of X^{i-1} that are not moved by Φ are not drawn. The image of the cancelling pair $h^i \cup h^{i+1}$ fits into the decomposition illustrated in Figure 3.3, with corners smoothed. Note that Φ maps $\partial X_{i-1} \cap (h^i \cup h^{i-1})$ (i.e. ∂D^n_+) to $\Phi(\partial X_{i-1}) \cap \Phi(h^i \cup h^{i-1})$. Therefore, the attaching maps of the remaining handles of X (with index i or higher) whose attaching regions have non-empty intersection with $\partial X_{i-1} \cap (h^i \cup h^{i-1})$ get dragged by Φ. It follows that we can extend Φ to the complement C of $X^{i-1} \cup h^i \cup i^{i+1}$ in $X \cup h^i \cup h^{i+1}$ via handle-wise identity maps. We take this extension as the induced diffeomorphism from this cancellation pair. In particular, the induced diffeomorphism from adding a cancelling pair to X is Φ^{-1}, and the induced diffeomorphism from removing such a pair is Φ.

For 0/1-pairs, i.e. $i = 0$, one can perform the same procedure as above using another two different decompositions of the n-ball as a union of a 1-handle and a 0-handle, as shown in Figure 3.6.

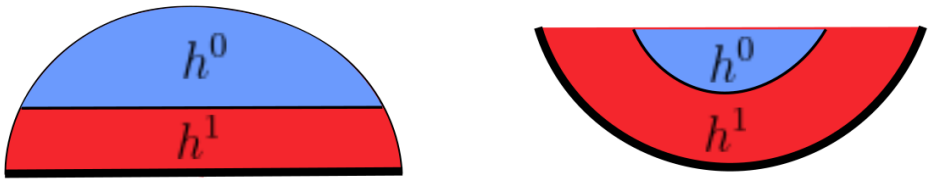

Figure 3.6: Two standard decompositions of the n-ball for 0/1-pairs.

Remark. There is an alternative view of the induced diffeomorphism from deleting/adding a cancelling pair. If X' is obtained from X by adding a cancelling pair, then we can take the composition $\Phi \circ i \colon X \to X' \to X$ where i is the natural inclusion map and Φ is the induced diffeomorphism described above. This can be considered as a self-embedding of X (viewed as a manifold rather than a handlebody). More precisely, it is an embedding of X, equipped with one handle structure, into X, equipped with a different, induced handle structure from Φ and X'. One can show that this map is isotopic to the identity map of X, as a manifold. Roughly, there is an isotopy of $\Phi \circ i$ that gradually enlarges the image $\Phi \circ i(X)$ to cover the entire X. From this point of view, Φ is indeed isotopic to the identity of X, as a manifold diffeomorphism. However, one must be very careful since $\Phi \circ i$ does not give rise to an isomorphism between handlebodies.

Combining the discussion so far, we have the following definition.

Definition 3.4. Given a finite sequence (m_i) of handle moves of (X, v_0, f_0) that transforms X to a manifold (X', v_1, f_1) with the same diffeomorphism type, there is a well-defined diffeomorphism $\Phi_{(m_i)} \colon X \to X'$ up to isotopy, called the induced diffeomorphism from (m_i). If X and X' are isomorphic as handle decompositions, then $\Phi_{(m_i)}$ is considered as a self-diffeomorphism of X and defines an element in $\pi_0 \mathrm{Diff}(X)$.

To end this section, we state the following conjecture that concerns the inverse without giving a proof.

Conjecture 3.5. *Let X be an n-dimensional connected manifold. Then every element $\Phi \in \mathrm{Diff}(X)$ can be factored into a composition of a finite sequence of diffeomorphisms, each of which is induced by a handle slide, a cancelling pair creation/cancellation or a level-preserving isotopy.*

The possible ideas behind the proof would be based on Cerf theory: given a diffeomorphism Φ of X, the composition $f_0 \circ \Phi^{-1}\colon X \to \mathbb{R}$ is also a Morse function on X. Cerf [6] proved that there exists a 1-parameter family of smooth functions f_t on X where $f_0 = f$ and $f_1 = f \circ \phi$, and this family can be deformed into a smooth function $G\colon X \times I \to \mathbb{R}$ on $X \times I$ that is Morse for almost all t except at finitely many isolated values of t where types of the critical points are classified, i.e. we can control the types of singularities at these isolated points. In particular, cusp singularities correspond to cancelling pairs and integral flowline between critical points of the same index correspond to handle slides. We plan to return to this topic in greater detail in future work.

3.2 Dimension 4

In this section, we focus on diffeomorphisms of 4-dimensional handlebodies. We will explore representing diffeomorphisms of 4-dimensional handlebodies by sequences of Kirby diagrams connected by handle moves. Readers that are not familiar with 4-manifold handle decompositions and Kirby calculus can refer to [12] for a detailed treatment. For a connected 4-manifold X, there exists a handle decomposition of X induced from a Morse function f on X together with a gradient-like vector field v, such that there is a unique 0-handle. If X has no boundary, we can assume a unique 4-handle by cancelling some 3-4 pairs, if necessary. The 2-skeleton X^2 of X can be described by a Kirby diagram that consists of dotted, unknotted circles (1-handles) and knots/links with framing numbers noted (2-handles). By [19], any diffeomorphism of a connected sum of finitely many copies of $S^1 \times S^2$ extends to a diffeomorphism of the corresponding boundary connected sum of the same number of copies of $S^1 \times D^3$. Thus, a Kirby diagram determines a closed 4-manifold up to its diffeomorphism type. Any two Kirby diagrams (together with the 3- and 4-handles) represent the same handlebody if and only if they are related by a sequence of handle moves.

If X has no 3- and 4-handles (so $X = X^2$), then a sequence of Kirby diagrams that starts and ends with the same diagram of X, connected by handle moves, induces a

self-diffeomorphism of X up to isotopy, since we can identify the starting and ending diagrams via the natural identification of diagrams which then leads to an isomorphism of handlebodies (cf. Definition 3.2 and Example 3.3).

It remains to deal with the attaching maps of 3- and 4-handles if X admits 3- and 4-handles. Note that although we can assume that a connected 4-manifold X admits a handle decomposition with at most one 4-handle as mentioned above, sequences of handle moves of X may introduce cancelling 3-4 pairs that are not recorded in detail in Kirby diagrams. A typical scenario is as follows: we start with a finite sequence of Kirby diagrams (D_i) together with attaching maps ϕ_i of the 3- and 4-handles representing handlebodies X_{D_i} connected by handle moves

$$(D_1, \phi_1) \to (D_2, \phi_2) \to \cdots \to (D_m, \phi_m)$$

where $\phi_i \colon \#_{k_i} S^1 \times S^2 \to \partial X^2_{D_i}$ and k_i is the number of 3-handles of X_{D_i}. We allow 3-handle moves to appear in the above sequence. In this case, two items in the sequence connected by a 3-handle move will share the same diagram but different attaching maps of 3- and 4-handles.

We denote the composition of the induced diffeomorphisms from the handle moves by $\Phi \colon X_{D_1} \to X_{D_m}$. We further assume D_m and D_1 are the same diagram, i.e. the sequence starts and ends with the same diagram, and X_{D_1} and X_{D_m} have the same attaching maps for 3- and 4-handles. It follows that X_{D_1} and X_{D_m} are isomorphic handlebodies. Thus we have a well-defined self-diffeomorphism of X up to isotopy (cf. Definition 3.2). In the special case when X has no 3-handles, we can simplify the data needed. We consider three cases separately.

1. There are no 3-handles involved.

   Let $\phi_1 \colon \partial D^4 \to \partial X^2_{D_1}$ and $\phi_m \colon \partial D^4 \to \partial X^2_{D_m}$ denote the attaching maps of the 4-handles of X_{D_1} and X_{D_m} respectively. Since $\mathrm{Diff}(S^3)$ is homotopy equivalent to $SO(4)$ by [14], the mapping class group of orientation-preserving diffeomorphisms $\pi_0 \mathrm{Diff}(S^3)$ is trivial. So ϕ_1 and ϕ_m are both isotopic to the identity and thus are

isotopic. By choosing an isotopy from f_m to f_1, we can line up these two attaching maps and thus extend the isomorphism between the 2-skeletons to the 4-handles (thus to an isomorphism between X_{D_1} and X_{D_m}). The only thing we need to check is that the choice of isotopy does not affect the isotopy class of Φ. Since $\pi_1\mathrm{Diff}(S^3) \cong \mathbb{Z}/2$ is generated by a path of rotations that fix an axis by [5], the effect of performing an isotopy along the collar of the 4-handle can be undone by rotating the inner part of the 4-handle. This tells us that we do not need to keep track of the attaching maps of the 4-handles in our sequence.

2. There is only one 3-handle involved.

   The union of the 3-handle with the 4-handle gives rise to a copy of $S^1 \times D^3$. To see this, note that we can take the standard decomposition of $S^1 \times D^3$ which consists of a 0-handle and a 1-handle, and take it upside and down.

   We can apply a similar argument with $\phi_1 \colon \partial(S^1 \times D^3) \to \partial X^2_{D_1}$ and $\phi_m \colon \partial(S^1 \times D^3) \to \partial X^2_{D_m}$ denoting the attaching maps of the 3- and 4-handles of X_{D_1} and X_{D_m} respectively. By [13], the group $\mathrm{Diff}(S^1 \times S^2)$ is homotopy equivalent to $O(2) \times O(3) \times \Omega O(3)$ with $\pi_0\mathrm{Diff}(S^1 \times S^2)$ being isomorphic to $(\mathbb{Z}/2)^3$ which is realized by rotations on S^1 and S^2, and loops of rotations around S^2, and these extend naturally to $S^1 \times D^3$. Note that here (but not below) we use $\mathrm{Diff}(S^1 \times S^2)$ to denote all diffeomorphisms including orientation-reversing ones. We isotope ϕ_1 and ϕ_m to diffeomorphisms ϕ_1' and ϕ_m' generated by these generators and use $\phi_1' \circ {\phi_m'}^{-1}$ to identify D_1 and D_m. It remains to show that the isotopy class of $\phi_1' \circ {\phi_m'}^{-1}$ is independent of choices. Two choices of isotopies give rise to a loop in $\pi_1\mathrm{Diff}(S^1 \times S^2) \cong \mathbb{Z} \times \mathbb{Z}/2$ which is generated by loops of rotations. Thus we can again "rotate" the interior of $S^1 \times D^3$ to cancel the effects of this loop.

3. There are two or more 3-handles involved.

   Similar to the previous cases, we are looking at $\pi_0\mathrm{Diff}(\#_k S^1 \times S^2)$ and $\pi_1\mathrm{Diff}(\#_k S^1 \times S^2)$ where k is the number of 3-handles involved. By [17,18] (see also [1]), $\pi_0\mathrm{Diff}(\#_k S^1 \times$

S^2) is described by the following short exact sequence:

$$1 \to \text{Twist}(\#_k S^1 \times S^2) \to \pi_0\text{Diff}(\#_k S^1 \times S^2) \to \text{Out}(F_k) \to 1$$

where $\text{Twist}(\#_k S^1 \times S^2) \cong {\mathbb{Z}_2}^k$ is the group of sphere twists generated by the twists along the k core spheres $S^2 \times \{pt\}$ of the k different summands, and $\text{Out}(F_k)$ is the group of outer automorphisms of the free group on k generators. (cf. Example 3.13 below). This short exact sequence splits and $\pi_0\text{Diff}(\#_k S^1 \times S^2)$ is isomorphic to the semidirect-product $\text{Twist}(\#_k S^1 \times S^2) \rtimes \text{Out}(F_k)$. The automorphism group $\text{Aut}(F_k)$ has a countable set of standard generators: for distinct $1 \leq i, j \leq k$, elements L_{ij} and R_{ij} defined via the formulas:

$$L_{ij}(a_k) = \begin{cases} a_j a_k & \text{if } k = i \\ a_k & \text{otherwise} \end{cases} \qquad R_{ij}(a_k) = \begin{cases} a_k a_j & \text{if } k = i \\ a_k & \text{otherwise} \end{cases}$$

and for $1 \leq k \leq n$, and elements

$$I_{ij}(a_k) = \begin{cases} a_k^{-1} & \text{if } k = i \\ a_k & \text{otherwise} \end{cases}$$

for $1 \leq i \leq n$. This induces a generating set of $\text{Out}(F_k)$. It follows that we can isotope the attaching maps of 3- and 4-handles f_1 and f_m as standard pairs in the above semi-direct product and use these to identify X_{D_1} and X_{D_m}. So in this case the extra information needed is contained in $\pi_1\text{Diff}(\#_k S^1 \times S^2)$, which is not yet sufficiently understood to the author's knowledge.

The following theorem is a refinement of Definition 3.4 in dimension 4.

Theorem 3.6. *For an oriented, compact, smooth 4-manifold X with a preferred handle structure σ, consider any finite sequence $\mathcal{S}$*

$$(D_1, \phi_1) \to (D_2, \phi_2) \to \cdots \to (D_m, \phi_m)$$

of Kirby diagrams D_i together with attaching maps $\phi_i\colon \#_r S^1 \times S^2 \to \partial X^2_{D_i}$ of 3- and 4-handles, connected by handle moves, where D_1 and D_m are identical as diagrams representing σ, along with identical attaching maps $\phi_1 = \phi_m$ of 3- and 4-handles. Here r is the number of 3-handles.

In this scenario, there exists a ***handle animation*** *self-diffeomorphism Φ induced from $\mathcal{S}$ as a composition of induced diffeomorphisms from each handle move in the sequence, which is well-defined up to isotopy. If X has less than or equal to one 3-handle ($r \leq 1$), then we do not need to keep track of the attaching maps of 3- and 4-handles.*

Remark. In fact, each attaching ϕ_i can be realized by a sequence of surgery diagrams connected by Kirby moves. In particular, $\#_k S^1 \times S^2$ may be represented as the boundary of the standard diagram of k dotted unknots of $\natural_k S^1 \times D^3$, and each ϕ_i is realized by a sequence of diagrams from this standard diagram to the boundary surgery diagram of D_i. See Example 3.13 in the next section.

3.3 Examples

In this section, we discuss examples of diffeomorphism representations of handlebodies in dimension 2, 3 and 4.

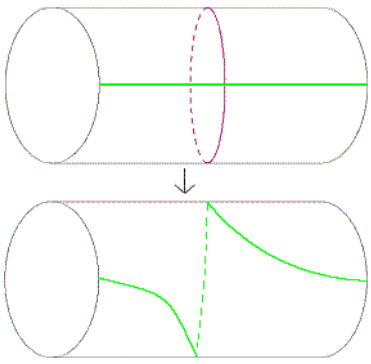

Figure 3.7: Dehn twist.

Example 3.7. We look at orientable surfaces first. Recall that the mapping class group $\pi_0\mathrm{Diff}(S, \partial S)$ of an orientable, compact surface S is generated by Dehn twists (see Figure 3.7) along essential curves (i.e. loops that do not bound disks) in S. Let S be a connected,

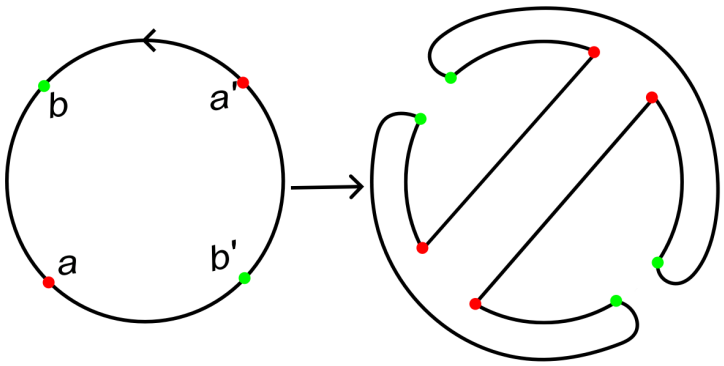

Figure 3.8: A punctured torus specified by an oriented circle with two pairs of points.

orientable surface with boundary. Then S can be specified by an oriented circle with labelled ordered pairs of points on the circle, annotated by $(a, a'), (b, b') \ldots$. To recover the surface by building up a handlebody, one first considers the circle as the boundary of a 2-disk, as a 0-handle, then attaches an oriented 1-handle to a neighbourhood of each pair of points in the way that the resulting surface is orientable. The orientation of the circle leads to an ordering of all labelled points on it. We call such a circle a *pointed circle*. If we further require that surgering out the pair of points out of the pointed circle gives rise to a connected 1-manifold, then such a circle specifies a surface with only one boundary component. Figures 3.8 and 3.9 indicate a punctured torus described in this way. The arrow in the former figure indicates that the two ordered pairs of points are surgered out, leading to a connected 1-manifold. Each ordered pair of points (a, a') and (b, b') determines an oriented core curve. See Figure 3.9: the red dotted circle with arrows is the core curve determined by (a, a'). Our first claim is the following theorem which is also described in [20] as Lemma 2.1 in a different language of *arc-slides* for surfaces with one boundary component.

Theorem 3.8. *Let S be an oriented surface determined by a pointed circle with pairs of annotated points on it. Assume that there is only one annotated point, say b', between an ordered pair of points a and a' on the pointed circle (using the orientation of the pointed circle). Then the Dehn twist along an oriented core curve l specified by the ordered pair (a, a') can be realized by sliding b' over the 1-handle specified by (a, a') once along the direction of l.*

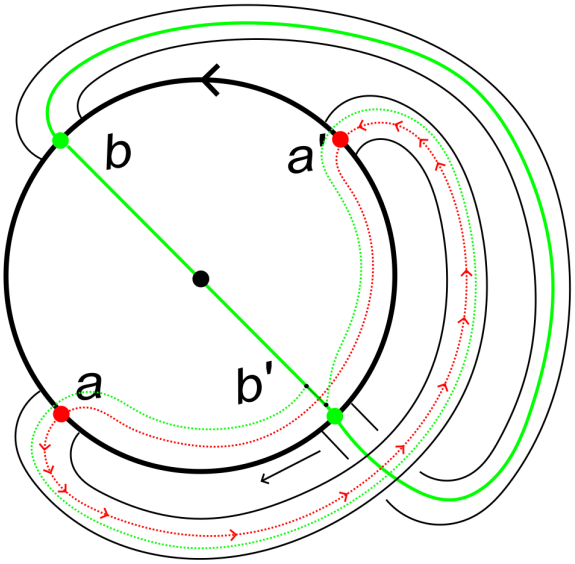

Figure 3.9: Realizing a Dehn twist of a punctured torus.

The proof makes use of the Alexander method, which roughly says that a diffeomorphism of S can be (partly) understood by looking at its effects on a collection of curves and arcs. It is briefly summarised below. For details, see Proposition 2.8 of [8].

Proposition 3.9. *(The Alexander method) Let S be an orientable surface, and let $\Phi \in \mathrm{Diff}(S, \partial)$. Fix a collection $\mathcal{C}$ of pairwise non-isotopic, essential, simple closed curves and simple, properly embedded arcs that fill S, meaning that the result of cutting along these curves and arcs is a disjoint union of disks and once-punctured disks, satisfying*

- *Curves in $\mathcal{C}$ are pairwise in minimal position, meaning that the geometric intersection number is realized.*
- *For distinct α, β and $\gamma \in \mathcal{C}$, at least one of $\alpha \cap \beta$, $\alpha \cap \gamma$ and $\beta \cap \gamma$ is empty.*

If Φ fixes all curves and arcs in $\mathcal{C}$ with orientations preserved, then Φ is isotopic to the identity.

Proof of Theorem 3.8. We compare the induced handle slide diffeomorphism $\Phi_{b' \to (a,a')}$ from sliding b' over the 1-handle specified by (a, a') and the Dehn twist T_l along l. First, observe that both diffeomorphisms can be arranged to have the same supports, namely a neighbourhood $N(l)$ of l away from the boundary of S. Note that $\Phi_{b' \to (a,a')}$ can be arranged to fix the boundary of S pointwise since the attaching region of b' is pushed

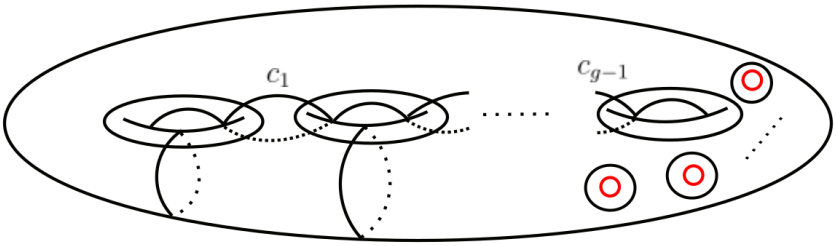

Figure 3.10: The Lickorish generators plus curves around each boundary component, as a collection of curves that fills S.

to its original position by the slides. We would like to apply the Alexander method to the composition $\Phi_{b'\to(a,a')} \circ T_l^{-1}$. We fix a collection $\mathcal{C}$ of essential, simple closed curves and simple, properly embedded arcs that *fill* S, meaning that the result of cutting along these curves and arcs is a disjoint union of disks and once-punctured disks, and satisfies the additional conditions as stated in Proposition 3.9 and Proposition 2.8 of [8]. Such a collection can always be found. For example, if the genus of S is g and if S has n boundary component, then it contains g holes and a puncture, so we can choose such a collection $\mathcal{C}$ by taking the Lickorish generators (see Section 4 of [8], namely by picking all meridians and longitudes of all holes, together with circles that go through consecutive holes, and circles separating the boundary components, as shown in Figure 3.10 for the case when S is a genus g surface with three boundary components. The boundary components are drawn as red circles. Each of the meridians and longitudes corresponds to a 1-handle determined by an ordered pair of points on the pointed circle as its core curve.

Let $\gamma \in \mathcal{C}$. Suppose that the (oriented) intersection number between γ and l is zero, then one can modify $\mathcal{C}$ by isotoping γ such that γ is disjoint from a neighbourhood of l. It follows that both T_l and $\Phi_{b'\to(a,a')}$ fix γ (see Proposition 3.2 of [8] for an argument for Dehn twists). If the intersection number between γ and l is non-zero, then one can again isotope γ if necessary such that it intersects a neighbourhood of l in minimal (cannot be reduced further), finitely many sub-arcs, with the two endpoints of each sub-arc contained in the two boundary components of $N(l) \cong I \times l$. In fact, one can further arrange for these sub-arcs to be parallel copies of $I \times \{pt\}$ in $N(l)$. Now, observe that $\Phi_{b'\to(a,a')}$ fixes the endpoints of each sub-arc but replaces a smaller piece of the interior of each sub-arc by an arc that twists along l once, since the sliding of b' drags it along l. But this is exactly

what a Dehn twist around l does. For example, in Figure 3.9, the short small sub-arc of the green solid curve determined by (b, b'), which is indicated by a short black interval, is mapped to the green dotted arc by both $\Phi_{b'\to(a,a')}$ and T_l. Now, by the Alexander method applied to $\Phi_{b'\to(a,a')} \circ T_l^{-1}$, we conclude that $\Phi_{b'\to(a,a')} \circ T_l^{-1}$ is isotopic to the identity which implies that $\Phi_{b'\to(a,a')}$ is isotopic to T_l. □

Remark. In fact, one can show that Theorem 3.8 is true in greater generality. In general, when there is more than one annotated point between (a, a'), one slides all these annotated points along the 1-handle specified by (a, a') to realize the Dehn twist along (a, a').

More generally, we can realize the entire mapping class groups.

Theorem 3.10. *Let S be an orientable surface (with or without boundary). Then there exists a handle structure of S such that for any embedded simple closed curve l in S, the Dehn twist T_l along l can be factored as a sequence of 1-handle slides starting and ending with isomorphic handle structures. Thus $\pi_0\mathrm{Diff}(S, \partial)$ are handle animation diffeomorphisms.*

Proof. If l is null homotopic, then T_l is isotopic to the identity map, thus we can take the empty sequence. Otherwise, T_l can be factored into a composition of Dehn twists along the Lickorish generators and boundary Dehn twists along the separating curves of the n boundary components, as shown in Figure 3.10. So it suffices to prove that there exists a handle structure such that all Lickorish generators can be realized by sequences of 1-handle slides.

Let n denote the number of boundary components of S, and let g denote the genus of S. We fix a handle decomposition of S that contains a 0-handle, $2g + n$ 1-handles, and a 2-handle. Denote the attaching spheres of the 1-handles by ordered labelled pairs of points

$$(x_1, x_1'), (x_2, x_2') \ldots, (x_{2g}, x_{2g}'), (y_1, y_1'), \ldots, (y_{2g}, y_{2g}'), (z_1, z_1'), \ldots, (z_n, z_n').$$

These are attached to the 0-handle in the following order

$$x_1, y_1, x_1', y_1', x_2, y_2, x_2', y_2' \ldots, x_g, y_g, x_g', y_g', z_1, z_1', \ldots, z_n, z_n'$$

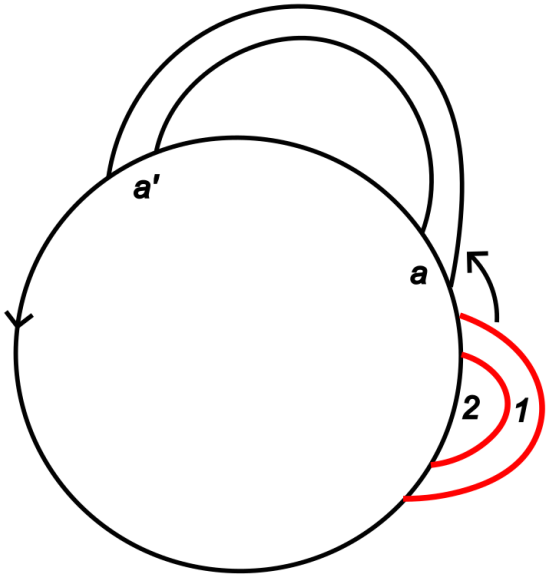

Figure 3.11: Realizing the mapping class group of the annulus.

with the 2-handle attached to the "big" boundary circle which has non empty intersection with all 1-handles. Figure 3.9 shows the 1-skeleton of this handle structure for S being a torus.

To realize a boundary Dehn twist along a separating curve of one of the n boundary components say (z_i, z_i'), we attach a 1-2 cancelling pair to this boundary circle (to the 0-handle of S) and slide the newly attached 1-handle over the 1-handle corresponding to (z_i, z_i') twice so that both feet are slid (with the newly attached 2-handle following), and finally cancel this pair. A primary example is the annulus, whose mapping class group is generated by the Dehn twist along its core curve. It has only one 1-handle, so we cannot recover the twist without adding cancelling pairs. See Figure 3.11. Another example is the pair of pants whose mapping class group has three free generators, each of which can be represented by attaching a 1-2 pair to each of the the corresponding boundary component, sliding this newly attached 1-handle around that boundary component with the 2-handle following, and finally cancelling the pair. Note that if we do not require that the boundary is fixed pointwise, then boundary Dehn twists are isotopic to the identity. We generally do require boundary to be fixed pointwise, and then we apply this requirement to each step in the composition realising a boundary Dehn twist..

Combining the above with Theorem 3.8, it remains to prove that Dehn twists along the Lickorish generators c_i (see Figure 3.10) for $i = 1, \ldots, g-1$ can be factored as sequences of 1-handle slides. This is illustrated in Figure 3.12, reading from the top to the bottom. This figure is meant to be a portion of S containing four 1-handles $(x_i, x_i'), (y_i, y_i'), (x_{i+1}, x_{i+1}')$ and (y_{i+1}, y_{i+1}') (which we relabelled as $(a, a'), (b, b'), (c, c'), (d, d')$) and the 0-handle of S. The red dotted curve in the top picture represents c_i. The Dehn twist along c_i is realized by first sliding b' over (c, c'), then c' over (b', b), then d over (b', b). then c over (b', b), a' over (b', b), and finally sliding b' over (c', c) to move it back to the original position. This sequence starts and ends with the same handle structure and realizes T_{c_1}. To see this, we apply the Alexander method again to the collection of curves that fill S shown in Figure 3.10. Except for the core curves determined by the four 1-handles $(x_i, x_i'), (y_i, y_i'), (x_{i+1}, x_{i+1}')$ and (y_{i+1}, y_{i+1}'), the remaining curves do not move under both the Dehn twist T_{c_i} along c_i and the above sequence of handle slides. Therefore, it suffices to show that the image of the core curves l_a, l_b, l_c and l_d determined by $(a, a'), (b, b'), (c, c'), (d, d')$ respectively under this sequence of slides coincide with the image of the same curves under the Dehn twist T_{c_i}. We illustrate the images of l_c and l_d along the sequence of handle slides in Figure 3.12, and the images of l_a and l_b can be obtained by symmetry. □

Remark. For orientable surfaces, level-preserving isotopies induce diffeomorphisms between isomorphic handlebodies, thus self-diffeomorphisms, that are isotopic to the identity.

Example 3.11. We describe an analogous case in dimension 3. We would like to realize the twist of a collar neighbourhood of the boundary torus of a solid torus. Denote the boundary torus of $D^2 \times S^1$ by $S^1_B \times S^1_R$. We take a collor neighbourhood $N = [-1, 1] \times S^1_B \times S^1_R$ and define a diffeomorphism of N by taking the product of the Dehn twist on $[-1, 1] \times S^1_R$ with the identity map on S^1_B. We extend it to a diffeomorphism of $D^2 \times S^1$ via the identity map. We denote this diffeomorphism by $\Phi_{S^1_R}$. We will describe a construction similar to what we did with the annulus in the previous example, by attaching a "*hula hoop*" (which we will describe below) to the boundary of the solid torus. The desired diffeomorphism induced by the Dehn twist will then realized by sliding the hula hoop around S^1_R.

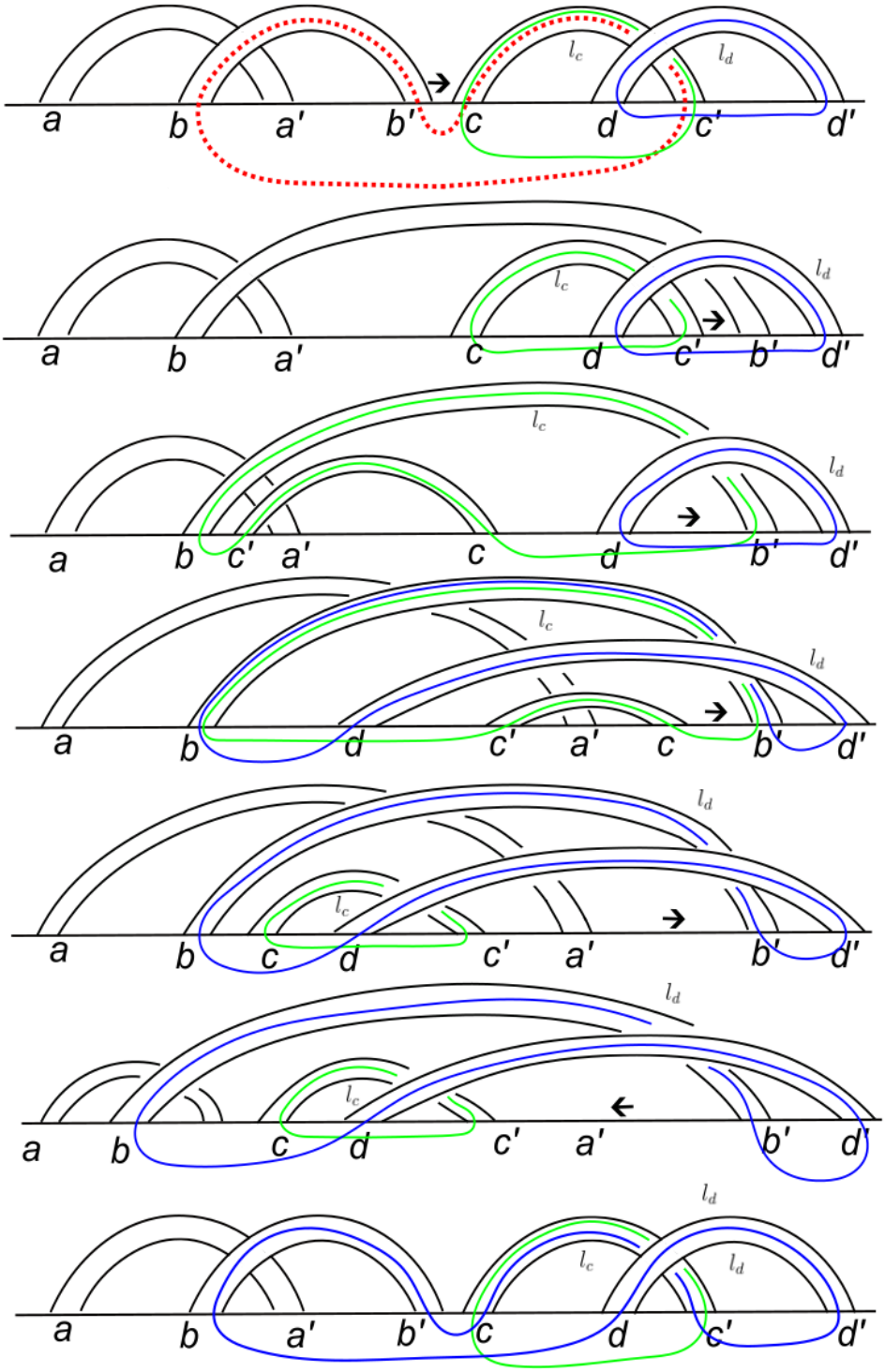

Figure 3.12: The Dehn twist along c_1 as a sequence of 1-handle slides.

We first give a handle structure to $S^1 \times D^2$. The standard decomposition of the annulus with one 0-handle and one 1-handle induces a product decomposition of the solid torus $S^1 \times D^2$ with one 0-handle and one 1-handle. From the last example, we see that an extra 1-2 pair is needed to realize the Dehn twist along the core circle of the annulus. The hula hoop is a general construction as follows.

Definition 3.12. For $n \geq 3$, the n-dimensional hula hoop is the n-manifold $S^1_1 \times \dots S^1_{n-2} \times D^2$ that admits the following product decomposition.

- The disk D^2 is decomposed as a 2-dimensional $1/2$-pair.
- Each circle S^1_i, $i \geq 1$ admits a standard decomposition as a 0-handle and a 1-handle.

In dimension 3, the hula hoop is the product of such a 2-dimensional 1-2 pair with S^1. The hula hoop itself with this decomposition is illustrated in Figures 3.13. It is attached to $S^B \times S^R$ as shown in Figure 3.14. Let $x_0 \in S^1_B$ be a fixed point, and let $a, b \in \{x_0\} \times S^1_R$ be two points that are close to each other. Attach a 1-handle to a neighbourhood of a and b in $S^1_B \times S^1_R$, and then attach a 2-handle to make a cancelling 1-2 pair, as indicated in Figure 3.14. Then we attach another 2-handle along the blue curve L. Finally, we attach a 3-handle to make a solid torus. It is diffeomorphic to a solid torus. In other words, we have attached two cancelling pairs, one 1-2 pair and one 2-3 pair. The 3-manifold $S^1 \times D^2$ with a hula hoop attached is shown in Figure 3.15 in terms of a Heegaard diagram. Note that B_1, B_2 specifies a 1-handle that cancels the 2-handle in the middle, and the 3-handle then cancels the remaining 2-handle, giving back $S^1 \times D^2$.

The Dehn twist along S^1_R is realized by sliding both feet of the 1-handle of the hula hoop over the original 1-handle in the solid torus, and going back to its original position. In Figure 3.15, this is done by sliding both B_1 and B_2 over A. As before, the rest of the higher dimensional handles will follow. To see this, we note that for each fixed point $x \in S^1_B$, the restriction of $\Phi_{S^1_R}$ to the slice $x \times S^1_R \times [-1, 1]$, which is an annulus, is given by the Dehn twist of along the core curve $x \times S^1_R \times 0$. We observe that sliding the hula hoop along the S^1_R direction realizes this Dehn twist in each slice by imagining cutting the hula

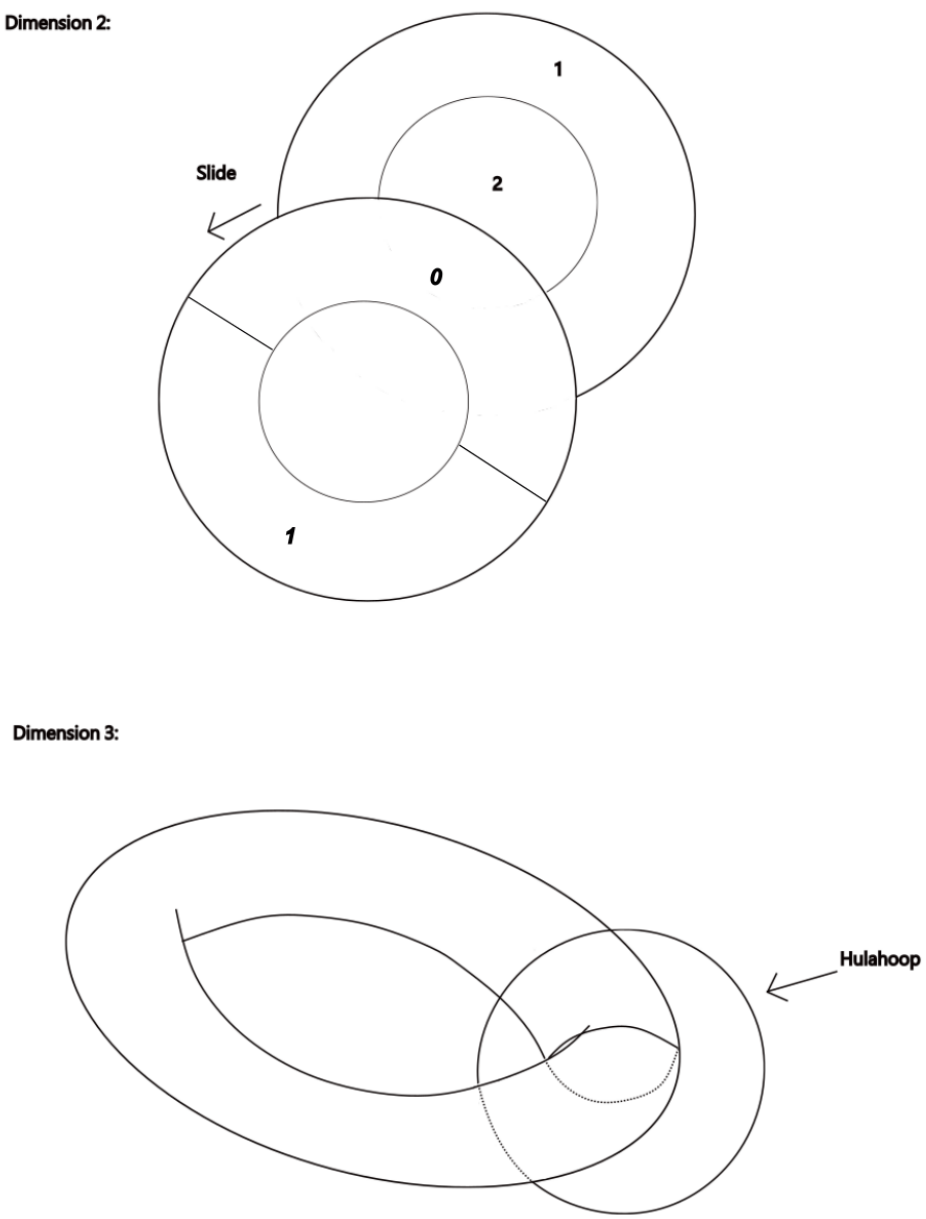

A comparison with dimension 2.

The hula hoop as two cancelling pairs.

Figure 3.13: The hula hoop construction.

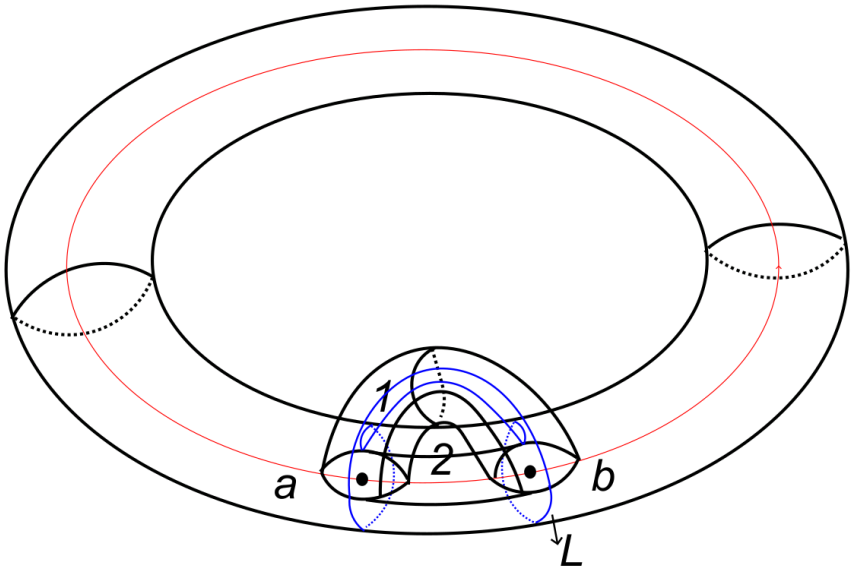

Figure 3.14: The 3-dimensional hula hoop attached to $S^1_B \times S^1_R$.

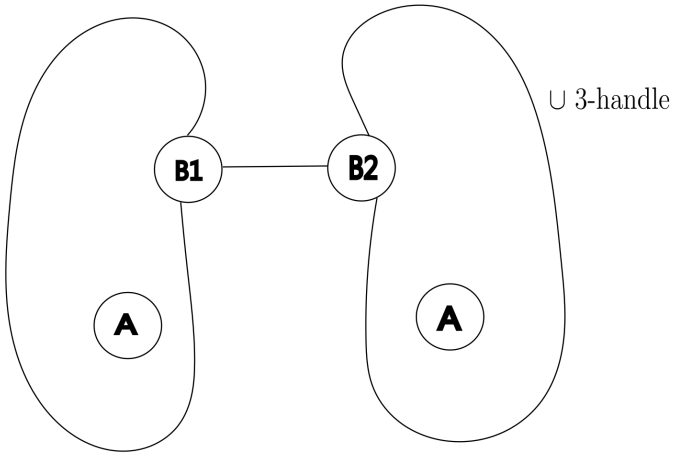

Figure 3.15: Solid torus with a hula hoop attached.

hoop into a S^1_B-parameter family of 2-dimensional 1-2 pairs, and applying the previous example.

Example 3.13. Consider the 3-manifold $M_k = \#_k S^1 \times S^2$, for $k \geq 1$ (cf. the discussion before Theorem 3.6). The manifold M_k can be constructed by removing $2k$ disjoint 2-spheres from S^3 and identifying the boundary in pairs. Thus it admits a handle structure with a 0-handle, k 1-handles, k 2-handles and a unique 3-handle. Alternatively, M_k can be viewed as the boundary of either $\natural_k S^1 \times D^3$ or $\natural_k S^2 \times D^2$. Here we think of it as the boundary of $\natural_k S^1 \times D^3$, which admits a handle structure that contains a 0-handle and k

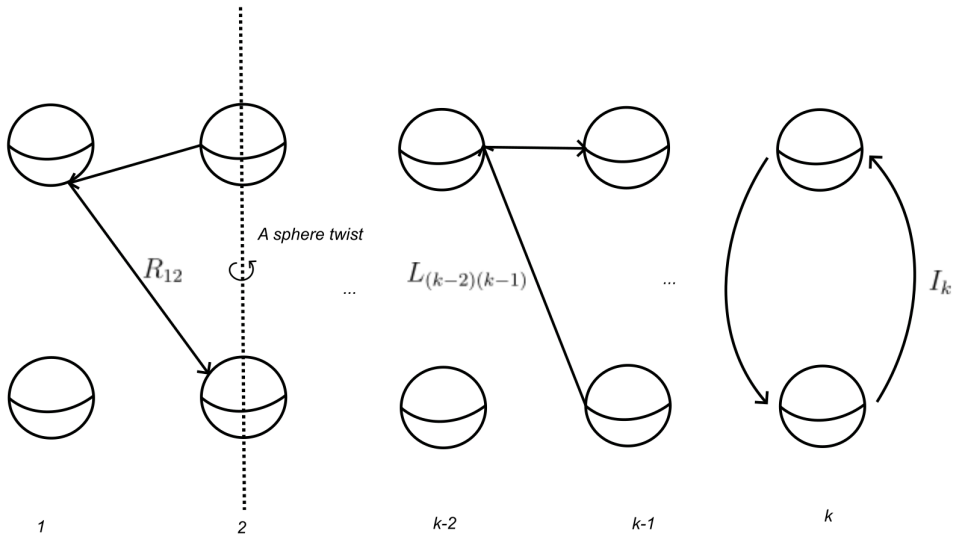

Figure 3.16: The manifold $\natural_k S^1 \times D^3$ and generators of the mapping class group of M^k.

1-handles as in Figure 3.16. We would like to realize the mapping class group of M_k by handle moves of 4-manifolds.

Recall that a sphere twist R_S of M_k around an embedded 2-sphere $S \subset M_k$ can be described by fixing a neighbourhood $U \cong S \times [0,1]$ of S and taking the diffeomorphism $U \to U$ defined by

$$(x, y) \to (r(y) \cdot x, y)$$

where $r\colon [0,1] \to SO(3)$ is a loop that rotates $\mathbb{R}^3$ about an axis by a full turn. The group of sphere twists $R(M_k) \cong (\mathbb{Z}/2)^k$ is generated by the twists about the core spheres (separating spheres) $\{*\} \times S^2$ in each of the k summands and is a normal abelian subgroup of $\pi_0\mathrm{Diff}(M_k)$. These can be described by rotating the corresponding pairs of 2-spheres (representing 1-handles) by 2π. More precisely, to realize the sphere twist around the i-th core (separating) sphere in M_k, we take a Kirby diagram of $\natural_k S^1 \times D^3$ as shown in Figure 3.16, and perform a level-preserving isotopy by rotating the i-th 1-handle by 2π. This gives rise to a self-diffeomorphism of $\natural_k S^1 \times D^3$ whose restriction to the boundary realizes the sphere twist we want.

Furthermore, the generators R_{ij} (again, cf. the discussion before Theorem 3.6) can be realized by dragging the top sphere (i.e. the top attaching region) of the i-th 1-handle and sliding it over the bottom sphere of the j-th 1-handle. Similarly, the generators L_{ij} can be

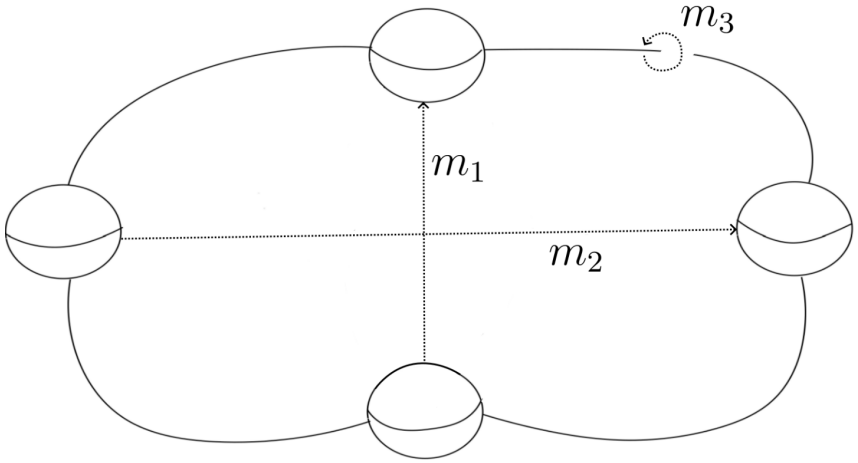

Figure 3.17: The Kirby diagram of $T^2 \times D^2$.

realized by dragging the top sphere (i.e. the top attaching region) of the i-th 1-handle and sliding it over the top sphere of the j-th 1-handle. Finally, the generators I_i are realized by exchanging the position of the two boundary points of the attaching sphere of the i-th 1-handle using an isotopy. These are shown in Figure 3.16.

We now turn to examples in dimension 4. We will look at barbell diffeomorphisms and Montesinos twin twists introduced in Chapter 2. Unless otherwise stated, all of our 2-handles in Kirby diagrams without framing numbers are 0-framed.

Example 3.14. We consider $T^2 \times D^2$ whose boundary is a 3-torus. There is a natural handle structure of $T^2 \times D^2$ defined by taking the natural handle structure of the torus (which contains a 0-handle, two 1-handles and a 2-handle, see Figure 3.9) and taking the product structure. In particular, it has one 0-handle, two 1-handles and one 2-handle. See Figure 3.17 for a Kirby diagram of $T^2 \times D^2$. The two meridians of the two 1-handles, and the meridian of the attaching circle of the 2-handle form 3 circles of the boundary 3-torus which we denote by m_1, m_2 and m_3 respectively.

We now describe Dehn twists along the boundary circles analogous to the hula hoop construction in Example 3.11. Take a collar neighbourhood $N = [-1, 1] \times m_1 \times m_2 \times m_3$ of $\partial(T^2 \times D^2)$. The boundary Dehn twist along m_i for $i = 1, 2, 3$ is the product of the Dehn twist on $[-1, 1] \times m_i$ with the identity maps on the other two circles. We would like to realize the twist along m_2. We attach a 4-dimensional hula hoop as defined in

Definition 3.12. The 4 extra cancelling pairs needed, as a 4-dimensional hula hoop, will be attached to a neighbourhood of $m_1 \times m_3$ in S^3. For each point in m_3, a 3-dimensional hula hoop is attached. The 4-dimensional hula hoop is diffeomorphic to $S^1 \times S^1 \times D^2$ and we decompose it into one 1-handle, three 2-handles, three 3-handles and one 4-handle by taking the product with the 3-dimensional hula hoop (cf. Figure 3.13). Figure 3.18 shows the handle diagram of $T^2 \times D^2$, not including the 3- and 4-handles, with this 4-dimensional hula hoop attached. The 2-handles are denoted by x, y, z and u.

The 3-handles are attached in the following way. The first 3-handle is attached to a neighbourhood of the obvious sphere determined by the region bounded by A, C and C', and the 2-handles z and y. In particular, this region is a 2-sphere with three boundary components, each of which bounds a disk in either z or y. This 3-handle cancels with the 2-handle z. The second 3-handle is attached to a neighbourhood of a 2-sphere determined by the 2-handles x, u and z and the 1-handles attaching regions A, C and C'. In particular, the path following x and u that is connected by A, C and C' defines a 2-sphere with 3 boundary components with each boundary component bounding a disk in a 2-handle. This 3-handle cancels with the 4-handle. Finally, the attaching region of the 3-handle that cancels u is indicated in the first picture of Figure 3.18 in blue. It is attached to a blue sphere as a result of gluing four pentagons (denoted by 1,2,3 and 4) together. Each pentagon has 3 edges on A, C and C', and three more edges on x, u and z. The four large pink arcs are internal in the four pentagons. One imagines that each pentagon, as a disk, is attached to the blue lines in the four regions, and contains one of the four pink arcs. Gluing them together gives rise to a 2-sphere with three holes, and each hole bounds a disk in a 2-handle.

The boundary Dehn twist along m_2 can now be realized by first sliding both feet of the new 1-handle (with attaching regions C and C') over B, then sliding one of the new 2-handles over the original 2-handle **twice** as denoted in the third diagram of Figure 3.18. This sequence of moves brings the diagram back to the starting position. As before, the higher dimensional handles (3- and 4-handles) get dragged along the way. In the end, we cancel the three cancelling pairs.

Note that in this example, although there are more than one (indeed two) 3-handles involved in our sequence of handle moves, we can keep tracking their attaching maps to see that they are identical in the starting and ending diagrams.

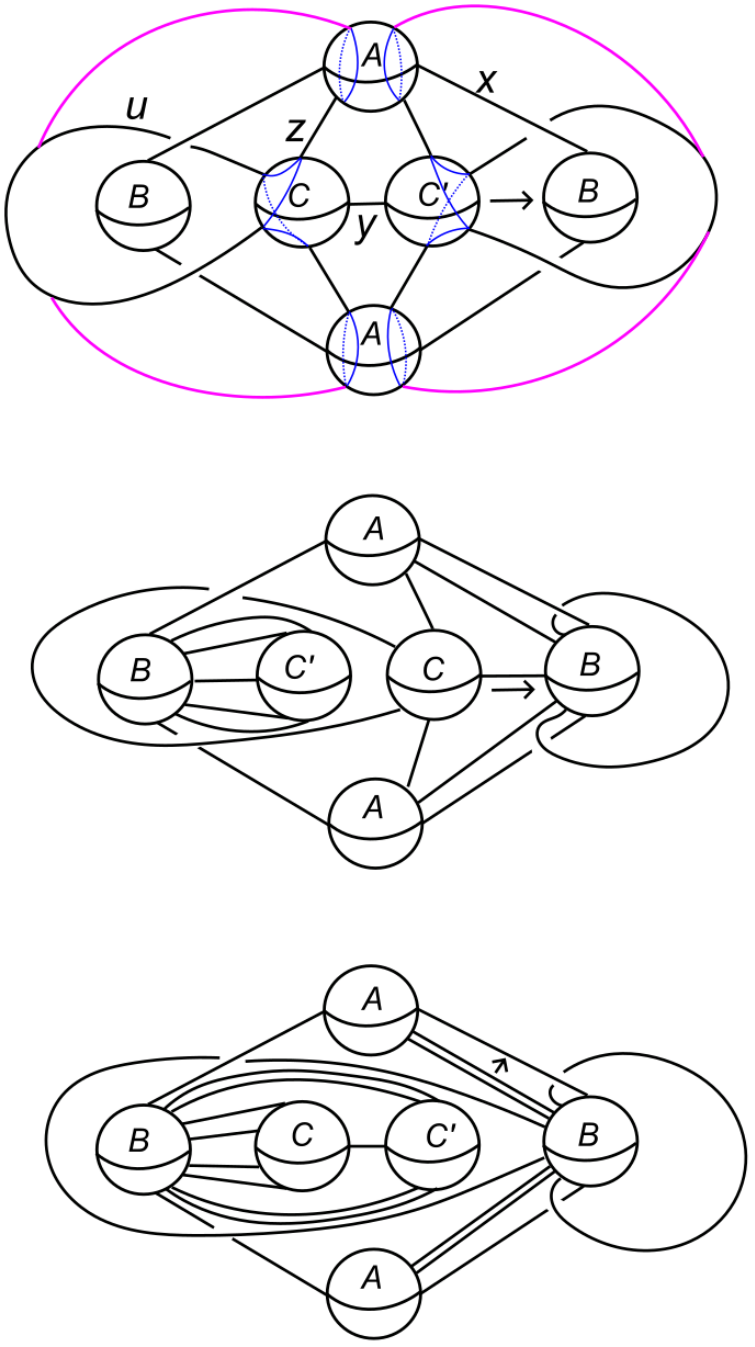

Figure 3.18: The twin twist along the boundary of $T^2 \times D^2$.

Example 3.15. Recall from Section 2.2 that a Montesinos twin twist Φ_W of a twin W embedded in a 4-manifold is supported in a collar neighbourhood of a 3-torus. Since Φ_W

is only non-trivial on a collar neighbourhood of the boundary 3-torus, there is not much difference between Φ_W along the boundary 3-torus of E^4 (cf. Figure 2.14) and boundary Dehn twists of $T^2 \times D^2$ discussed in the previous example. We just need to figure out the correspondence between the two collections of 3 boundary circles. To do this, we first put their handle diagrams in the same position by transferring them to dotted-circle notation. See the lower picture of Figure 3.19 for a Kirby diagram of E^4 with a hula hoop attached. The hula hoop is drawn (roughly) in the dotted box. The upper picture of Figure 3.19 is the same diagram in dotted circle notation. The manifold $T^2 \times D^2 \cup$ hula hoop can be obtained from the upper picture by replacing the 2-handle in the centre of the diagram (denoted by centre 2-handle in Figure 3.19) by a dotted circle. If we make this change, then we can pair Figures 3.17 and 3.18 with Figure 3.19 such that m_2 in Figure 3.17 corresponds to a meridian of the centre 2-handle in Figure 3.19. We can now observe that the twin twist restricting to a boundary collar neighbourhood of E^4 is the same as the boundary Dehn twist along m_2 of $T^2 \times D^2$ restricting to a boundary collar. We further observe that sliding both feet of a 1-handle over the 1-handle B in Figure 3.18 induces the same diffeomorphism of this collar neighbourhood as pushing the corresponding 1-handle in Figure 3.19 through the centre 2-handle. It follows that we can realize the twin twist by following the same process as in Example 3.14 and Figure 3.18 with the exception that we replace 1-handle slides over B by pushing the attaching regions of the corresponding 1-handle through the centre 2-handle. This realizes the Montesinos twin twist of E^4.

In fact, we can consider twins in other ambient 4-manifolds. For example, Figure 3.20 shows E^4 embedded in S^4 in a standard way, with two additional 3-handles and a 4-handle not drawn. To see how it is interpreted as a diagram of S^4, one starts with the top picture and performs two handle slides. Then the 1-handle cancels with the green 2-handle, leaving us the bottom picture which is an unlink which are then cancelled by two 3-handles, giving back to the standard Kirby diagram diagram of S^4. It follows that we can realize this twin twist as a diffeomorphism of S^4 using the previous paragraph. More generally, recall from Section 2.4 the unknotted twins $W(i)$ in S^4 proposed by Gay in [9]. We can draw Kirby diagrams of the pairs $(S^4, W(i))$. For example, a Kirby diagram of S^4

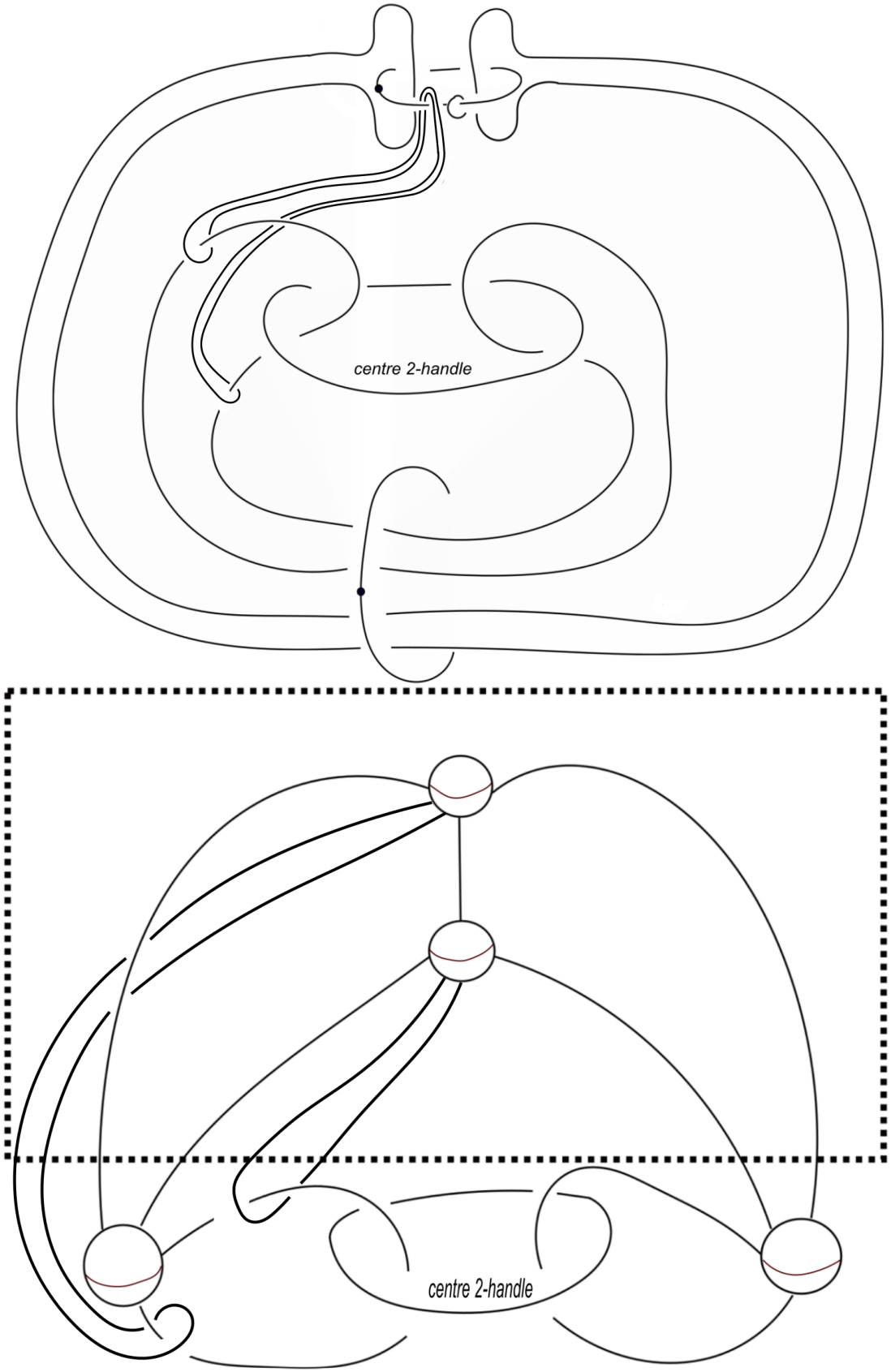

Figure 3.19: The twin twist along the boundary of E^4.

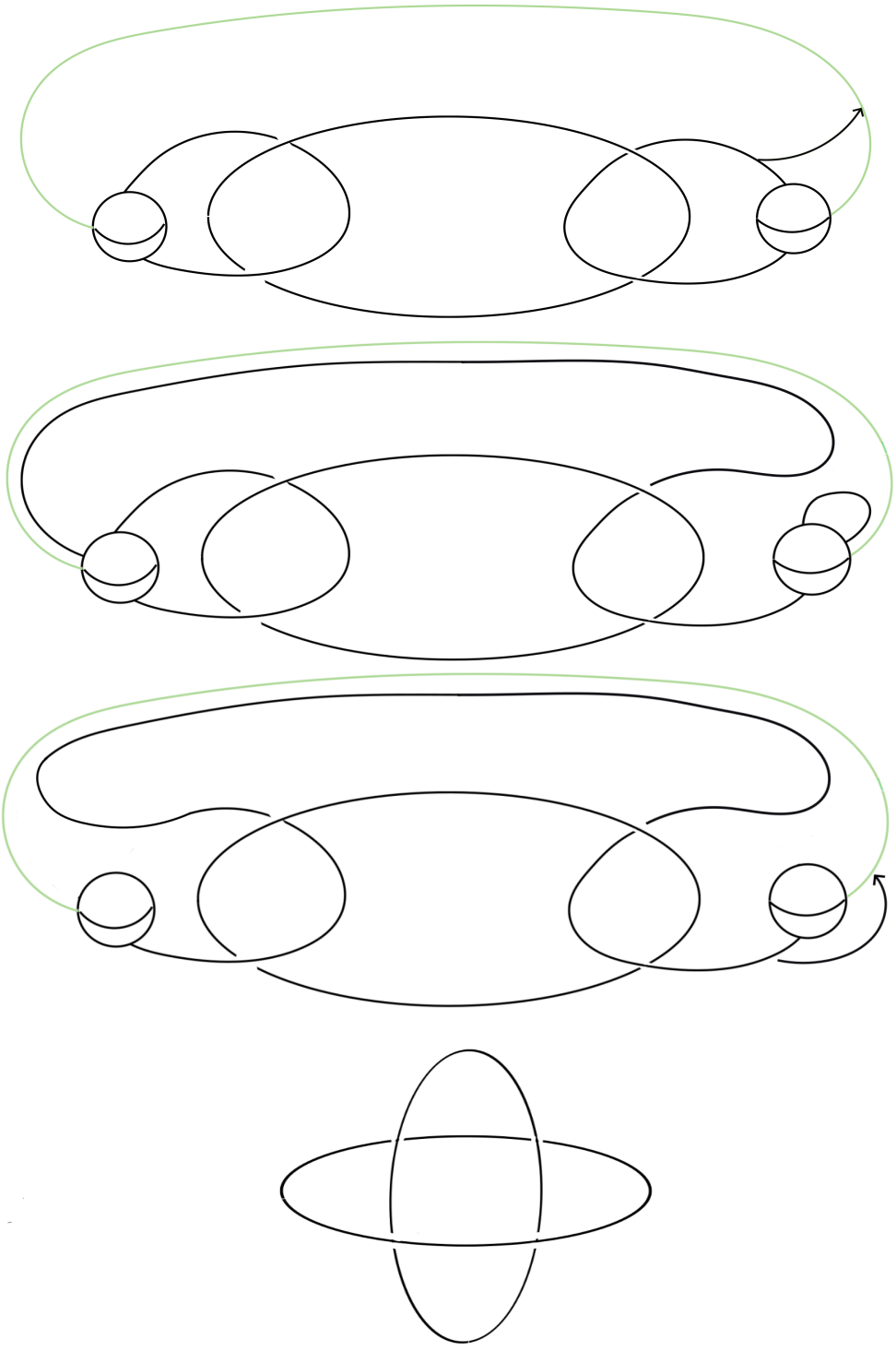

Figure 3.20: The standard Montesinos twin embedded in S^4.

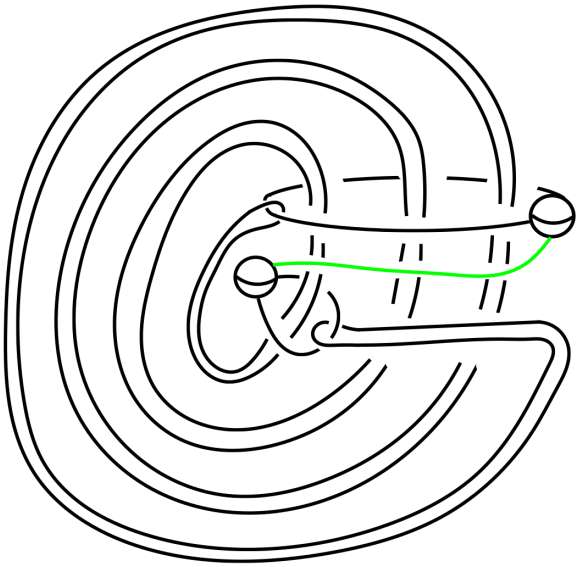

Figure 3.21: A Kirby diagram of the pair $(S^4, W(3))$.

with a neighbourhood of the twin $W(3)$ (cf. Figure 2.19) embedded in it is shown in Figure 3.21. As in the previous case, the green 2-handle makes sure this diagram represents S^4. We call Figure 3.21 a diagram of the pair $(S^4, W(3))$. Therefore, we can attach a hula hoop to such diagrams to realize the induced twin twist $\Phi_{W(i)}$. Combining with Theorem 2.12 and Theorem 2.13, we have the following theorem.

Theorem 3.16. *For any element in the subgroup $\mathcal{M}_0$ of $\pi_0\mathrm{Diff}(S^4)$ generated by half-unknotted Montesinos twin twists, there exists a handle structure σ of S^4 such that this element is realized by a sequence of Kirby diagrams starting and ending with the same diagram representing σ, connected by handle moves. The same is true for the subgroup $\mathcal{B}_0$ generated by half unknotted barbell diffeomorphisms.*

Example 3.17. We now recall a barbell manifold embedded in S^4 proposed by Budney–Gabai as shown in Figure 3.22. To draw a Kirby diagram of it, it is helpful to think of it as a pair (S^4, E^4), i.e. we consider the induced twin from this barbell built by pushing one cuff along the bar and performing a finger move near the other cuff as discussed in Section 2.3. We start from a diagram that contains an unlink, which represents the connected sum of two copies of $S^2 \times D^2$. Each unknot represents a 2-handle that gives rise to a copy of the 2-sphere which consists of the obvious disk in the 0-handle and a 2-disk contained

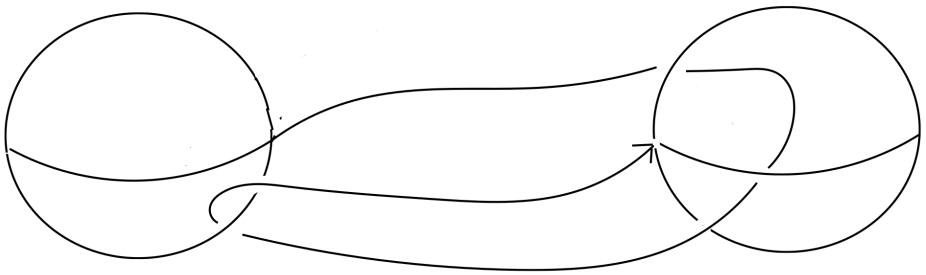

Figure 3.22: Conjecturally non-trivial barbell $\mathcal{B}_{yx}$ in S^4.

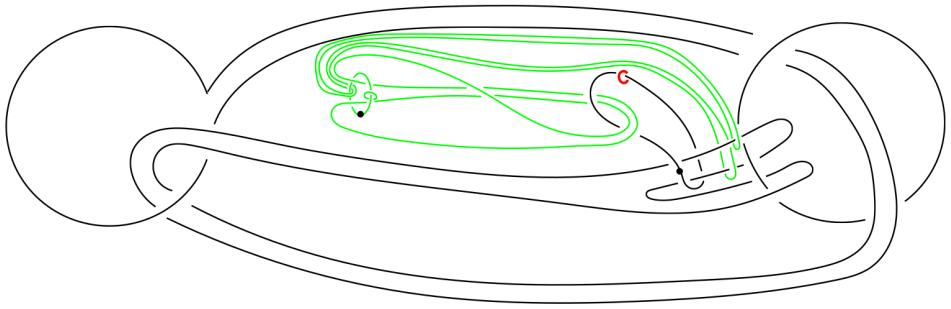

Figure 3.23: A Kirby diagram of the pair $(S^4, \mathcal{B}_{yx})$ with a hula hoop attached.

in the 2-handle. To build the twin, we push a small sub-arc of an unknot along the bar to make a finger move near the other, and lock it up by a dotted circle. Finally, add a meridian 2-handle (drawn in red) to cancel everything. See Figure 3.23. To recover the barbell, we take the obvious Whitney disk going over the dotted circle and resolve the two intersection points. Finally, add a meridian 2-handle to cancel everything. See Figure 3.23.

To realize the twin twist along this twin (hence the corresponding barbell diffeomorphism), we observe that Figure 3.23 and the upper part of Figure 3.19 (with the hula hoop removed) have a lot in common. In fact, if we remove the meridian 2-handle (drawn as a small red circle) from Figure 3.23, then it becomes a manifold with boundary a 3-torus just as E^4. Therefore, we can attach a hula hoop as before (drawn in green in Figure 3.23) and follow the same process.

We can also consider embedded barbells in $S^1 \times D^3$. We start by taking the simplest diagram of $S^1 \times D^3$, namely one 1-handle (two 2-spheres) put in the vertical direction. Figure 3.24 is an example of the barbell used by Budney–Gabai that generates non-trivial

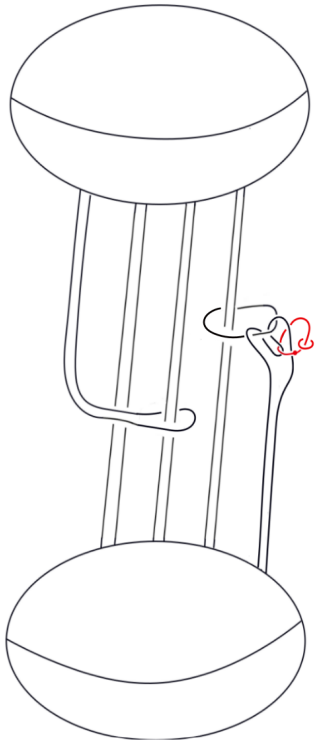

Figure 3.24: Budney-Gabai's barbell in $S^1 \times D^3$.

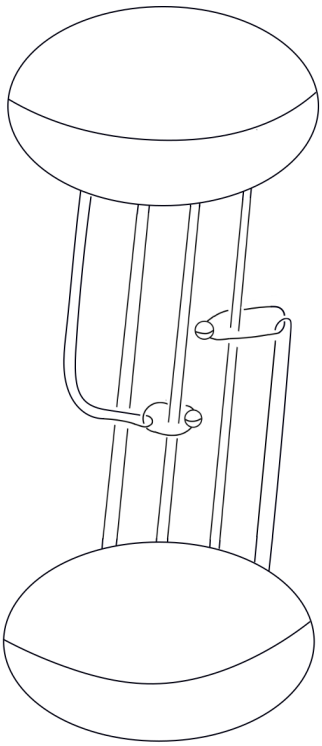

Figure 3.25: A modified twin based on Budney–Gabai's barbell in $S^1 \times D^3$.

diffeomorphisms of $S^1 \times D^3$. We twist several times the bar along the S^1 coordinate of $S^1 \times D^3$, i.e. we push it through the 1-handle of $S^1 \times D^3$, (here we abuse our notation and use a mixture of dotted circle notation and sphere notation). Again, we add a small meridian to the dotted circle and when it cancels one easily recovers $S^1 \times D^3$. Similarly, this barbell diffeomorphism can also be realized as before as a twin twist using a sequence of handle moves.

To end this section, we describe a Montesinos twin for which we cannot determine if it is originated from an embedded barbell. Figure 3.25 shows a twin where the two transverse intersection points appear at the linking of the 'long' circle with the 2-handle appearing as two half circles. It's not obvious to the author if one can find a Whitney disk for this pair of intersection points which would transfer this twin into a barbell manifold.

Chapter 4

Budney–Gabai's W_3 invariant and computations

Budney–Gabai [3,4] defined a rational homotopy invariant called W_3 on $\pi_0\mathrm{Diff}(S^1 \times D^3, \partial)$ and used it to detect isotopically non-trivial diffeomorphisms of $S^1 \times D^3$. In this chapter, we recall their construction and then discuss some extensions of their calculations.

4.1 The Fulton-MacPherson compactification of configuration spaces and the mapping space model

In this section, we briefly introduce the Fulton-MacPherson compactification of configuration spaces of manifolds, following [24] and [25]. We will need this notion in the definition of the W_3 invariant. However, we will mostly present the results and properties we need and will omit proofs. In the end of this section, we introduce the **mapping space model** due to D.Sinha in [25] about the space of properly embedded intervals with fixed endpoints in a 4-manifold M. This will be important for the construction of the W_3 invariant. For readers who are already familiar with these notions, this section serves the purpose of setting up our notations.

Given a manifold M embedded in some Euclidean space $\mathbb{R}^{N+1}$, we use $C_n(M)$ to denote the n-th ordered configuration space of M, i.e. the space of ordered, distinct n-tuples of

points in M. We define the Fulton-MacPherson compactification of this configuration space of M by $C_n[M] = \mathrm{Bl}_\Delta M^n$, i.e. the blow-up along the fat diagonal (the subspace in which at least two points coincide). We will now introduce the precise definition in a manageable way. We set up some notations before introducing it.

- For $m, n \geq 1$, let $C_m(n)$ be the space of ordered m-tuples of distinct points in the indexing set $\{1, 2, \ldots, n\}$. Note that $C_m(n)$ is empty if $m > n$.
- For $(i, j) \in C_2(n)$, let $\pi_{ij} \colon C_n(M) \to S^N$ be the map that sends $(x_i) \in M^n \subset (\mathbb{R}^{N+1})^n$ to the unit vector in the direction of $x_i - x_j$.
- For $(i, j, k) \in C_3(n)$, let $s_{ijk} \colon C_n(M) \to [0, \infty]$ be the map that sends (x_i) to $(|x_i - x_j|/|x_i - x_k|)$.
- Let $A_n[M]$ be the product $M^n \times (S^N)^{C_2(n)} \times [0, \infty]^{C_3(n)}$.
- Define $\alpha_n \colon C_n(M) \to A_n[M]$ to be the product $\mathrm{Inc} \times (\pi_{ij}) \times (s_{ijk})$ where $\mathrm{Inc} \colon C_n(M) \to M^n$ is the natural inclusion.

Then $C_n[M]$ is defined as the closure of the image of $C_n(M)$ in $A_n[M]$. We summarize some of the important properties of $C_n[M]$ following the first few sections of [25].

- The homeomorphism type of $C_n[M]$ is independent of the embedding of M in $\mathbb{R}^{N+1}$.
- If M is compact, then $C_n[M]$ is compact.
- The inclusion $\mathrm{Inc} \colon C_n(M) \to M^n$ factors through a surjective projection $C_n[M] \to M^n$.
- An embedding $f \colon M \to N$ induces a map $\mathrm{ev}_n(f) \colon C_n[M] \to C_n[N]$ extending the natural induced map on $C_n(M)$.
- $C_n[M]$ is a manifold with corners with $C_n(M)$ as its interior, equipped with a preferred stratification structure.
- The inclusion $C_n(M) \to C_n[M]$ is a homotopy equivalence.

Example 4.1. For $M = I$, the space $C_2[I]$ is a union of two triangles. More generally, $C_n[I]$ is a disjoint union of n-simplices, having one component for each ordering of n points.

For us, a **stratification** of a space X is a collection of disjoint subspaces $\{X_c\}$ called strata, such that the intersection of the closures of any two strata is the closure of some stratum. There is a preferred stratification structure of $C_n[M]$ that can be defined combinatorially in the following way.

Definition 4.2. Let Φ_n denote the category of rooted, connected **trees**, with n leaves labelled by $1,\ldots,n$, and with no bivalent internal vertices. Each tree admits a natural orientation when a root vertex is fixed by defining the direction pointing away from the root as positive. For T and $T' \in \Phi_n$, there is a unique morphism between T and T' if they are isomorphic up to contraction of some non-leaf edges. Two leaves are called **root-joined** if the unique paths to the root vertex intersect only at the root vertex.

Definition 4.3. Given a set S, an **exclusion relation** R is a subset of $C_3(S)$ satisfying

- if $(x, y, z) \in R$, then $(y, x, z) \in R$ and $(x, z, y) \notin R$;
- if $(x, y, z) \in R$ and $(w, x, y) \in R$, then $(w, x, z) \in R$.

The collection of all exclusion relations of S is denoted by $\mathrm{Ex}(S)$.

Definition 4.4. A **parenthesization** of a set S is a collection of nested subsets of S with each of them having cardinality greater than one.

There exists a map from $\mathrm{Ex}(n)$ of the indexing set $\{1, 2, \ldots, n\}$ to the collection of parenthesizations of the same set. For $R \in \mathrm{Ex}(n)$, this is given by taking the following sets.

- $A_{\sim i,\neg k}$ that contain all j such that (i, j, k) is in R and also i if such a j exists.

Definition 4.5. For a parenthesization P of $\{1, 2, \ldots, n\}$ given by a collection $\{A_\alpha\}$ of nested subsets, there is a tree $T(P) \in \Phi_n$ defined in the following way:

- Each A_α gives an internal vertex v_α.

- There is an edge between v_α and v_β if $A_\alpha \subset A_\beta$ but there are no proper inclusions $A_\alpha \subset A_\gamma \subset A_\beta$.
- A root vertex with edges connecting it to all internal vertices corresponding to maximal A_α.
- Leaves (i.e. vertices without edges with positive orientation) with an edge connecting the i-th leaf to either the vertex v_α where A_α is the minimal set containing i, or to the root vertex if no such A_α exists.

For $x = (x_i, u_{ij}, d_{ijk}) \in C_n[M]$, we can define an exclusion relation $R(x) \in \mathrm{Ex}(n)$ by letting $(i,j,k) \in R(x)$ if $d_{ijk} = 0$. Then Definition 4.5 gives rise to a tree denoted by $T(x)$. For $T \in \Phi_n$, let $C_T(M)$ denote the space of points $x \in C_n[M]$ such that $T(x) = T$ and let $C_T[M]$ be its closure. This defines a stratification of $C_n[M]$ (see Section 3 of [25]).

We will also make use of another space $C'_k[M]$, defined as the pullback of the k-fold product of the unit tangent bundle of M to $C_k[M]$. Intuitively, it contains points decorated with tangent vectors. It is equipped with a natural stratification induced from the one on $C_k[M]$. The following diagram describes their relationship.

$$\begin{array}{ccc} C'_k[M] & \longrightarrow & (STM)^k \\ \downarrow & & \downarrow \\ C_k[M] & \longrightarrow & M^k \end{array}$$

There is one more variant of $C_n[M]$ as intorduced in [3, 4, 25] that is involved in Budney–Gabai's invariants. Define $C_n(M, \partial)$ as the subspace of $C_{n+2}(M)$ such that the first and last points are fixed (and distinct) points x_0 and x_1 in the boundary of M. The compactification of $C_n(M, \partial)$, denoted by $C_n[M, \partial]$, is defined as the closure of the image of the map

$$\mathrm{Inc} \times (\pi_{ij}) \times (s_{ijk}) \colon C_{n+2}(M) \to A_{n+2}[M]$$

restricting to the subdomain $C_n(M, \partial)$. Similarly, there is a space $C'_n[M, \partial]$ defined as the subspace of $C'_{n+2}[M]$ that maps down to $C_n[M, \partial]$. This will be the setup we are going to

make use of in the coming sections (and chapters).

There is a stratification on $C_n[M, \partial]$, hence on $C'_n[M, \partial]$ defined in a similar way as in Definition 4.5 using a (full) subcategory Φ'_n of Φ_n. This subcategory contains trees whose roots have valence at least 2 and such that each set of leaves over the same vertex is **consecutive** for all non-root vertices, meaning that if the indices i and j are leaves over the same vertex, then $i < k < j$ implies that k is also a leaf over this vertex. Here, a leaf is said to be **over** a vertex if this vertex is contained in the unique path from the leaf to the root.

From now on, we will work with the **linearly ordered component** of $C'_n[I, \partial]$ for which the order of the points in the configuration agrees with the order they occur in the interval, and with all vectors pointing to the positive direction. We still use the same notation $C'_n[I, \partial]$, but the reader should keep in mind that equivalent constructions can be performed in other components as well.

Example 4.6. Consider $C_2[I, \partial]$ as the closure of the image of the map

$$\mathrm{Inc} \times (\pi_{ij}) \times (S_{ijk}) \colon C_4[I] \to A_4[I]$$

restricting to $C_2(I, \partial) = \{(0, x, y, 1) \colon 0 < x < y < 1\}$ where we restrict to one component only. This space can be parameterized in the following way:

- The interior contains points with $0 < x < y < 1$.
- Three boundary faces $0 < x = y < 1$, $x = 0$ and $y = 1$.
- Two extra faces denoted by $x = y = 0$ and $x = y = 1$.

Following the bijection $\mathcal{F}_4$, we list the largest subset in each of the corresponding parenthesizations:

- The interior corresponds to $\{1, 2, 3, 4\}$.
- The three (standard) boundary faces (with the vertices removed) correspond to $\{2, 3\}$, $\{1, 2\}$ and $\{3, 4\}$.

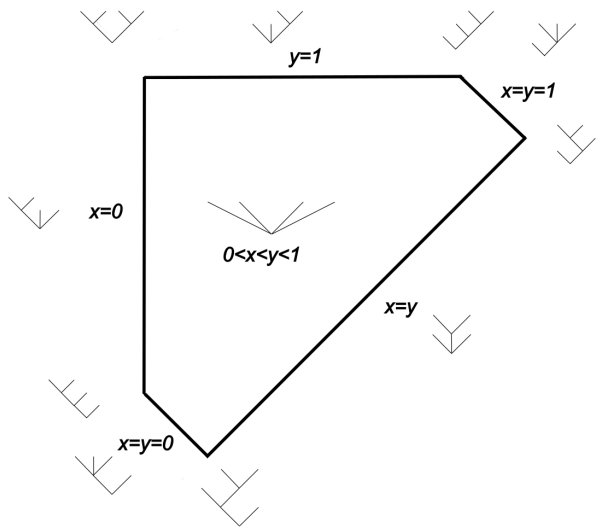

Figure 4.1: The space $C_2[I, \partial]$ as the fourth Stasheff polytope with trees annotated.

- The two extra faces correspond to $\{1, 2, 3\}$ and $\{2, 3, 4\}$.
- The vertex $x = 0, y = 1$ corresponds to two sets $\{1, 2\}$ and $\{3, 4\}$.

  It is parameterized by the fourth Stasheff polytope as shown in Figure 4.1. The corresponding trees at different strata are also shown in Figure 4.1. In fact, the $(n+2)$-th Stasheff polytopes also parameterize higher-dimensional compactifications $C_n[I, \partial]$. Reader can refer to Theorem 4.19 of [25] for details.

Definition 4.7. Let $x = (x_i, v_i) \times (u_{ij}) \times (s_{ijk}) \in C'_T[M, \partial]$ where $v_i \in T_{x_i}M$. Then x is called **aligned** with respect to T if for all i and j that are not root-joined (thus we have $x_i = x_j$), we have $v_i = v_j$ and u_{ij} is the image of v_i under the Jacobian of the embedding of M in $\mathbb{R}^N$. The subspace of aligned points is called the aligned sub-stratum and is denoted by $C^\alpha_T[M, \partial]$.

Definition 4.8. A map $f\colon C'_n[I, \partial] \to C_n[M, \partial]$ that respects the substratification by aligned points, meaning that $C^\alpha_T[I, \partial]$ gets mapped to $C^\alpha_T[M, \partial]$, is called **stratum-preserving and aligned**.

With the preparations so far, we can now state the **mapping space model** due to D. Sinha in [25] that helps understanding of the space $\mathrm{Emb}(I, M)$ of properly embedded intervals with fixed endpoints. For a compact manifold M, the embedding cal-

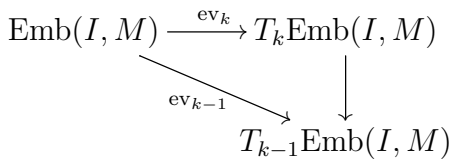

Figure 4.2: The embedding calculus tower.

culus tower of Goodwillie–Weiss (see [27]) provides an approximation of the space of smooth embeddings of the interval in M as shown in Figure 4.2. The maps ev_k are called the k-th **evaluation maps**. The space of aligned stratum-preserving maps is denoted by $\mathrm{Map}(C'_n[I,\partial], C'_n[M,\partial])$ and is weakly homotopy equivalent to the n-th element $T_n\mathrm{Emb}(I,M)$ in the tower of embedding calculus, as long as the dimension of M is 4 or greater.

Furthermore, the composition of this (weak) homotopy equivalence with the k-th evaluation map (which we still denote by ev_k) is given by sending f to the map $(x_1, x_2, \ldots, x_n) \mapsto (f(x_1), \ldots, f(x_n), f'(x_1), \ldots, f'(x_n))$ with $f'(x_1) = f'(x_2) = \cdots = f'(x_n) = 1$ since they are unit-normalized. Note that we omit the tangent vectors in $C'_n[I,\partial]$ as they are all positive.

4.2 Definitions and construction

In this section, we recall the construction of the W_3 invariant defined by Budney–Gabai in [3] and [4]. We will define a homomorphism

$$W_3 \colon \pi_0\mathrm{Diff}(S^1 \times D^3, \partial) \to \pi_2\mathrm{Emb}(I, S^1 \times D^3; I_0) \to \pi_5 C'_3[S^1 \times D^3] \otimes \mathbb{Q}$$

as a composition of two maps.

We start by defining the first map called the **scanning map**

$$s_{s_0} \colon \pi_0\mathrm{Diff}(S^1 \times D^3, \partial) \to \pi_2\mathrm{Emb}(I, S^1 \times D^3; I_0).$$

The manifold $S^1 \times D^3$ is naturally diffeomorphic to $S^1 \times I \times I \times I$ by embedding D^3

in $\mathbb{R}^3$ as the standard cube $[-1,1]^3$. Pick a point $s_0 \in S^1$, and let $I_0 = s_0 \times I \times 0 \times 0$ be our base point for $\mathrm{Emb}(I, S^1 \times D^3; I_0)$. For an element $[\Phi] \in \pi_0\mathrm{Diff}(S^1 \times D^3, \partial)$ represented by a difeomorphism Φ of $S^1 \times D^3$, we connect the end points of the images $\Phi(s_0 \times [-1,1] \times x \times y) \subset S^1 \times I \times I \times I \cong S^1 \times D^3$ with the endpoints of $I_0 = s^0 \times I \times 0 \times 0$ by straight arcs in the boundary faces $s_0 \times 0 \times I \times I$ and $s_0 \times 1 \times I \times I$, and by varying x and y, and naturally translating each $\Phi(s_0 \times [-1,1] \times x \times y)$ so that its endpoints coincide with the endpoints of I_0, to obtain an element $s([\Phi]) \in \pi_2\mathrm{Emb}(I, S^1 \times D^3; I_0)$. In other words, we make use of two of the three intervals to get a double loop of embedded intervals. An isotopy of Φ induces homotopies of the image $\Phi(s_0 \times [-1,1] \times x \times y) \subset S^1 \times I \times I \times I \cong S^1 \times D^3$ relative to the boundary faces. Therefore, the map s is well-defined up to isotopy.

We now define the second map, which will be denoted by

$$\overline{ev}_3 \colon \pi_2\mathrm{Emb}(I, S^1 \times D^3; I_0) \to \pi_5 C'_3[S^1 \times D^3] \otimes \mathbb{Q}.$$

This will make use of the mapping space model and involves of the second and third stages of the embedding calculus tower.

We start with analyzing the second stage. As discussed in the end of the previous section, the k-th element of the embedding calculus tower $T_k\mathrm{Emb}(I, S^1 \times D^3)$ can be modelled by stratum-preserving, aligned maps $C'_{k+2}[I, \partial] \to C'_{k+2}[S^1 \times D^3, \partial]$. For $[f] \in \pi_2\mathrm{Emb}(I, S^1 \times D^3; I_0)$ represented by a map

$$f \colon S^n \to \mathrm{Emb}(I, S^1 \times D^3; I_0)$$

we have an induced aligned, stratum-preserving map:

$$ev_2(f) \colon S^n \times C'_2[I, \partial] \to C'_2[S^1 \times D^3, \partial].$$

The space $C_2[I]$ is a truncated triangle (see Figure 4.1) with two vertices blown up into two extra edges denoted by $x = y = 0$ and $x = y = 1$. On these faces, the map $ev_k(f)$ gives a constant interval which is the image of I_0. Therefore, it is enough ignore the fixed

first and last coordinates and view this map as a stratum-preserving, aligned map

$$f\colon S^n \times C_2[I] \to C_2'[S^1 \times D^3].$$

In practice, as Budney–Gabai indicated in [3], it is often helpful to just think of $C_{k+2}'[M, \partial]$ as $C_k'[M]$ but keep in mind that extra stratification information is encoded to make sure the spaces have the correct homotopy types.

For a stratum-preserving, aligned map $f\colon S^1 \times C_2[I] \to C_2'[S^1 \times D^3]$, we will construct a map

$$\overline{ev}_2(f)\colon S^3 \to C_2'[S^1 \times D^3]$$

referred as the closure map of $ev_2(f)$. By the aligned and stratum-preserving property, the restriction of f to each of the 3 edges $t_1 = t_2$, $t_1 = 0$ and $t_2 = 1$ has codomain diffeomorphic to $C_1'[S^1 \times D^3]$ which is diffeomorphic to $S^1 \times D^3 \times S^3$. In particular, such a restriction gives a map $S^1 \times C_1[I] \to S^1 \times D^3 \times S^3$. For each $x \in S^1$, gluing $x \times C_1[I]$ with I_0 along the endpoints gives rise to an element in $\Omega_1(S^3)$ (their endpoints coincide because of the aligned and stratum-preserving property). Varying the value of $x \in S^1$ and doing the above at the same time leads to an element in $\pi_1\Omega_1(S^1 \times D^3 \times S^3) \cong \pi_2 S^3 = 0$. Therefore, these restrictions are null homotopic. Attaching null homotopies to f along the edges gives rise to a map $D^3 \to C_2'[S^1 \times D^3]$ which is constant on the boundary, i.e. this is an element in $\pi_3 C_2'[S^1 \times D^3]$. These null homotopies can be constructed through the following Proposition mentioned in Ryan Budney's talk at Glasgow [2].

Proposition 4.9. *Let $f\colon S^n \times C_2[I] \to C_2'[S^1 \times D^3]$ be an aligned stratum-preserving map with $n \geq 1$. The restriction of f to the boundary facets of $C_2[I]$ is null homotopic.*

Proof. For $f\colon S^n \times C_2[I] \to C_2'[S^1 \times D^3]$, we lift it to the universal cover $F\colon S^n \times C_2[I] \to \overline{C_2'[S^1 \times D^3]} \subset C_2'[\overline{S^1 \times D^3}]$. This map can be thought of as a map $(p, t_1, t_2) \to (q_1, q_2, v_1, v_2)$ where $p \in S^n$, and v_1 and v_2 are the corresponding velocity vectors. The points q_1 and q_2 are points in $\mathbb{R} \times D^3$. Along the $t_1 = t_2$ facet, as t_1 approaches t_2, the velocity vectors agree with the direction of the collision, as given by $\lim_{t_1 \to t_2} \frac{q_2 - q_1}{t_2 - t_1}$. The map

$(q_1, q_2, \frac{q_2-q_1}{t_2-t_1}, \frac{q_2-q_1}{t_2-t_1})$ defines an extension to the entire triangle, and the restrictions to the $t_1 = 0$ and $t_2 = 1$ facets can be straight-line homotoped to constant maps since they point to convex spaces (actually half spaces). Similarly, as t_1 approaches 0, the corresponding vector is given by the formula $\lim_{t_1\to 0}\frac{f(t_2+t_1)-q_2}{t_1}$ which also defines an extension to the entire triangle. In addition, the restriction to the other two edges $t_1 = t_2$ and $t_2 = 0$ can be homotoped to the constant map by straight-line homotopies.

The null homotopy for the edges $t_1 = 0$ and $t_2 = 1$ can be constructed in a similar manner. We give details for the $t_1 = 0$ edge to illustrate this, and a null homotopy for the $t_2 = 1$ edge can be constructed using the same idea. The restriction of a map $f\colon S^n \times C_2[I] \to C_2'[S^1 \times D^3]$ to the edge $t_1 = 0$ is given by

$$(p, 0, t_2) \longmapsto (f_p(0), f_p(t_2), \lim_{t_1\to 0}\frac{f_p(t_1) - f_p(0)}{t_1}, v_2).$$

As before, we define an extension of it to the remaining part of the triangle:

$$(p, t_1, t_2) \longmapsto (f_p(t_1), f_p(t_2), \frac{f_p(t_1) - f_p(0)}{t_1}, v_2).$$

On the $t_1 = t_2$ edge, this map is given by:

$$(p, t_2, t_2) \to (f_p(t_2), f_p(r_2), \frac{f_p(t_1) - f_p(0)}{t_1}, \lim_{t_1\to t_2}\frac{f_p(t_1) - f_p(t_2)}{t_1 - t_2})$$

where the last coordinate is null homotopic by the null homotopy described in the last paragraph. Now, observe that the vector $\frac{f_p(t_1)-f_p(0)}{t_1}$ is confined to a hemisphere for all values of t_1, and hence it is null homotopic through the straight line homotopy. □

Therefore, we have constructed an element

$$\overline{ev}_2(f)\colon S^3 \to C_2'[S^1 \times D^3].$$

which lives in $\pi_3 C_2'[S^1 \times D^3]$. This element is determined by $ev_2(f)$ up to choices of null

homotopies. Then we have defined an invariant

$$\overline{ev}_2 \colon \pi_2 \mathrm{Emb}(I, S^1 \times D^3; I_0) \to \pi_3 C'_2[S^1 \times D^3]/\{\text{some extra relations}\}$$

where the extra relations arise from the choices of null homotopies. One can refer to Section 3 of [3] for details about these relations (and we will discuss a more general situation in Section 5.2 in the next Chapter).

Before we proceed with the third stage to define $\overline{ev}_3$, we state a lemma we need whose proof can be found in Section 3 of [3]. Recall that the Whitehead product operation for a topological space X is a graded quasi-Lie algebra structure on the homotopy groups of X. For $f \in \pi_k X$ and $g \in \pi_l X$

$$[f, g] \colon S^{k+l-1} \to S^k \vee S^l \to X$$

where the first map is given by the attaching map of the top cell of $S^k \times S^l$ and the second map is the wedge $f \vee g$. A basic example is $X = S^2$ and $f = g = \mathrm{Id} \in \pi_2 S^2$. The Whitehead product is twice the Hopf map $2\nu \colon S^3 \to S^2$.

Lemma 4.10. *Consider the fibration $F \to C_k(S^1 \times D^3) \to C_{k-1}(S^1 \times D^3)$. The fiber has the homotopy type of a $(k-1)$-times punctured $S^1 \times D^3$ which is homotopy equivalent to $S^1 \vee_{k-1} S^3$. It follows that the rational homotopy groups of $C_k[S^1 \times D^3]$ are generated by the Whitehead products of the elements $t_l.\omega_{ij}$ with relations*

- $[\omega_{ij}, \omega_{lm}] = 0$ *if* $\{i, j\} \cap \{l, m\} = \emptyset$
- $[\omega_{ij}, \omega_{jl}] = [\omega_{jl}, \omega_{li}] = [\omega_{li}, \omega_{ij}]$
- $t_l.[f, g] = [t_l.f, t_l.g]$.

Here ω_{ij} is the element in $\pi_3 C_k[S^1 \times D^3] \otimes \mathbb{Q}$ such that all points are fixed except the j-th point orbits around the i-th point, and t_l are generators of $\pi_1 C_k[S^1 \times D^3]$, for $i, j, l \in \{1, 2, \ldots, k\}$.

For $k = 3$, the 5th rational homotopy group of $C'_3[S^1 \times D^3] \simeq (S^1) \times S^1 \vee S^3 \times (S^1 \vee S^3 \vee S^3) \times (S^3)^3$ is generated by the Whitehead products of pairs of elements in $\{t_l^q.\omega_{ij}$ for all $i, j, l \in \{1, 2, 3\}, q \in \mathbb{Z}\}$ where t_1, t_2, t_3 are generators of the fundamental group and $\omega_{ij} \colon S^3 \to C_3[S^1 \times D^3]$ with the j-th point orbits around the i-th point. They satisfy the following relations:

- $\omega_{ii} = 0$, $\omega_{ij} = \omega_{ji}$ *for* $i \neq j$
- $t_l.\omega_{ij} = \omega_{ij}$ *for* $l \notin \{i, j\}$
- $t_j.\omega_{ij} = t_i^{-1}.\omega_{ij}$
- $t_p.[f, g] = [t_p.f, t_p.g]$ *for all* $f, g \in \pi_3 C_3[S^1 \times D^3]$
- $[\omega_{ij}, \omega_{lm}] = 0$ *if* $\{i, j\} \cap \{i, m\} = \emptyset$
- $[\omega_{ij}, \omega_{jl}] = [\omega_{jl}, \omega_{li}] = [\omega_{li}, \omega_{ij}]$

Note that the factors $(S^3)^3$ contribute zero since $\pi_5 S^3 \cong \mathbb{Z}/2$.

For $[f] \in \pi_2 \mathrm{Emb}(I, S^1 \times D^3)$ such that $ev_2(f) \colon S^2 \times C_2[I] \to C'_2[S^1 \times D^3]$ is null homotopic, one can define a map

$$\overline{ev_3}(f) \colon D^5 \to C'_3[S^1 \times D^3]$$

with ∂D^5 being sent to a fixed point, by attaching null homotopies along the 4 boundary facets of $C_3[I]$ to the map

$$ev_3(f) \colon D^2 \times C_3[I] \to C'_3[S^1 \times D^3].$$

More generally, for all $[f] \in \pi_2 \mathrm{Emb}(I, S^1 \times D^3)$, the restrictions of $ev_3(f)$ to the boundary facets (after being closed up by attaching null homotopies along the 3 boundary edges of each facet as in the second stage) are torsion since $\pi_4 C'_2[S^1 \times D^3] = \pi_4(S^1 \times D^3 \times S^1 \times$

$D^3 \times S^3 \times (S^3)^2$) is finite. This means that we can define an element

$$\frac{1}{m}\overline{ev_3}(mf)\colon D^5 \to C_3'[S^1 \times D^3]$$

in $\pi_5 C_3'[S^1 \times D^3] \otimes \mathbb{Q}$ where m is the least common multiple of the orders of the restrictions to the boundary facets.

As before, attaching null homotopies along the boundary facets involves choices. When $m = 1$, we have defined a map

$$\overline{ev}_3\colon \pi_2 \mathrm{Emb}(I, S^1 \times D^3; I_0) \to \pi_5 C_3'[S^1 \times D^3] \otimes \mathbb{Q}/\{\text{additional relations}\},$$

with the following additional relations being satisfied in the codomain:

- $[t_2^\alpha.\omega_{23}, t_2^\beta.\omega_{23}] = 0$
- $[t_1^\alpha.\omega_{12}, t_1^\beta.\omega_{12}] = 0$
- $t_1^{\alpha-\beta}t_3^{-\beta} + t_1^\beta t_3^{\beta-\alpha} = t_1^\alpha t_3^{\alpha-\beta} + t_1^{\beta-\alpha}t_3^{-\alpha}$

for all $\alpha, \beta \in \mathbb{Z}$. See [3] and [4] for details of these relations. Composing with the scanning map s gives an invariant

$$W_3\colon \pi_0 \mathrm{Diff}(S^1 \times D^3, \partial) \to \pi_5 C_3'[S^1 \times D^3] \otimes \mathbb{Q}/\{\text{additional relations}\}.$$

concluding our construction. We denote the above relations by R. In particular, we can deduce the following proposition from these relations.

Proposition 4.11 (Proposition 3.4 in [3])**.** *The group $\pi_5 C_3'[S^1 \times D^3] \otimes \mathbb{Q}/R$ is generated by $[t_2^\alpha.\omega_{12}, t_2^\beta.\omega_{23}] = t_1^\alpha t_3^\beta[\omega_{12}, \omega_{23}]$ for $\alpha, \beta \in \mathbb{Z}$.*

We will denote this codomain by Λ. The last relation

$$t_1^{\alpha-\beta}t_3^{-\beta} + t_1^\beta t_3^{\beta-\alpha} = t_1^\alpha t_3^{\alpha-\beta} + t_1^{\beta-\alpha}t_3^{-\alpha}$$

is called the **Hexagon relation** and will be very important in the calculations of W_3 as we shall see in later sections.

4.3 A generalization of the Pontryagin-Thom construction

In this section, we describe a generalization of the Pontryagin-Thom construction to the setting of oriented, framed cobordism groups and the stable homotopy groups of wedge product of spheres. Although it seems to be widely known, the author is not aware of a well-written source of this construction. This will be needed in the calculations of the W_3 invariant in later sections of Chapter 4 and Chapter 5.

We first briefly recall the usual Pontryagin-Thom construction. Let $[M, N]$ denote the homotopy classes of maps between M and N and $[M, N]_*$ denote the homotopy classes of based maps. For N simply-connected, e.g. N is a sphere, the forgetful map $[M, N]_* \to [M, N]$ is a bijection. Let $\Omega^{fr}_{m-q:M}$ denote the group of framed cobordism classes of framed submanifolds of M of codimension q. Given a manifold M of dimension m, a map $f\colon M \to S^q$, and two regular values p_0 and p_1 in S^q, the submanifolds $f^{-1}(p_0)$ and $f^{-1}(p_1)$ are framed bordant by transporting the framings along a path.

The **Pontryagin-Thom collapse** map is defined as follows: given a framed submanifold Y of codimension q in M, we take a tubular neighbourhood $U \cong Y \times \mathbb{R}^q$ of it and send everything outside of this disk bundle to a base point, and inside the disk bundle we project to $\mathbb{R}^q$ and take the quotient of the disk bundle that sends the boundary to the base point too. This gives a map from M to S^q that is well defined up to framed cobordism.

Theorem 4.12 (Pontryagin-Thom)**.** *Given an m-manifold M, there is an isomorphism $[M, S^q] \to \Omega^{fr}_{m-q:M}$ given by taking the preimage of a regular value with the Pontrjagin-Thom collapse as an inverse.*

For $M = S^m$, by the Freudenthal suspension theorem, we can take the colimit of the

following sequence:

$$\pi_m S^q \to \pi_{m+1} S^{q+1} \to \cdots \to$$

where the maps are induced by the suspension maps, and the colimit is the n-th stable homotopy group of spheres, denoted by π_n^s, where $n = m - q$. Therefore, the theorem implies a one to one correspondence between the stable homotopy groups of spheres and the bordism group Ω_n^{fr} of n-manifolds in $\mathbb{R}^\infty$ with a trivilization of the tangent bundle. The smash product in π_n^s corresponds to the Cartesian product in Ω_n^{fr}.

We now consider the case when $N = S^1 \vee S^n$ and $M = S^m$.

Theorem 4.13. *There is an isomorphism $[S^m, S^1 \vee S^n] \cong \Theta_N^{fr}$. Here Θ_N^{fr} is the set of finite collections of cobordism classes of disjoint framed codimension-n submanifolds in $S^1 \vee S^n$. The map is given by taking the preimage of a regular value in $S^n \subset S^1 \vee S^n$ and the preimage of a regular value in $S^1 \subset S^1 \vee S^n$ where the former gives rise to disjoint codimension-n submanifolds in S^m and the latter gives rise to disjoint codimension-1 spheres in S^m separating the codimension-n submanifolds. Further, each codimension-n submanifold is assigned an integer a_k, called the degree that is given by the signed number of codimension-1 spheres that separate it from the others.*

Proof. Let the wedge point of $S^1 \vee S^3$ be y_0. Given a map $f\colon S^m \to S^1 \vee S^n$, we take a point y_1 in the circle $S^1 \subset S^1 \vee S^n$ that is not y_0. The preimage $f^{-1}(y_1)$ is a union of codimension-1 (closed) oriented submanifolds in $S^m \setminus y_0$ which we denote by M_k, so $f^{-1}(S^1 \vee S^n \setminus y_1)$ is a copy of S^m with a finite number of codimension-1 oriented submanifolds removed. Note that since we can locally homotope f such that the restriction to $f^{-1}(S^1 \subset S^1 \vee S^3)$ becomes smooth, then any point in S^1 other than y_0 is a regular point by dimension reasons. In addition, take any regular point y in $S^n \subset S^1 \vee S^n$. The preimage is a disjoint union of codimension-n submanifolds N_l in $S^m \setminus f^{-1}(y_0)$.

The neighbourhood of each M_k gets mapped in the following way: take the disk bundle of its framing $M_k \times D^1 \subset M_k \times \mathbb{R}$ and project to the $\mathbb{R}$ factor, and take the quotient that sends the boundary of D^1 to the base point to get a map between circles. The manifolds N_l are separated by M_k in the following way: collapsing the neighbourhoods $M_k \times D^1$ into

$\{\text{pt}\} \times D^1$ gives a quotient of S^m as a wedge of L long strings at y_0 with the other end of each long string connected with an m-dimensional sphere, and each long string consists a sequence of at least 1 arcs such that the total number of arcs K is the total number of M_k, and L is the total number of N_l. Furthermore, each N_l is contained in an S^m in this space. We record the number of arcs each long string contains. See Figure 4.3 for an example when $m = 2$. Note that all of the circles and spheres are oriented, and the orientations are recorded by the numbers in the figure. This gives the forward direction.

Up to homotopies of f, different choices of regular values lead to framed cobordisms between the corresponding preimages by choosing paths between these choices. Similar to the original Pontryagin-Thom construction, a homotopy between two maps gives a framed cobordism.

Conversely, given a collection of disjoint representatives M_k of codimension n framed submanifolds of S^m, each of which is assigned a degree L_k, we can choose a (closed) tubular neighbourhood $U_k \cong M_k \times D^n$ for each of them and choose a bigger tubular U'_k neighbourhood for each such that they are still disjoint. Then define a map $f' \colon S^m \to S^1 \vee S^n$ as follows. In the tubular neighbourhoods $M_k \times D^n$, f' first projects onto the D^n part and then sends $0 \in D^n$ to the antipodal point y'_0 of y_0 in $S^n \subset S^1 \vee S^n$. The remaining part of $\text{Int}D^n$ (which is an annulus) is then mapped to $S^n \setminus \{y_0, y'_0\}$ by the identity map between the annuli. It follows that ∂D^n is mapped to y_0. Furthermore, the remaining part of the larger tubular neighbourhoods $U'_k \setminus U_k \cong M_k \times S^{n-1} \times I$ is projected to I and then the end points of I are assigned to y_0 with $\text{Int}I$ wrapping around the circle part L_k times. Finally, the rest of S^n is sent to y_0. This gives the backward direction. One checks that they are inverses of each other. □

Remark. Alternatively, one can lift a map $f \colon S^m \to S^1 \vee S^n$ to the universal cover of $S^1 \vee S^n$ which is $\mathbb{R} \vee_\infty S^n$ and perform the above computations by taking preimages of points in the various lifted S^n.

In this case, we have $\pi_n(S^1 \vee S^n) \cong \mathbb{Z}[t, t^{-1}]$. This can be seen by passing to the universal cover. One way of representing the generators is as follows: given a polynomial

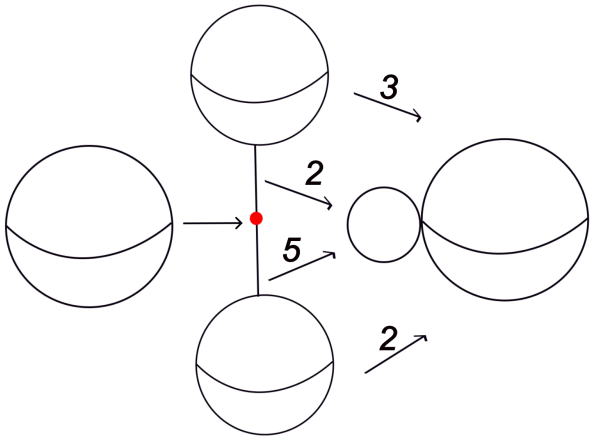

Figure 4.3: A representation of the element $2t^5 + 3t^2$.

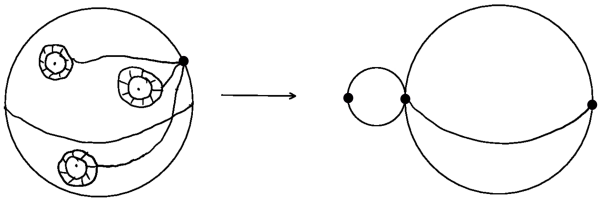

Figure 4.4: The backward map for $M = S^2$.

$h = a_0 + a_1 t^{k_1} + \cdots + a_m t^{k_m}$, squash S^n into a sequence of $m+1$ copies of S^n (labeled by S^n_i) connected by m copies of arcs (labeled by I_{k_i}), and map $S^n_i \subset S^1 \vee S^n$ to S^n by a degree a_i map. Further, the arcs I_{k_i} are mapped to $S^1 \subset S^1 \vee S^n$ by a degree k_i map (with endpoints being sent to y_0).

Figure 4.3 and 4.4 give an example when $m = n = 2$. In this case everything can be easily visualised. For $n = 2$, for such a map f, the preimage $f^{-1}(S^1 \vee S^n \setminus y_1)$ is a copy of S^2 with n punctures. The preimage of any regular value in S^2 gives m points in the domain, each of which is separated from the rest by a circle. Conversely, given a collection of points in S^2 and corresponding indices, we take a disk around each of the points and an annulus outside the disk. The resulting map is now easy to describe: the boundary of disks are quotiented to the wedge point of $S^1 \vee S^2$ and the annuli part (the dashed part in Figure 4.4) is collapsed into an interval with endpoints being sent to y_0 and the interior naturally circles around S^1. See Figure 4.4. Note that the paths in the domain S^2 from the base point to each tubular neighbourhood are not necessary but just auxiliary: everything outside of the tubular neighbourhoods get mapped to the wedge point y_0.

The above can be generalized to the case of $(\vee_k S^1) \vee (\vee_l S^n)$ by picking up a regular point in each of the spheres (and circles) away from the wedge point and taking a preimage to obtain collections of disjoint submanifolds up to the sloping point. In the following sections, we will make use of the case when $n = 3$, $k = 1, 2, 3$ and $l = 1, 2$.

4.4 Computing the W_3 invariant

In this section and Section 4.5, we discuss the strategy for computing the W_3 invariant

$$W_3 \colon \pi_0 \mathrm{Diff}(S^1 \times D^3, \partial) \to \pi_2 \mathrm{Emb}(I, S^1 \times D^3; I_0) \to \Lambda$$

Budney–Gabai proposed two different approaches in the calculations of the W_3 invariant of unknotted barbell diffeomorphisms of $S^1 \times D^3$. The first is to write the image of a barbell diffeomorphism on the scanning map as a linear combination of certain **fundamental classes** they denote by $G(p, q)$ in $\pi_2 \mathrm{Emb}(I, S^1 \times D^3)$. Budney–Gabai (see Theorem 8.1 in [3]) provided a formula to calculate the invariant W_3 of $\theta_k(v, w)$ (see Section 2.1) using this approach. We will not discuss the first approach in this paper. The second method, which is proposed in [4], is through intersection theory and the Pontryagin-Thom construction. This approach is only completed in [4] for the calculations for the barbells δ_k (see Theorem 3.1 in [4]), but not for other unknotted barbells in $S^1 \times D^3$. We aim to complete the calculations for unknotted barbells in $S^1 \times D^3$ using this approach.

Our plan is outlined below. The scanning map s_{s_0} depends on the choice of a fixed point $s_0 \in S^1$. For a class $[\Phi] \in \pi_0 \mathrm{Diff}(S^1 \times D^3, \partial)$, the image $s_{s_0}([\Phi])$ can be analyzed by a case-by-case method by choosing a suitable representative Φ and looking at the image $\Phi(s_0 \times D^3)$ in detail. For the scanning map, we will focus on its effects on the subgroup generated by barbell diffeomorphisms of unknotted barbells in $S^1 \times D^3$ introduced in Section 2.1, this will be done in Section 4.5. For the second map

$$\overline{ev}_3 \colon \pi_2 \mathrm{Emb}(I, S^1 \times D^3; I_0) \to \Lambda$$

we will discuss a machinery that would potentially work for classes in $\pi_2\mathrm{Emb}(I, S^1 \times D^3; I_0)$ other than the image of such barbell diffeomorphisms, though we will only go into the calculations of barbell diffeomorphisms throughout. This will be in this section (Section 4.4).

In the rest of this section, we discuss ideas for calculating the map

$$\overline{ev}_3 \colon \pi_2\mathrm{Emb}(I, S^1 \times D^3; I_0) \to \Lambda.$$

For an element $[f] \in \pi_2\mathrm{Emb}(I, S^1 \times D^3)$, we start by analyzing (the homotopy class represented by) the map

$$\overline{ev}_2(f) \colon D^1 \times D^1 \times C_2[I] \to C_2[S^1 \times D^3] \simeq S^1 \times (S^1 \vee S^3).$$

Budney–Gabai proposed a method of constructing cobordism classes of certain families of disjoint, framed submanifolds that detect such maps as we shall disclose now. Let $\delta \in \partial D^3$ be a fixed unit direction. For $i \in \mathbb{Z}$, we define the **cohorizontal submanifold**

$$t^i\mathrm{Co}_1^2 = \{(p_1, p_2) \in C_2[\mathbb{R} \times D^3] \colon t^i.p_2 - p_1 = \lambda\delta \text{ for some } \lambda > 0\}.$$

This submanifold intersects the image of $t_1^i.\omega_{12} \colon S^3 \to C_2[S^1 \times D^3]$ transversely at exactly one point (cf. Lemma 4.10). Namely, suppose that we pick a representative of the lift $\overline{t_1^i.\omega_{12}}$ of $t_1^i.\omega_{12}$ to $C_2[\mathbb{R} \times D^3]$ by shooting the first point from the base point say $(0,0)$ to $(i,0) \in \mathbb{R} \times D^3$, and letting the second point loop around $(0,0)$, then the unique intersection point between this image and $t^i\mathrm{Co}_1^2$ is obtained by taking the halfline to the δ-direction that starts from $(i,0)$. See Figure 4.5 for a 2-dimensional cartoon picture. The horizontal rectangles in Figure 4.5 represent fundamental domains, and the solid red sphere (drawn as a 2-sphere but aiming to represent a 3-sphere) loops around the point p_1 and creates a cohorizontal pair. The dotted red sphere represents the image of the second point under the action of t^6. The horizontal arrow represents the cohorizontal direction δ. Therefore, we have the following.

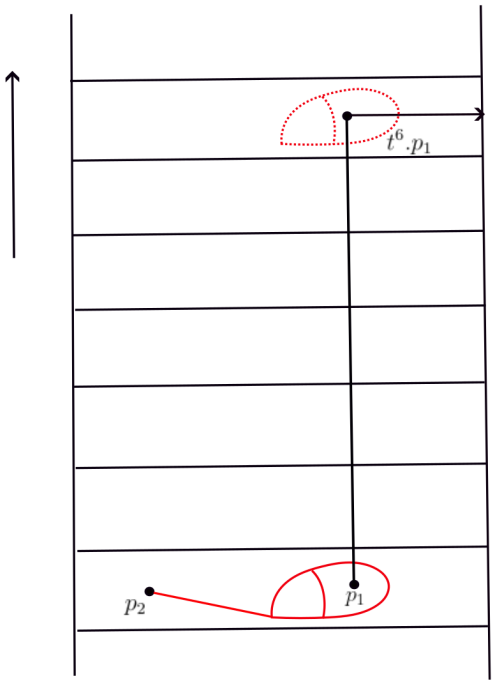

Figure 4.5: The cohorizontal submanifold $t^6\mathrm{Co}_1^2$ in $\mathbb{R} \times D^3$ detects $t^6.\omega_{12}$.

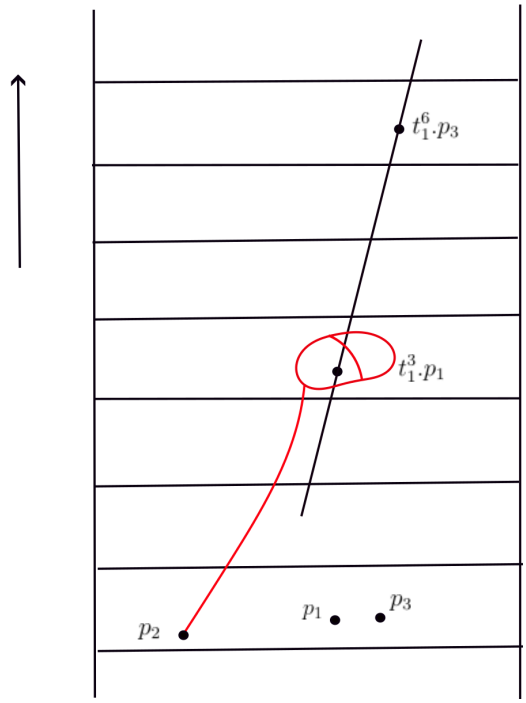

Figure 4.6: The collinear submanifold $\mathrm{Col}_{3,6}^1$ in $\mathbb{R} \times D^3$ detects $t^3.\omega_{12}$.

Lemma 4.14. *The preimage of $t^i\mathrm{Co}_1^2$ under the map $\overline{t_1^i.\omega_{12}}\colon S^3 \to C_2[\mathbb{R} \times D^3]$ is a codimension-3 oriented submanifold, which in this case is a single point. For $j \neq i$, the preimage of $t^i\mathrm{Co}_1^2$ under $\overline{t_1^j.\omega_{12}}$ is empty. Therefore, we say that $t^i\mathrm{Co}_1^2$ detects $t^i.\omega_{12}$.*

Thus, we can use cohorizontal submanifolds to detect the map f. In particular, we lift it to $C_2[\mathbb{R} \times D^3]$ and take the preimage of the cohorizontal submanifolds $t^i\mathrm{Co}_1^2$ under this lift. The preimage is given by a disjoint union of (signed) points for all i. Counting the signed number of points gives the coefficient of $t^i\mathrm{Co}_1^2$, and taking the sum gives $[f]$.

Next, we consider the third stage map $\overline{ev}_3(f) \in \Lambda$. By Proposition 4.11, such a class is a linear combination of Whitehead brackets $[t_2^\alpha.\omega_{12}, t_2^\beta.\omega_{23}] = t_1^\alpha t_3^\beta[\omega_{12}, \omega_{23}]$ with coefficients being detected by the following two collections of **collinear submanifolds**:

$$\mathrm{Col}_{\alpha,\beta}^1 = \{(p_1, p_2, p_3) \in \overline{C_3[S^1 \times D^3]}\colon (p_2, t^\alpha.p_1, t^\beta.p_3) \text{ lie on a straight line in } \mathbb{R} \times D^3 \text{ in order}\}$$

$$\mathrm{Col}_{\alpha,\beta}^3 = \{(p_1, p_2, p_3) \in \overline{C_3[S^1 \times D^3]}\colon (t^\alpha.p_1, t^\beta.p_3, p_2) \text{ lie on a straight line in } \mathbb{R} \times D^3 \text{ in order}\}.$$

See Figure 4.6 for a picture of $\mathrm{Col}_{\alpha,\beta}^1$ with $\alpha = 3$ and $\beta = 6$.

The universal cover $\overline{C_3[S^1 \times D^3]}$ can be interpreted as a subspace of $C_3[\mathbb{R} \times D^3]$ in the sense that it contains points of the latter space with disjoint $\mathbb{Z}$-orbits (also see Figure 9 of [3] for details).

Lemma 4.15. *The two collections of collinear submanifolds* $\mathrm{Col}^1_{\alpha,\beta}$ *and* $\mathrm{Col}^3_{\alpha,\beta}$ *are disjoint. If we consider* $t_2^\alpha.\omega_{12}$ *and* $t_2^\beta.\omega_{23}$ *as elements of* $\pi_3 C_3[S^1 \times D^3]$ *by taking their images under the inclusion maps* $C_2[S^1 \times D^3] \to C_3[S^1 \times D^3]$ *given by*

$$\mathrm{Inc}_{12} \colon (p_1, p_2) \to (p_1, p_2, p_0)$$

$$\mathrm{Inc}_{23} \colon (p_2, p_3) \to (p_0, p_2, p_3)$$

for some $p_0 \in S^1 \times D^3$ *which we can choose to be distinct to the other coordinates, then the former collinear submanifold* $\mathrm{Col}^1_{\alpha,\beta}$ *detects* $t_2^\alpha.\omega_{12}$ *and the latter collinear submanifold* $\mathrm{Col}^3_{\alpha,\beta}$ *detects* $t_2^\beta.\omega_{23}$ *in the sense that the (transverse) intersections between* $\mathrm{Col}^1_{\alpha,\beta}$ *and* $t_2^\alpha.\omega_{12}$ *(and* $\mathrm{Col}^3_{\alpha,\beta}$ *and* $t_2^\beta.\omega_{23}$*) are exactly one point, and for* $\alpha' \neq \alpha$ *and* $\beta' \neq \beta$*, the (transverse) intersections between* $\mathrm{Col}^1_{\alpha,\beta}$ *and* $t_2^{\alpha'}.\omega_{12}$ *(and* $\mathrm{Col}^3_{\alpha,\beta}$ *and* $t_2^{\beta'}.\omega_{23}$*) are zero.*

In addition, the preimage of the pair $(\mathrm{Col}^1_{\alpha,\beta}, \mathrm{Col}^3_{\alpha,\beta})$ *under (the lift of) the Whitehead product* $[t_2^\alpha.\omega_{12}, t_2^\beta.\omega_{23}]$ *is a 2-dimensional Hopf link with linking number 1 in* S^5*. Therefore, we say that the pair* $(\mathrm{Col}^1_{\alpha,\beta}, \mathrm{Col}^3_{\alpha,\beta})$ *detects the Whitehead product* $[t_2^\alpha.\omega_{12}, t_2^\beta.\omega_{23}]$*.*

Proof. The property of being disjoint follows directly from the orderings of the triples.

We show that the former collinear submanifold $\mathrm{Col}^1_{\alpha,\beta}$ detects $t_2^\alpha.\omega_{12}$. The latter one can be argued in a similar way.

By choosing an appropriate representative of $t_2^\alpha.\omega_{12}$, we can arrange its image to be $p_1 \times (\gamma \vee S) \times p_0$ where p_1 is a fixed point in $0 \times D^3 \subset \mathbb{R} \times D^3$, and γ is a null homotopic path from a fixed point $p_2 \in 0 \times D^3 \subset \mathbb{R} \times D^3$ to a 3-sphere S that loops around $t_1^\alpha.p_1 \in \alpha \times D^3 \subset \mathbb{R} \times D^3$. Again, see Figure 4.6 for a picture of $\mathrm{Col}^1_{\alpha,\beta}$ with $\alpha = 3$ and $\beta = 6$.

Now, we can deduce that the intersection between this image and the submanifold $\mathrm{Col}^1_{\alpha,\beta}$ consists of a unique point. Namely, $t_3^\beta.p_0$ and $t_1^\alpha.p_1$ determines a straight line which

intersects S at a unique point.

To see the last statement, we recall that $C_3[S^1 \times D^3]$ is homotopy equivalent to $S^1 \times (S^1 \vee S^3_{12}) \times (S^1 \vee S^3_{13} \vee S^3_{23})$. The elements ω_{12} and ω_{23} represent the homotopy classes of the inclusion maps of the 3-spheres S^3_{12} and S^3_{23} respectively. The actions of t_2^α and t_2^β reflect the actions of the second and third circles in the wedge. Fixing a base point appropriately, we can take the Whitehead product $[t_2^\alpha.\omega_{12}, t_2^\beta.\omega_{23}]$ by composing the wedge map with the attaching map of the top cell of $S^3 \times S^3$:

$$S^5 \to S^3 \vee S^3 \xrightarrow{t_2^\alpha.\omega_{12} \vee t_2^\beta.\omega_{23}} C_3[S^1 \times D^3].$$

The preimage of the pair $(\mathrm{Col}^1_{\alpha,\beta}, \mathrm{Col}^3_{\alpha,\beta})$ under this composition is the same as the preimage of two points: say x_1 in S^3_{12} and x_2 in S^3_{23} that are distinct from the wedge points. Since the attaching map

$$S^5 \cong \partial D^6 \cong \partial(D^3 \times D^3) \cong \partial D^3 \times D^3 \cup D^3 \times \partial D^3 \to S^3 \vee S^3$$

is given by $(\psi_1 \times \overline{\psi_2} \cup \overline{\psi_2} \times \psi_1)$, where ψ_i is the attaching map of the 3-cell the i-th 3-sphere and $\overline{\psi_i}$ is the corresponding characteristic map, one concludes that the preimage of the two points x_1 and x_2 is a disjoint union of two 2-spheres with linking number 1. □

The preimage of the pair $(\mathrm{Col}^1_{\alpha,\beta}, \mathrm{Col}^3_{\alpha,\beta})$ under (the lift of) $\overline{ev}_3(f)$ is a disjoint union of pairs of codimension 3 (thus dimension 2) oriented submanifolds in S^5, and the linking numbers of these pairs determines the coefficient of $[t_2^\alpha.\omega_{12}, t_2^\beta.\omega_{23}]$ in the linear combination representing $\overline{ev}_3(f)$.

To end this section, we state a lemma that helps us simplify calculations involving collinear submanifolds by reducing the above linking number computation strategy to linking number computations that only involve cohorizontal submanifolds.

Lemma 4.16 ([3]). *Given a smooth map $f\colon S^5 \to C_3[S^1 \times D^3]$, we can assume generically that it has no cohorizontal triples. As before, we fix $\delta \in \partial D^3$. Define the cohorizontal*

manifold for $k, j \in \{1, 2, 3\}$

$$t^i \mathrm{Co}_j^k = \{(p_1, p_2, p_3) \in C_3[S^1 \times D^3] \colon t^i.p_j - p_k = \lambda\delta \text{ for some } \lambda > 0\}.$$

In other words, we allow one of the three coordinates to be free with the other two being cohorizontal. Then the linking numbers of the preimage of the pair $(\mathrm{Col}^1_{\alpha,\beta}, \mathrm{Col}^3_{\alpha,\beta})$ *under the lift of* f *to the universal cover* $\overline{f} \colon S^5 \to \overline{C_3[S^1 \times D^3]}$ *are the same as the linking numbers of the preimage of the pair* $(t^\alpha Co_2^1 - t^{\alpha-\beta} Co_3^1, t^{\beta-\alpha} Co_1^3 - t^\beta Co_2^3)$ *under* f *for all* $\alpha, \beta \in \mathbb{Z}$.

This lemma allows one to perform the calculations at the third stage entirely by using the idea of cohorizontal submanifolds rather than running into the difficulties of visualizing collinear triples.

We will present some ideas behind the proof of this lemma in Section 5.2 in a more general setting.

4.5 W_3 invariant of unknotted barbells in $S^1 \times D^3$

As discussed in Chapter 2, unknotted barbells in $S^1 \times D^3$ are determined by elements of the free group of three generators $\mathrm{F}_3[\nu_R, \nu_B, t]$ where ν_R and ν_B are meridian circles of the cuff spheres and t represents the circle factor. In fact, the operation of taking induced barbells from elements of $\mathrm{F}_3[\nu_R, \nu_B, t]$ factors through the quotient map

$$\mathrm{F}_3[\nu_R, \nu_B, t] \to \langle \nu_B \rangle \backslash F_3 / \langle \nu_R \rangle$$

that kills words starting with powers of ν_B or ending with powers of ν_R, because if the bar starts from a cuff sphere and immediately links this sphere, then these linkings can be undone through an isotopy that drags this cuff away from the bar.

Recall from Section 2.1 the special classes of barbells defined by Budney–Gabai denoted by $\theta_k(v, w)$, with $k \in \mathbb{Z}^+$, $(v)_i, (w)_j \in \mathbb{Z}^{k-1}$. These are specified by a positive integer k and two vectors v and $w \in \mathbb{Z}^{k-1}$. Starting with two disjoint unknotted 2-spheres B and

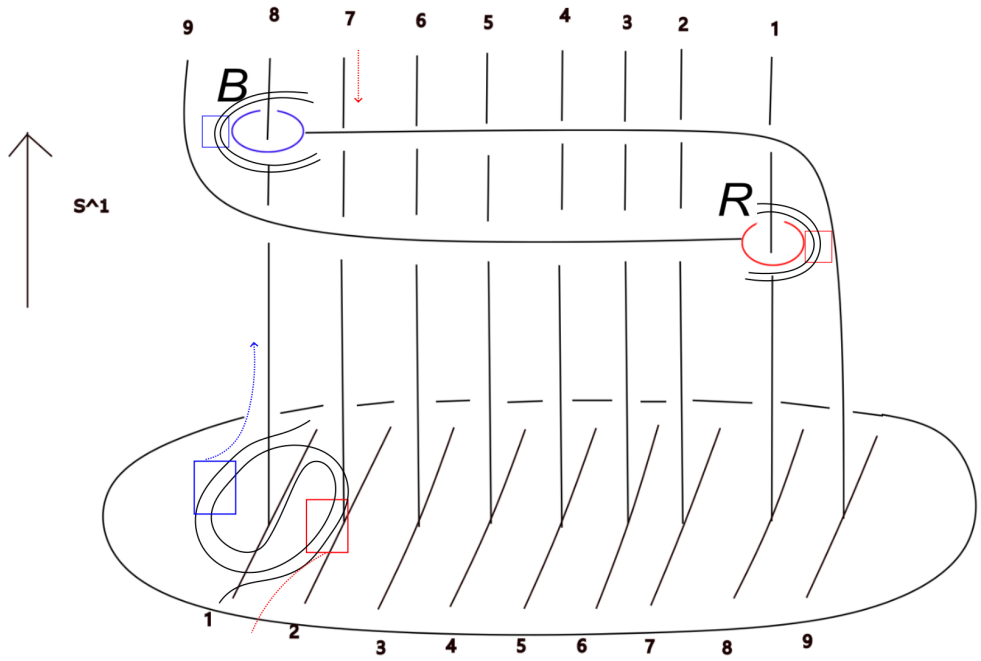

Figure 4.7: The embedded barbell $\delta'_{10} = \theta_{10}((0,\dots,0,1,0),(0,\dots,0,1,0))$.

R (one in blue and one in red) embedded in $S^1 \times D^3$, we need to specify a bar connecting them. The positive number k indicates the number of times the bar wraps around the circle direction going from R to B. Each entry of the two vectors indicates the signed number of times each vertical strand of the bar wraps around the two spheres (refer to Figures 2.5 and 4.7 for examples). In this section, we study the W_3 invariants for barbells $\theta_k(v,w)$, using the ideas described in the previous section, and describe their properties. We also provide a method for calculating W_3 for general unknotted barbells in $S^1 \times D^3$.

As in Chapter 2, we denote the induced barbell diffeomorphism from an embedded barbell $\mathcal{B}$ by $\Phi_{\mathcal{B}}$. However, when there is no ambiguity, we sometimes do not distinguish $\mathcal{B}$ and $\Phi_{\mathcal{B}}$.

We first state an important calculation done by Budney–Gabai in [3].

Theorem 4.17 (Section 3 and Figure 10 of [4])**.** *The W_3 invariants of barbell diffeomorphisms induced from*

$$\delta_k = \theta_k((0,\dots,1,0),(0,\dots,0,1))$$

for $k \geq 4$ are nonzero and linearly independent. Therefore, the induced barbell diffeomorphisms Φ_{δ_k} from δ_k are isotopically nontrivial and linearly independent for $k \geq 4$.

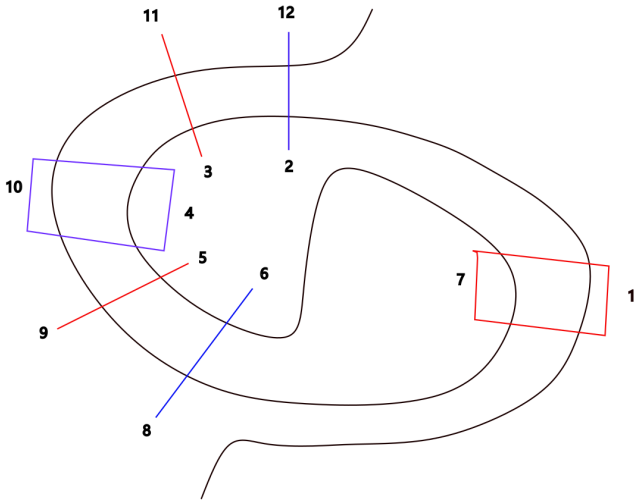

Figure 4.8: The type 1 intersection for point 1.

Let δ'_k denote the barbell in $S^1 \times D^3$ whose defining vectors are $v = w = (0, 0, \ldots, 0, 1, 0)$ (cf. Chapter 2.1), i.e.

$$\delta'_k := \theta_k((0, 0, \ldots, 0, 1, 0), (0, 0, \ldots, 0, 1, 0)).$$

See Figure 4.7 (which is a repetition of Figure 2.5 for the case $k = 10$, with more annotations which we will explain below). We calculate the W_3 invariant for this barbell.

The first step is analyzing the image $s_{s_0}([\Phi_{\delta'_k}])$ under the scanning map s_{s_0}, where $\Phi_{\delta'_k}$ is the induced barbell diffeomorphism from δ'_k. We will need a trick from [4]. By assumption, δ'_k intersects the 3-ball $\{s_0\} \times D^3$ transversely at the bar at $k-1$ isolated points but not at the cuff spheres. At each of the $k-1$ intersection points on the bar, following the approach in [3, 4] (in particular, see Proposition 6.3 of [3] and Proposition 2.2 of [4]), we twist the corresponding embedded $k-1$ arcs (drawn as short arcs in the horizontal plane in Figure 4.7) controlled by the two parameter families (blue and red) artificially into the shape shown in Figure 4.8 (ignoring the colored arcs on sides of the colored boxes for now). Virtually, there are five strands in Figure 4.8, two in the blue box, two in the red box, and one in the middle.

Lemma 4.18. *([3, 4]) The barbell diffeomorphism $\Phi_{\delta'_k}$ is isotopic to a diffeomorphism*

whose restriction to the 3-ball $\{s_0\} \times D^3$ has the following effects on each twisted arc (as in Figure 4.8) from each of the $k-1$ intersection points: it grabs the two strands in the blue box on the left side, following the bar (as the dotted blue arrow indicated in Figure 4.7 for the first interval) until getting to the blue cuff, loops around the blue cuff sphere and comes back, and at the same time, grabs the two strands in the red box on the right side, following the bar (as the dotted red arrow indicated in Figure 4.7 for the first interval) until getting to the red cuff, loops around the red cuff sphere and comes back.

Therefore, up to translating the endpoints to coincide with the endpoints I_0 as discussed in the definition of s_{s_0} in Section 4.2, the image $s_{s_0}([\Phi_{\delta'_k}])$ is given by a sum denoted by

$$[\delta'_k]_1 + [\delta'_k]_2 + \cdots + [\delta'_k]_{k-1}$$

of $k-1$ 2-parameter families of embedded intervals, each of which is given by twisting one of the $k-1$ arcs to the shape of Figure 4.8, following the above description, and finally untwisting.

We now use Lemma 4.18 to detect the second stage map

$$\overline{ev}_2(s_{s_0}([\Phi_{\delta'_k}])) = \overline{ev}_2(s_{s_0}([\Phi_{\delta'_k}]_1) + \cdots + \overline{ev}_2(s_{s_0}([\Phi_{\delta'_k}]_{k-1}).$$

Each term $\overline{ev}_2(s_{s_0}([\Phi_{\delta'_k}]_i)$, $i = 1, 2, \ldots, k-1$ is a map

$$D^1 \times D^1 \times C_2[I] \to C_2[S^1 \times D^3]$$

and we will apply Lemma 4.14 to each of these separately. Suppose that we fix the direction pointing horizontally to the left side being our choice of the cohorizontal direction δ, then the points contained in the cohorizontal submanifolds

$$t^i\mathrm{Co}_1^2 = \{(p_1, p_2) \in \overline{C_2[S^1 \times D^3]} \colon t^i.p_2 - p_1 = \lambda\delta \text{ for } \lambda > 0\}$$

happen near the the cuffs when the strands of the bar inside the blue and red boxes (see

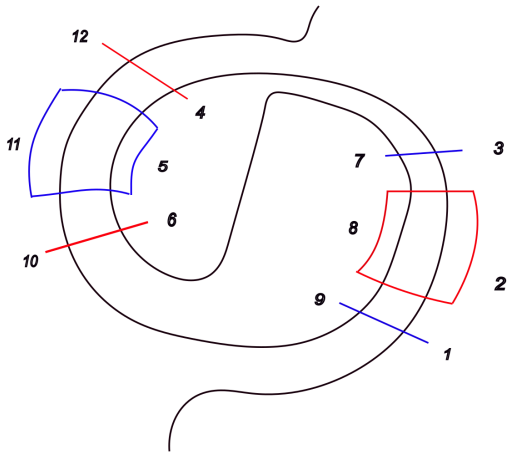

Figure 4.9: The type 2 intersection for points 2 to $k-2$.

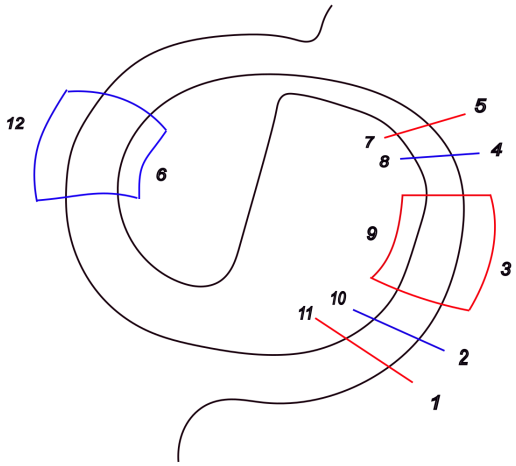

Figure 4.10: The type 3 intersection for point $k-1$.

Figure 4.8) get dragged to the farthest point respectively, i.e. looping around the blue and red cuffs in Figure 4.7. At these moments, the vertical strands inside the red and blue boxes create cohorizontal pairs.

In fact, if we assume that the bar links each of the two cuff spheres for only once, and assume that starting from B, it links the red cuff R first, then the blue cuff B, then $k-1$ intersection points are classified into 3 types, fitting in the following lemma.

Lemma 4.19. *Let e_i be the vector whose only non-zero entry is the i-th entry and is 1. Assume that a barbell $\theta_k(e_i, e_j)$ in $S^1 \times D^3$, $k \geq 1$ with $i+j \geq k$ is isotoped to a position such that the cuff spheres are disjoint from $\{s_0\} \times D^3 \subset S^1 \times D^3$ for some point $s_0 \in S^1$, and the bar intersects $\{s_0\} \times D^3$ at $k-1$ points transversely, then these intersection points are classified into three types, based on the patterns of the cohorizontal pairs shown in Figures 4.8, 4.9 and 4.10. The colored arcs on the sides of the blue and red boxes indicate intersections with the spanning disks of the two cuff spheres, i.e. the natural 3-balls they bound. Furthermore, the barbell $\theta_k(e_i, e_j)$ produces $(k-i-1)$ type 1 intersection points, $(-k+j+i+1)$ type 2 intersection points and $(k-j-1)$ type 3 intersection points.*

Proof. For an intersection point (that is contained in an interval in $\{s_0\} \times D^3$) arising from $\theta_k(e_i, e_j)$, the corresponding barbell diffeomorphism creates intersections between this interval and the spanning disks of the two unknotted cuff spheres, i.e. the natural

3-ball they bound in $S^1 \times D^3$. Since $i + j \geq k$, the blue sphere is on the left of the red sphere, meaning that the nearest intersections that appear on the sphere of one colour are always of the other colour. In fact, one can check point by point that there are only three possible patterns of such intersections as shown in Figures 4.8, 4.9 and 4.10.

Since the nonzero coordinate of the first vector e_i is at the i-th position, it follows that the blue cuff links the i-th vertical strand, counting from right to left. This indicates that counting from the left to right, the first $(k - i - 1)$ intersection points are of type 1. Similarly, the last $(k - j - 1)$ intersection points are of type 3 since e_j indicates that the red cuff links the j-th vertical strand, counting from right to left. The remaining $(k-1) - (k-i-1) - (k-j-1) = (-k+j+i+1)$ intersection points in the middle are of type 2. □

We now analyze point 1 of $\delta'_k = \theta_k((0,\dots,0,1,0),(0,\dots,0,1,0)) = \theta_k(e_{k-2}, e_{k-2})$ which is a type 1 point. The two blue and two red arcs in Figure 4.8 happen at the moment when the farthest point is reached for both red and blue cuff spheres. We parameterize the interval by $[0, 13]$. The two sets of strands contained in the red and blue boxes are looping around the red and blue circles, and each creates 8 cohorizontal points (so 16 in total). In this type 1 case, there are no arcs on the red box side because the strands do not cross the spanning disks of the cuff spheres along the way of reaching the farthest point at the red cuff sphere.

The next lemma describes cohorizontal points arising from this type 1 intersection point.

Lemma 4.20. *The preimage of the cohorizontal points arising from the first intersection point of δ'_k are as shown in Figure 4.11. The square on the left hand side is parameterized by $[0,1] \times [0,1]$, and the axes of the triangle picture are parameterized by $[0, 13]$. The cohorizontal points appearing at the centre of the square are listed below.*

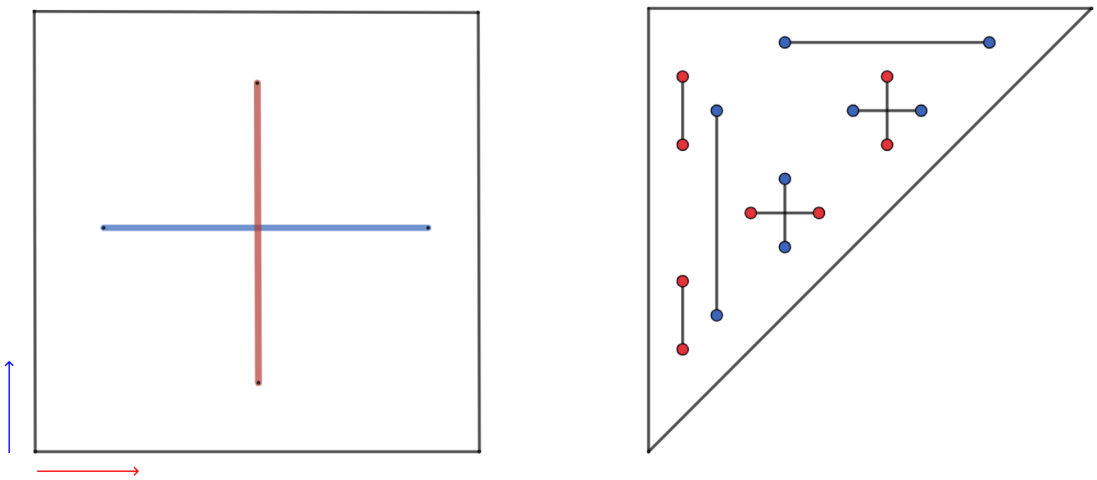

Figure 4.11: The preimage of the cohorizontal manifolds for the second stage map $D^1 \times D^1 \times C_2[I] \to C_2[S^1 \times D^3]$.

$$\begin{array}{cccc} (1,3) & (3,7) & (2,4) & (2,10) \\ (1,5) & (5,7) & (4,6) & (6,10) \\ (1,9) & (7,9) & (4,8) & (8,10) \\ (1,11) & (7,11) & (4,12) & (10,12). \end{array}$$

Proof. Figure 4.11 is a Budney–Gabai style picture as Figures 12 and 13 of [4] but we interpret it in a slightly different way. In the square, there is a cross of two intervals, one in blue and one in red. Cohorizontal points only appear in these two intervals. The two axes of the square are annotated as red and blue, meaning the former one controls the two strands in the red box, and the latter one controls the two strands in the blue box, in Figure 4.8.

At the center of the square they intersect. This point corresponds to the moment when both of the two sets of strands contained in the red and blue boxes are at the farthest position, looping around the two cuff spheres. At this point, both of the red and blue dots in the triangle picture are present, corresponding to the double points mentioned in the paragraph before this lemma.

When fixing the blue coordinate at 0.5 and freely moving the red coordinate, i.e. on the blue interval in the square, the blue cohorizontal points in the triangle picture stay.

The 4 pairs of red cohorizontal points

$$\{(1,3),(1,5)\},\{(1,9),(1,11)\},\{(3,7),(5,7)\},\{(7,9),(7,11)\}$$

gradually come together as we approache the two end points of the blue interval, tracing out a circle for each pair. This is shown as intervals connecting each pair in the triangle picture. After passing these two endpoints, no cohorizontal points are present. To see this, imagine that we fix the two strands that come from the blue box, keeping them at the farthest position, and move the two strands in the red box back to the initial position, then when these two strands cross the vertical strand that the red cuff R links, the 4 pairs of red cohorizontal points merge together in pairs, and then disappear.

Similarly, varying the blue coordinate along the red interval traces out 4 circles of blue cohorizontal points corresponding to the pairs

$$\{(2,4),(2,10)\},\{(4,6),(4,8)\},\{(6,10),(8,10)\},\{(4,12),(10,12)\}.$$

□

Pulling back the orientations of the normal bundles of the cohorizontal submanifolds $t^i\mathrm{Co}_1^2$ (codimension 3) along $\overline{ev}_2(s_{s_0}([\Phi_{\delta_k'}]_1))$ gives orientations to the 8 circles. Now observe that this disjoint union of unlinked codimension 3 (1-dimensional) oriented submanifolds in D^4 is null-cobordant. This implies that the second stage map $\overline{ev}_2(s_{s_0}([\Phi_{\delta_k'}]_1))$ is null homotopic.

Next, we move forward to detect the third stage map

$$\overline{ev}_3(s_{s_0}([\Phi_{\delta_k'}]_1))\colon D^1\times D^1\times C_3[I]\to C_3'[S^1\times D^3]$$

as an element in $\pi_5 C_3'[S^1\times D^3]$. By Lemma 4.16, we need to understand the preimage of the following pair:

$$(t^\alpha\mathrm{Co}_2^1-t^{\alpha-\beta}\mathrm{Co}_3^1,t^{\beta-\alpha}\mathrm{Co}_1^3-t^\beta\mathrm{Co}_2^3).$$

for each $\alpha, \beta \in \mathbb{Z}$. As defined in Lemma 4.16, for each of the cohorizontal submanifolds in the above pair, one of the three coordinates is free to move with the remaining two being cohorizontal (remember that we assume no cohorizontal triples as in Lemma 4.16). This implies that each cohorizontal submanifold will only appear on two of the three facets of $C_3[I]$.

In fact, these are represented by a disjoint union of 2-spheres embedded in $D^1 \times D^1 \times C_3[I]$. We draw $C_3[I]$ as a tetrahedron with coordinates t_1, t_2 and t_3. We follow the convention in [4] and draw a tetrahedron as a triangle with the t_2 coordinate pointing out of the page. We omit the square $D^1 \times D^1$ in our pictures as it will stay the same as the square in Figure 4.11. As outlined in Example 3.6 of [3], the third stage pictures are obtained from the second stage pictures by connecting the cohorizontal points in the preimage of the same cohorizontal submanifold at the same position on the two facets that are involved, by an interior arc, and closing the tetrahedron by attaching the null homotopies to the facets. The interior arc corresponds to varying the free coordinate (cf. Lemma 4.16).

Again, following the convention in [4], we draw the preimage in pairs with different colours (that may produce non-trivial linking numbers) as in Figures 4.12, 4.13, 4.14, 4.15, 4.16 and 4.17. These pictures show cohorizontal points at the centre of the square, i.e. when we are at the point $(0, 0) \in D^1 \times D^1$. Along the boundary facets, we attach null homotopies of the second stage map with the convention that we close the red spheres first and the blue spheres afterwards. In our pictures, this gives rise to a collection of circles, and when we vary in the two directions of $D^1 \times D^1$, these circles traces out a disjoint union of 2-spheres. One can refer to the construction of Figures 16 and 17 of [4] for comparison.

Following the approach in [4], we pull back the orientation of the normal bundles of the cohorizontal submanifolds (codimension 3) to give orientations to the 2-spheres (codimension 3). We now apply Lemma 4.16. For (the preimage of) each cohorizontal submanifold in the pair

$$(t^{\alpha}\mathrm{Co}_2^1 - t^{\alpha-\beta}\mathrm{Co}_3^1, t^{\beta-\alpha}\mathrm{Co}_1^3 - t^{\beta}\mathrm{Co}_2^3),$$

the power of t is determined by the number of times one needs to travel (along the bar) along the circle direction of $S^1 \times D^3$ from one point of a cohorizontal pair to the other. We then read off the linking numbers from Figures 4.12, 4.13, 4.14, 4.15, 4.16 and 4.17 and take the sum to get the following polynomial:

$$\overline{ev}_3(s_{s_0}([\Phi_{\delta_k'}]_1)) = -t_1^{k-2}t_3^{k-2} - t_1^{k-2}t_3^{k-2} + t_1^{2-k}t_3^0 + t_1^0 t_3^{2-k}.$$

For example, in Figure 4.12, there is only one linking pair (drawn in the middle of the picture). It takes $k-2$ times along the circle factor to go from the blue cuff sphere, along the bar, to where the cohorizontal pairs occur near the blue cuff (for $k = 10$, this is near strand 8, counting from right to left on the top in Figure 4.7). Thus we have $\alpha = k-2$. Similarly, we have $\beta - \alpha = 2 - k$. This implies that $\beta = 0$, so this picture contributes $\pm t_1^{2-k}t_3^0$ with the sign being determined by the orientations of this linking pair. To determine the orientations, note that the null-homotopy denoted by the blue arc attached to the $t_2 = t_3$ facet is determined by the pair of cohorizontal points $(4,6)$ and $(4,8)$ which admit negative and a positive normal bundle orientations respectively, with reference to the pull-back orientation of the normal bundle of $t^\alpha \mathrm{Co}_2^1$ in $C_3[S^1 \times D^3]$ and with the direction pointing horizontally to the left side being our choice of the cohorizontal direction δ, and thus is oriented by the direction pointing from $(4,6)$ to $(4,8)$. Similarly, the red arc representing a null-homotopy attached to the same $t_2 = t_3$ facet is oriented by pointing from $(3,7)$ to $(5,7)$, leading to a positive linking. Therefore, Figure 4.7 gives rise to the monomial $t_1^{2-k}t_3^0$. The contributions from the remaining figures can be calculated in this manner as well in the same way.

To finish the calculation of $W_3([\Phi_{\delta_k'}])$, we need to calculate the contributions from the remaining $k-3$ type 2 intersection points and the last type 3 intersection point. We will explain that this essentially follows from the following result by [4] (in particular, page 26 of [4]).

Lemma 4.21. *([4]) The barbell $\delta_k = \theta_k(e_{k-1}, e_{k-2})$ with $k \geq 4$ has one type 3 intersection*

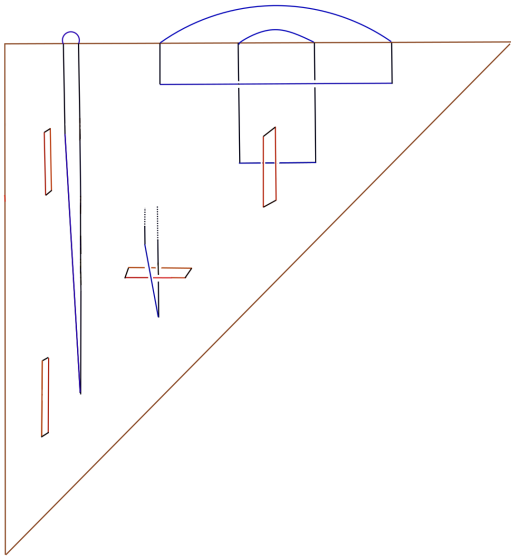

Figure 4.12: $(t^{\alpha}\mathrm{Co}_2^1, t^{\beta-\alpha}\mathrm{Co}_1^3)$, contributes $t_1^{2-k}t_3^0$.

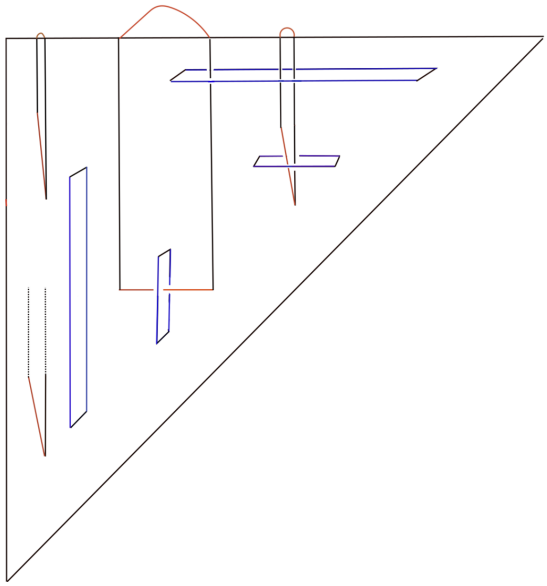

Figure 4.13: $(t^{\alpha}\mathrm{Co}_2^1, t^{\beta-\alpha}\mathrm{Co}_1^3)$, contributes 0.

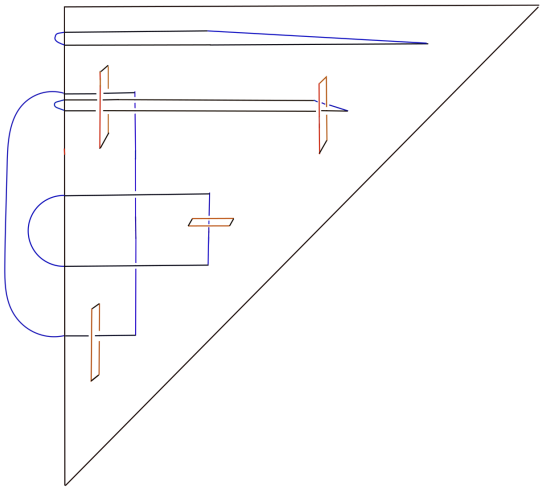

Figure 4.14: $(t^{\alpha-\beta}\mathrm{Co}_3^1, t^{\beta}\mathrm{Co}_2^3)$, contributes $t_1^0t_3^{2-k}$.

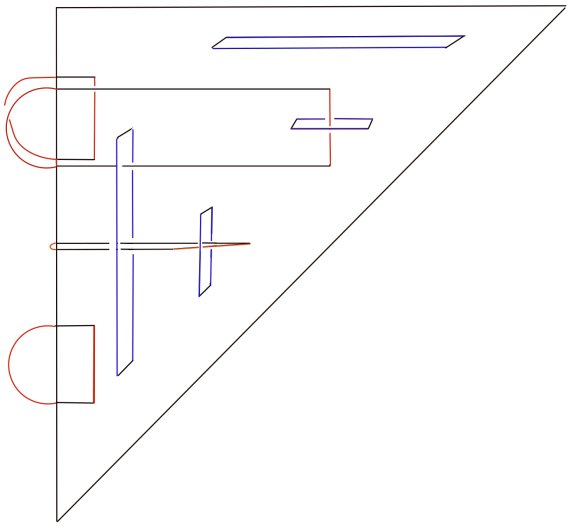

Figure 4.15: $(t^{\alpha-\beta}\mathrm{Co}_3^1, t^{\beta}\mathrm{Co}_2^3)$, contributes 0.

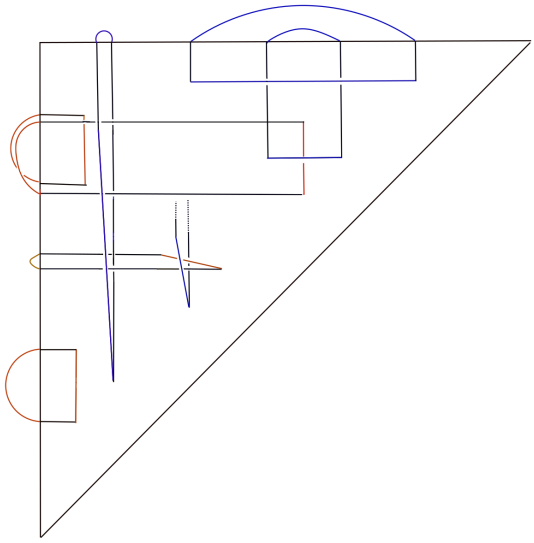

Figure 4.16: $(t^{\alpha}\mathrm{Co}_2^1, t^{\beta}\mathrm{Co}_2^3)$, contributes $-t_1^{k-2}t_3^{k-2}$.

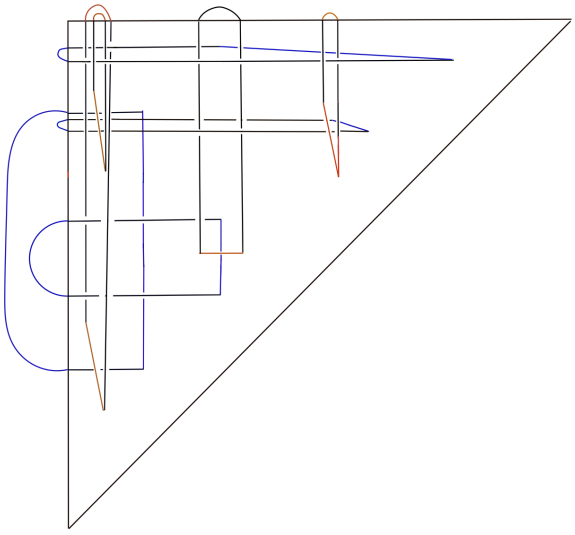

Figure 4.17: $(t^{\alpha}\mathrm{Co}_2^1, t^{\beta}\mathrm{Co}_2^3)$, contributes $-t_1^{k-2}t_3^{k-2}$.

point that contributes

$$-t_1^{2-k}t_3^{1-k} - t_1^{2-k}t_3^{1-k} - t_1^{2-k}t_3^1 + t_1^{1-k}t_3^{-1} + t_1^{k-1}t_3^1 + t_1^1t_3^{k-1} + t_1^{-1}t_3^{1-k} - t_1^1t_3^{2-k}$$

and $k-2$ type 2 intersection points, each of which contributes

$$t_1^{-1}t_3^{1-k} + t_1^{1-k}t_3^{-1} - t_1^{2-k}t_3^1 - t_1^1t_3^{2-k}.$$

Lemma 4.21 concerns the barbell δ_k (see Figure 4.18) which has no type 1 but only type 2 and type 3 intersection points. Although δ_k and δ_k' are different barbells, by Lemma 4.19, the type 2 intersection points of both barbells can be calculated following the same process, but with modifications to the exponents of t_1 and t_3 terms based on the number of times one needs to travel (along the bar) along the circle direction of $S^1 \times D^3$ from one point of a cohorizontal pair to the other, as mentioned before. For example, in the top left picture of Figure 16 of [4], the linking number of the preimage of the pair $(t^{\alpha}\mathrm{Co}_2^1, t^{\beta-\alpha}\mathrm{Co}_1^3)$ was calculated. We can use the same picture to calculate the same linking number for δ_k' instead of δ_k by changing the exponents of t by changing $1-k$ to $2-k$, and $k-1$ to $k-2$, leading to $-t_1^{2-k}t_3^0$ rather than $-t_1^{2-k}t_3^1$ in [4].

Therefore, using Figures 16 and 17 of [4], we can calculate W_3 of δ_k' in full. In particular,

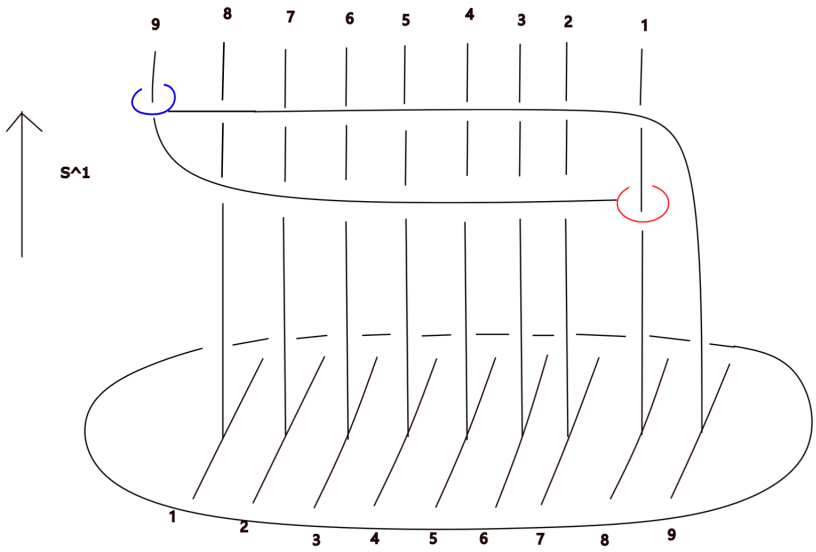

Figure 4.18: The embedded barbell δ_{10}.

one can verify that the $k-3$ type 2 intersection points contribute 0 (more to discuss below in Lemma 4.23) and the last intersection point contributes:

$$t_1^0 t_3^{k-2} + t_1^{k-2} t_3^0 - t_1^{2-k} t_3^{2-k} - t_1^{2-k} t_3^{2-k}.$$

Again, changes to the t powers need to be made to the formulas in [4] based on the number of times a cohorizontal point needs to travel (along the bar) along the circle direction to get to the cuff sphere with the same colour (with signs accounted by the pulled back orientations as in [4]). Taking the sum of the above two polynomials and applying the Hexagon relation twice, we deduce that $W_3(\delta'_k) = 0$ for $k \geq 3$.

Proposition 4.22. *For $k \geq 3$, we have*

$$\begin{aligned} W_3(\delta'_k) &= -t_1^{k-2}t_3^{k-2} - t_1^{k-2}t_3^{k-2} + t_1^{2-k}t_3^0 + t_1^0 t_3^{2-k} + t_1^0 t_3^{k-2} + t_1^{k-2}t_3^0 - t_1^{2-k}t_3^{2-k} - t_1^{2-k}t_3^{2-k} \\ &= -(t_1^{k-2}t_3^{k-2} + t_1^{k-2}t_3^{k-2}) - (t_1^{2-k}t_3^{2-k} + t_1^{2-k}t_3^{2-k}) + (t_1^{2-k}t_3^0 + t_1^0 t_3^{k-2}) + (t_1^0 t_3^{2-k} + + t_1^{k-2}t_3^0) \\ &= 0 \end{aligned}$$

by applying the Hexagon relation (see the discussion before Proposition 4.11).

More generally, by Lemma 4.19, we can write down a generalised formula for calculating

the W_3 invariant of any $\theta_k(e_i, e_j)$ with $i + j \geq k$ since the shapes of the triangle and tetrahedron pictures we presented (together with Figures 16 and 17 presented in Section 3 of [4]) remain unchanged. For $\theta_k(e_i, e_j)$ with $1 \leq i \leq j \leq k-1$ and $k \geq 3$, if we use the convention that e_i controls the position of the red cuff and e_j controls the position of the blue cuff, then the exponents $\alpha, \beta, \alpha - \beta, \beta - \alpha$ of t in each of the cohorizontal submanifolds in the pair

$$(t^{\alpha}\mathrm{Co}_2^1 - t^{\alpha-\beta}\mathrm{Co}_3^1, t^{\beta-\alpha}\mathrm{Co}_1^3 - t^{\beta}\mathrm{Co}_2^3),$$

can be described in terms of i and j (via colour constituents as proposed on p.26 of [4]): $\pm i$ for the red constituent part and $\pm j$ for the blue constituent part.

Therefore, we have the following theorem.

Theorem 4.23. *For $k \geq 3$, the polynomial we obtain from a type 1 intersection from $\theta_k(e_i, e_j)$ with $i + j \geq k$ is*

$$-t_1^j t_3^i - t_1^i t_3^j + t_1^{-i} t_3^{j-i} + t_1^{j-i} t_3^{-i}.$$

Based on Budney–Gabai's calculations, we also have the formula for a type 2 intersection point:

$$-t_1^{-j} t_3^{i-j} + t_1^{-i} t_3^{j-i} + t_1^{j-i} t_3^{-i} - t_1^{i-j} t_3^{-j}$$

and for a type 3 intersection point:

$$-t_1^{-j} t_3^{-i} - t_1^{-i} t_3^{-j} - t_1^{-j} t_3^{i-j} + t_1^{-i} t_3^{j-i} + t_1^{i} t_3^{i-j} + t_1^{i-j} t_3^{i} + t_1^{j-i} t_3^{-i} - t_1^{i-j} t_3^{-j}.$$

Combining Lemma 4.19 and Theorem 4.23 allows us to write down the W_3 invariant for any $\theta_k(e_i, e_j)$ with $k \geq 3$ and $i + j \geq k$. For example, one can verify that when $i = j = k - 1$,

$$W_3(\Phi_{\delta_k'}) = W_3(\Phi_{\theta_k(e_{k-1}, e_{k-1})}) = 0$$

using Theorem 4.23.

We mentioned in the beginning of Section 4.4 that Budney–Gabai discovered an alternative method of calculating the W_3 invariant for $\theta_k(e_i, e_j)$ for all possible i and j in [3]. In particular, they produced a formula for $\theta_k(e_i, e_j)$ in terms of their fundamental classes $G(p, q) \in \pi_2\mathrm{Emb}(I, S^1 \times D^3)$:

$$\begin{aligned}[\theta_k(e_i, e_j)] = (k-i-1)(D(-j,i) - D(i-j,-i)) \\ + (k-j-1)(D(i,-j) - D(i-j,j)) + (i+j+1-k)D(i,-j)\end{aligned}$$

for $k \geq 4$ where $D(i,j) = -G(j,-i) + G(-j,i) - G(i,-j) + G(-i,j)$, and they calculated that $W_3(G(i,j)) = t_1^{i-j}t_3^{-j}$. See Example 3.6 of [3]. One can verify that for $i + j \geq k$, our formula in Theorem 4.23 coincides with their formula. For example,

$$\begin{aligned}&W_3(D(-j,i) - D(i-j,-i)) \\ &= (-t_1^{i-j}t_3^{-j} + t_1^{j-i}t_3^{j} - t_1^{i-j}t_3^{i} + t_1^{j-i}t_3^{-i}) - (-t_1^{-j}t_3^{i-j} + t_1^{j}t_3^{j-i} - t_1^{-j}t_3^{-i} + t_1^{j}t_3^{i}) \\ &= t_1^{i}t_3^{j} - t_1^{-j}t_3^{-i} + t_1^{-i}t_3^{j-i} + t_1^{i-j}t_3^{j} \\ &= -t_1^{j}t_3^{i} - t_1^{i}t_3^{j} + t_1^{-i}t_3^{j-i} + t_1^{j-i}t_3^{-i}\end{aligned}$$

by the Hexagon relation (cf. the end of Section 4.2) which indicates that the two formulae for a type 1 intersection point coincide.

Remark. So far we have calculated W_3 of $\theta_k(e_i, e_j)$ with $i + j \geq k$. To deal with $\theta_k(e_i, e_j)$ with $j \leq k - 1 - i$ (see Figure 4.19) using the method we discussed in this Chapter, there are three more types of intersection points that need to be considered. These are barbells such that there is no "overlap" between the two cuff spheres. In Figure 4.19, if we use the same scanning disk as before, then points on the left of the red cuff (including the one just below it) belong to type 4, points on the right of the blue cuff (including the one just below it) belong to type 6, and points in between the two cuff spheres belong to type 5. The scanning pictures of these are shown in Figure 4.20. Computing these types will improve Lemma 4.19 and Theorem 4.23. We may return to this point in future research.

We now discuss some properties of $W_3(\theta_k(v, w))$. The following lemma is partly a

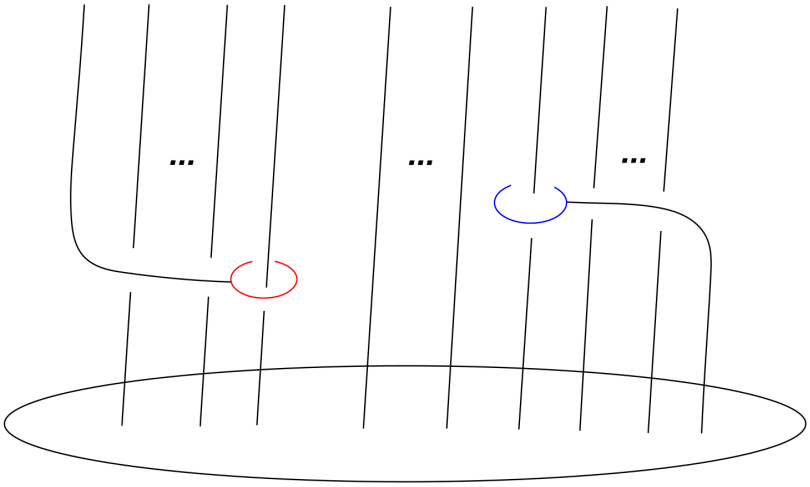

Figure 4.19: $\theta_k(e_i, e_j)$ with $i + j < k$.

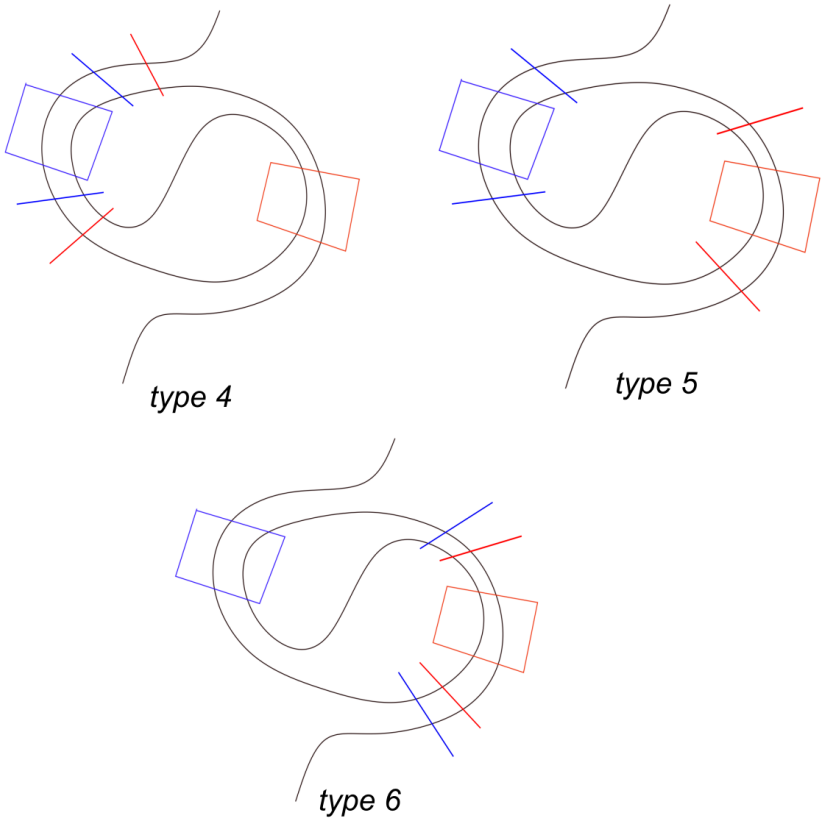

Figure 4.20: The extra three points of intersection points for $\theta_k(e_i, e_j)$ with $i + j < k$.

restatement of Corollary 7.18 in [3] (which is phrased in terms of certain fundamental classes $G(p,q)$ in $\pi_2\mathrm{Emb}(I, S^1 \times D^3)$ mentioned above) but in a different context and can be checked using Theorem 4.23 together with the Hexagon relation.

Lemma 4.24. *For $k > 0$, and suppose $i + j \geq k$, we have*

$$W_3(\theta_k(e_i, e_j)) = -W_3(\theta_k(e_j, e_i)).$$

Proof. By Theorem 4.23, we have

$$\begin{aligned}
&W_3(\theta_k(e_i, e_j)) = \\
&(k-i-1)(-t_1^j t_3^i - t_1^i t_3^j + t_1^{-i} t_3^{j-i} + t_1^{j-i} t_3^{-i}) + \\
&(-k+j+i-1)(-t_1^{-j} t_3^{i-j} + t_1^{-i} t_3^{j-i} + t_1^{j-i} t_3^{-i} - t_1^{i-j} t_3^{-j}) + \\
&(k-j-1)(-t_1^{-j} t_3^{-i} - t_1^{-i} t_3^{-j} - t_1^{-j} t_3^{i-j} + t_1^{-i} t_3^{j-i} + t_1^i t_3^{i-j} + t_1^{i-j} t_3^i + t_1^{j-i} t_3^{-i} - t_1^{i-j} t_3^{-j})
\end{aligned}$$

coming from the three types of intersection points. Note that the contribution of a type 2 intersection point is itself anti-symmetric. We show that the contributions of type 1 intersection points of $W_3(\theta_k(e_i, e_j))$ cancel with the contributions of type 3 intersection points of $W_3(\theta_k(e_j, e_i))$:

$$\begin{aligned}
&(k-i-1)(-t_1^j t_3^i - t_1^i t_3^j + t_1^{-i} t_3^{j-i} + t_1^{j-i} t_3^{-i}) + \\
&(k-i-1)(-t_1^{-i} t_3^{-j} - t_1^{-j} t_3^{-i} - t_1^{-i} t_3^{j-i} + t_1^{-j} t_3^{i-j} + t_1^j t_3^{j-i} + t_1^{j-i} t_3^j + t_1^{i-j} t_3^{-j} - t_1^{j-i} t_3^{-i}) \\
&= (k-i-1)(-(t_1^{-i} t_3^{-j} + t_1^j t_3^i) - (t_1^{-j} t_3^{-i} + t_1^i t_3^j) + (t_1^{-j} t_3^{i-j} + t_1^{j-i} t_3^j) + (t_1^j t_3^{j-i} + t_1^{i-j} t_3^{-j})) \\
&= (k-i-1)(-(t_1^{-i} t_3^{-j} + t_1^j t_3^i) - (r_1^{i-j} t_3^{-j} + t_1^j t_3^{j-i}) + (t_1^{-j} t_3^{i-j} + t_1^{j-i} t_3^j) + (t_1^j t_3^{j-i} + t_1^{i-j} t_3^{-j})) \\
&= 0.
\end{aligned}$$

Similarly, the contributions of type 3 intersection points of $W_3(\theta_k(e_i, e_j))$ cancels with the contributions of type 1 intersection points of $W_3(\theta_k(e_j, e_i))$. □

Remark. In fact, there is a direct way of proving Lemma 4.24 for all $1 \leq i, j \leq k-1$. We shrink $\theta_k(e_i, e_j)$ such that it is embedded in a smaller (4-dimensional) solid torus in

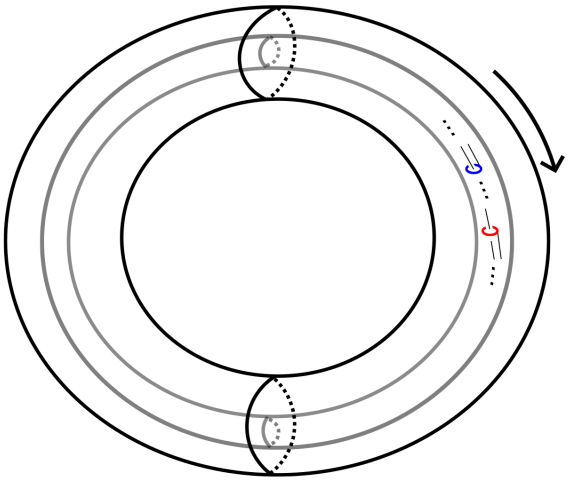

Figure 4.21: Anti-symmetric relation of $\theta_k(e_i, e_j)$.

$S^1 \times D^3$. Let ψ denote the rotation of this smaller solid torus in $S^1 \times D^3$ by π. See Figure 4.21 for a 3-dimensional picture. Now if we conjugate $\Phi_{\theta_k(e_i,e_j)}$ by ψ, the claim is we get $\Phi^{-1}_{\theta_k(e_j,e_i)}$. In other words, we have

$$\psi \Phi^{-1}_{\theta_k(e_j,e_i)} \psi^{-1} = \Phi_{\theta_k(e_i,e_j)}.$$

To see this, note that the image $\psi(\theta_k(e_i, e_j))$ is equal to $\theta_k(e_j, e_i)$ with the role of the two cuff spheres switched, and this switch corresponds to taking the inverse of the induced barbell diffeomorphism. But now since $\pi_0 \mathrm{Diff}(S^1 \times D^3, \partial)$ is abelian, we get exactly the antisymmetric relation we want.

The following lemma is a key observation for calculating the W_3 invariant of $\theta_k(v, w)$.

Lemma 4.25. *The W_3 invariant of $\theta_k(v, w)$ satisfies*

$$W_3(\theta_k(v, w)) = \Sigma v_i w_j W_3(\theta_k(e_i, e_j))$$

Proof. The idea is that we can analyze each set of cohorizontal points that arises from one of the possible pairs of vertical strands (one going through the red cuff and one going through the blue cuff) separately and take the sum. We now elaborate on this.

By isotoping $\theta_k(v, w)$ if necessary, we saw that the W_3 invariant is determined by the

$k-1$ intersections of the bar with the 3-ball $s_0 \times D^3$. First, note that

$$W_3(\theta_k(ae_i, e_j)) = aW_3(\theta_k(e_i, e_j))$$

for $a \in \mathbb{Z}$ where a indicates that the blue cuff B wraps around the i-th strand a times, counting from right to left. This is because $\theta_k(ae_i, e_j)$ produces a parallel copies of the 8 cohorizontal spheres, counting with a sign rather than only 8 cohorizontal spheres, near the blue cuff sphere for $\theta_k(e_i, e_j)$. Similarly, we have

$$W_3(\theta_k(e_i, be_j)) = bW_3(\theta_k(e_i, e_j)).$$

Next, if for $1 \leq i, j \leq k$, we let e_{ij} be the vector with all entries 0 except the i-th and j-th place being 1, then we have

$$W_3(\theta_k(e_{ij}, e_l)) = W_3(\theta_k(e_i, e_l)) + W_3(\theta_k(e_j, e_l)).$$

To see this, we observe that for each of the $k-1$ intersection points, $\theta_k(e_{ij}, e_l)$ has blue cohorizontal points near both the i-th strand and the j-th strand, counting from right to left. Each of these two sets of cohorizontal points pairs with the red cohorizontal points (near the l-th strand, counting from left to right) separately, precisely leading to the cohorizontal points of $\theta_k(e_i, e_l)$ and $\theta_k(e_j, e_l)$. Similarly, we have

$$W_3(\theta_k(e_l, e_{ij})) = W_3(\theta_k(e_l, e_i)) + W_3(\theta_k(e_l, e_j)).$$

More generally, we observe that

$$W_3(\theta_k(ae_i + be_j, ce_k + de_l) = acW_3(e_i, e_k) + adW_3(e_i, e_l) + bcW_3(e_j, e_k) + bdW_3(e_j, e_l).$$

for $a, b, c, d \in \mathbb{Z}$ since the cohorizontal points that arise from this barbell can be analysed separately in pairs in a similar way, leading to above combination. Now, the theorem follows from the combination of the above. $\square$

Essentially, Budney–Gabai proved the same result in a slightly different context (by directly homotoping $s_{s_0}(\theta_k(v,w))$ into a sum of their fundamental classes). See Theorem 8.1 of [3]. In the proof of Lemma 4.25, we break up the W_3 invariant of $\theta_k(v,w)$ into a sum of the W_3 of a set of "sub-barbells" $\theta_k(e_i,e_j)$ (where $i=j$ is allowed), each of which gives a parallel copy of a set of tetrahedron pictures.

More generally, any unknotted barbell in $S^1\times D^3$ represented by a word in $\langle\nu_R\rangle\backslash F_3/\langle\nu_B\rangle$ can be calculated in a very similar way. We first observe the following lemma.

Lemma 4.26. *Let $\mathcal{B}$ be an unknotted barbell in $S^1\times D^3$ represented by an element*

$$\nu_B^{i_1}t^{j_1}\nu_R^{k_1}\cdots\nu_B^{i_n}t^{j_n}\nu_R^{k_n}$$

in $\langle\nu_R\rangle\backslash F_3/\langle\nu_B\rangle$, where $n\in\mathbb{Z}$. Define $|\mathcal{B}|=j_1+\cdots+j_n$, i.e. it is the total signed number of times the bar of $\mathcal{B}$ loops around the circle factor of $S^1\times D^3$. Then $W_3(\mathcal{B})$ is equal to the sum

$$\sum_{i,j,\alpha,\beta} c_{i_\alpha k_\beta} W_3(\mathcal{B}_{i_\alpha k_\beta})$$

of W_3 invariants of a finite sequence of "sub-barbells" $\mathcal{B}_{i_\alpha k_\beta}$ with $\alpha,\beta\in\{1,2,\dots,n\}$, and coefficients $c_{i_\alpha k_\beta}$. Each $\mathcal{B}_{i_\alpha k_\beta}$ is an unknotted barbell satisfies the condition that the bar links each of the two cuff spheres only once positively, and is represented by a word in the form

$$t^{j_1}t^{j_2}\dots t^{j_{\alpha-1}}\nu_B^\alpha t^\alpha\dots t^\beta\nu_R^\beta\dots t^{j_n}$$

when $\alpha\le\beta$, and in the form

$$t^{j_1}t^{j_2}\dots t^{j_\beta}\nu_R^\beta t^{\beta+1}\dots t^{\alpha-1}\nu_B^\alpha\dots t^{j_n}$$

when $\alpha>\beta$. Also, $|\mathcal{B}_{i_\alpha k_\beta}|=|\mathcal{B}|$ for all α,β. Further, the coefficients satisfies

$$c_{i_\alpha k_\beta}=i_\alpha k_\beta.$$

Proof. The idea is the same as the proof of Lemma 4.25. We first break the information

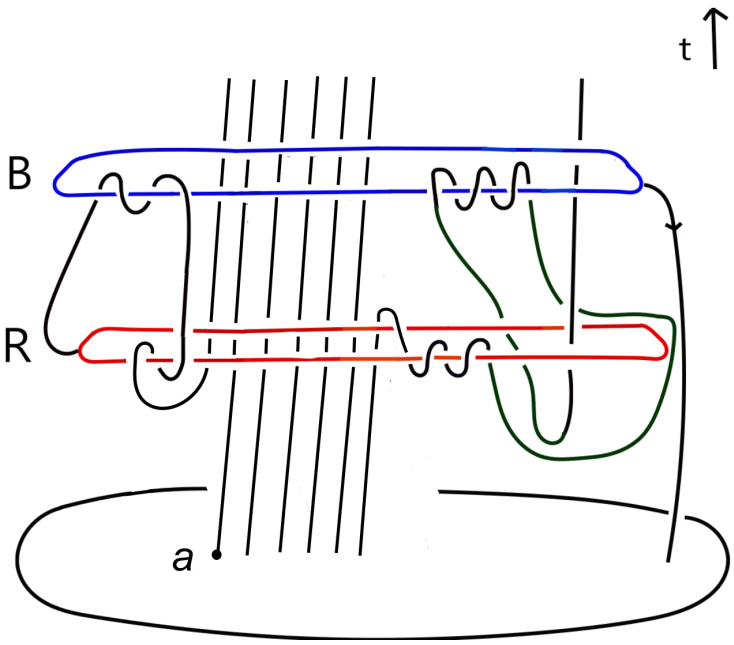

Figure 4.22: The barbell manifold $t^{-1}\nu_R\nu_B{}^3\nu_R{}^{-3}t^{-6}\nu_R\nu_B{}^2$.

of cohorizontal points from $\mathcal{B}$ into barbells in the form of

$$\cdots t^{j_1} \cdot \nu_B^{i_\alpha} t^{j_\alpha} \cdots \nu_R^{k_\beta} \cdots t^{j_n},$$

i.e. barbells that keep only a single power of ν_B and a single power of ν_R but keep all powers of t. Each such barbell leads to triangle and tetrahedron diagrams that contain a piece of information of cohorizontal points of $\mathcal{B}$. Next, we further observe that the exponents i_α and k_β have the effects of contributing to parallel copies of cohorizontal points of

$$\cdots t^{j_1} \cdot \nu_B^{1} t^{j_\alpha} \cdots \nu_R^{1} \cdots t^{j_n}$$

leading to coefficients $c_{i_\alpha k_\beta} = i_\alpha k_\beta$. □

Example 4.27. Take the barbell represented by the word $t^{-1}\nu_R\nu_B{}^3\nu_R{}^{-3}t^{-6}\nu_R\nu_B{}^2$ as in Figure 4.22. Note that $|t^{-1}\nu_R\nu_B{}^3\nu_R{}^{-3}t^{6}\nu_R\nu_B{}^2| = -7$. Scanning through a chosen D^3 as in Figure 4.22 gives rise to 7 intersection points that can be analyzed separately. For example, at the first intersection point a (counting from left to right), we can similarly draw its intersection with the spanning disks of the cuff spheres as in Figure 4.23.

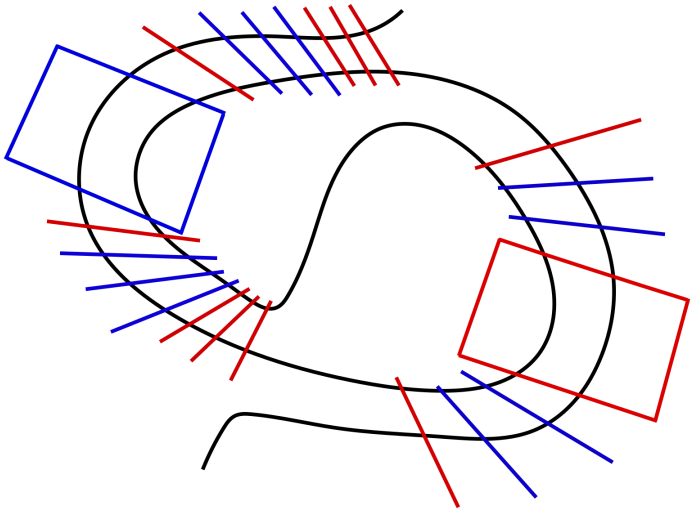

Figure 4.23: The intersection between the arc through point a and the spanning disks of the cuff spheres.

In this case, one takes all possible pairs of two symmetric red arcs with two symmetric blue arcs, and every such pair leads to exactly the same pattern of linking number diagrams. The W_3 invariant of $t^{-1}\nu_R{\nu_B}^3{\nu_R}^{-3}t^{-6}\nu_R{\nu_B}^2$ is the sum of all these possible pairs at each intersection point of the bar with the scanning disk D^3. In particular, the above barbell can be factored into the following sub-barbells:

- $3t^{-1}\nu_R\nu_B t^{-6}$
- $2t^{-1}\nu_R t^{-6}\nu_B$
- $9t^{-1}\nu_B\nu_R^{-1}t^{-6}$
- $6t^{-1}\nu_R^{-1}t^{-6}\nu_B$
- $3t^{-1}\nu_B t^{-6}\nu_R$
- $2t^{-7}\nu_R\nu_B$.

For example, Figure 4.24 shows the barbell $t^{-1}\nu_R\nu_B t^{-6}$. In fact, this barbell is isotopic to the barbell $\theta_7(e_6, e_1)$ by dragging the blue cuff B in Figure 4.24 downwards along the bar to the t negative direction for one time. Therefore, its W_3 invariant can be calculated using Theorem 4.23. Further, one can verify, by drawing pictures, that except

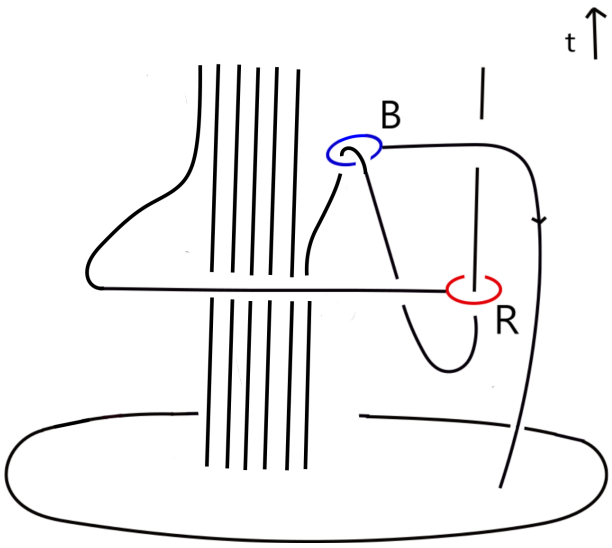

Figure 4.24: The barbell $\theta_k(e_7, -e_1)$.

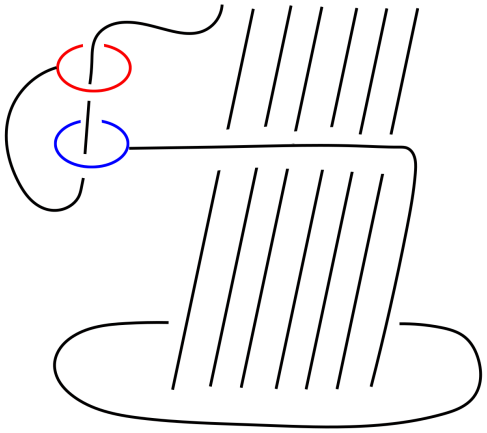

Figure 4.25: The barbell $t^{-7}\nu_R\nu_B$.

for $t^{-7}\nu_R\nu_B$, each of the above sub-barbells can be identified with some $\theta_k(\pm e_i, \pm e_j)$ for some $i, j \in \{1, \ldots, 7\}$, and $k \leq 8$. In particular, we have

$$W_3(t^{-1}\nu_R\nu_B{}^3\nu_R{}^{-3}t^{-6}\nu_R\nu_B{}^2) =$$
$$3W_3(\theta_8(e_6, e_7)) + 2W_3(\theta_8(e_6, e_7)) + 9W_3(\theta_8(-e_7, e_1)) +$$
$$6W_3(\theta_8(-e_6, e_7) + 3W_3(\theta_8(e_1, e_1)) + 2W_3(t^{-7}\nu_R\nu_B),$$

in which all terms can be easily calculated using Theorem 4.23 except $W_3(t^{-7}\nu_R\nu_B)$ (See Figure 4.25).

The barbell $t^{-7}\nu_R\nu_B$ is not isotopic to a $\theta_k(v, w)$. However, we can calculate its W_3

invariant fairly easily by observing that its bar intersects $s_0 \times D^3$ at 7 points and all of these 7 points give rise to tetrahedron pictures with the same shape as a type 3 intersection point shown in Figure 4.10. In particular, we can make use of Figure 17 of [4] together with the strategy we have been discussing throughout this section to obtain a slightly variant formula as in Theorem 4.23. Namely, we take the formula for type 3 points in Theorem 4.23, and plug in $i = j = 7$.

Remark. For a barbell represented by a word

$$\cdots t^{j_1} \cdot \nu_B^1 t^{j_\alpha} \cdots \nu_R^1 \cdots t^{j_n}$$

such that at least one of $j_1, \ldots, j_n$ is positive, one can calculate its W_3 invariant by framing a variation of Theorem 4.23 following essentially the same strategy we have been discussing in this section and then to calculate the W_3 of a barbell represented by any random word. However, we do not have time to finish these discussions in this thesis and may return to this in the future.

We end this section (and chapter) with a discussion of the question of which barbells give rise to linearly independent barbell diffeomorphisms. First, note that $\pi_0\mathrm{Diff}(S^1 \times D^3, \partial)$ is abelian. This can be seen by noting that we can shrink the supports of any two diffeomorphisms to two smaller 4-dimensional solid tori to make them commute. Therefore, it makes sense to talk about linear independence of diffeomorphisms (up to isotopy) in this group. Budney–Gabai (using Lemma 4.21) proved that

$$W_3(\delta_k) = W_3(\theta_k(e_{k-1}, e_{k-2}))$$

for $k \geq 4$ are linearly independent. Thus $\delta_k = \theta_k(e_{k-1}, e_{k-2})$ for $k \geq 4$ are linearly independent diffeomorphisms of $S^1 \times D^3$.

For $k \geq 6$, we can apply Theorem 4.23 to calculate $W_3(\theta_k(e_{k-1}, e_{k-3}))$. By setting all terms $t_1^p t_3^q = 0$ of $W_3(\theta_k(e_{k-1}, e_{k-3}))$ except when $p - q = k - 1$, we get

$$-(k-1)t_1^2 t_3^{3-k}$$

which is nonzero. Furthermore, if a finite combination of $\theta_n(e_{n-1}, e_{n-3})$, for $1 \leq n \leq k$, (i.e. k is the largest n)

$$a_6\theta_6(e_5, e_3) + a_7\theta_7(e_6, e_4) + \cdots + a_k\theta_k(e_{k-1}, e_{k-3}) = 0$$

equals 0, then setting all terms $t_1^p t_3^q$ except when $p - q = k - 1$ kills $\theta_n(e_{n-1}, e_{n-3})$ with $n < k$. This implies that the coefficient a_k before $\theta_k(e_{k-1}, e_{k-3})$ is 0. Therefore, we deduce that the set $\{\theta_k(e_{k-1}, e_{k-3})\}_{k\geq 6}$ is linearly independent. Furthermore, by Corollary 8.2 of [3], the same argument applied to $\delta_k = \theta_k(e_{k-1}, e_{k-2})$ gives rise to

$$-(k-1)t_1^1 t_3^{2-k} \neq 0$$

which implies that the set $\{\delta_k, \theta_k(e_{k-1}, e_{k-3})\}_{k\geq 6}\}$ is linearly independent.

By applying Theorem 4.23 again to $W_3(\theta_k(e_{k-1}, e_{k-m}))$ for $k > m + 1$, and following the same argument above, namely by setting all terms $t_1^p t_3^q$ in $W_3(\theta_k(e_{k-1}, e_{k-m}))$ to zero except when $p - q = k - 1$, one deduces that the set of barbells

$$\{\theta_k(e_{k-1}, e_{k-m})\}_{m\in\{3,\ldots,[(k-1)/2]-1\},k\geq 2m-1}$$

is linearly independent. Here $[(k-1)/2]$ denotes the integer part of $(k-1)/2$. Therefore, we have the following theorem.

Theorem 4.28. *The elements $\theta_k(e_{k-1}, e_{k-3})$ for $k \geq 6$ of $\pi_0\mathrm{Diff}(S^1 \times D^3, \partial)$ are linearly independent. Further, these elements are linearly independent to*

$$\delta_k = \theta_k(e_{k-1}, e_{k-2}) = \theta_k((0, \ldots, 0, 1), (0, \ldots, 0, 1, 0))$$

for $k \geq 4$.

More generally, there exist linearly independent elements $\theta_k(e_{k-1}, e_{k-m})$ of $\pi_0\mathrm{Diff}(S^1 \times D^3, \partial)$ for $m \in \{3, 4, \ldots, [(k-1)/2] - 1\}$ with $k \geq 2m - 1$. Here $[(k-1)/2]$ is the integer part of $(k-1)/2$.

We can also consider $\theta_k(e_{k-2}, e_{k-m})$ with $k \geq 4$, $m \in \{3, 4, \ldots, k-2, k-1\}$ and $k - m > 2$, and apply Theorem 4.23. Setting all terms of $W_3(\theta_k(e_{k-2}, e_{k-m}))$ in the form of $t_1^p t_3^q$ to zero except when $p - q = k - 2$ gives rise to

$$-(k-2)t_1^{m-2}t_3^{m-k}$$

which is non-zero if $k - m \neq m - 2$, i.e. $2m \neq k + 2$. By the Hexagon relation together with Theorem 4.23,

$$W_3(\theta_k(e_{k-2}, e_{k-m}) + \theta_k(e_{k-2}, e_{m-2})) = 0$$

in this quotient. It follows that for a fixed $k \geq 4$, there are $(k-3)/2$ linearly independent terms for k odd and $(k-2)/2$ linearly independent terms for k even.

For example, when $k = 10$, the linearly independent terms we get are

$$\theta_{10}(e_8, e_7), \theta_{10}(e_8, e_6), \theta_{10}(e_8, e_5), \theta_{10}(e_8, e_4).$$

Question 4.29. *More generally, for a fixed $\alpha, \beta \geq 1$, $m > \alpha$ and $n > \beta$, one can ask if the barbells $\theta_{k_1}(e_{k_1-\alpha}, e_{k_1-m})$ and $\theta_{k_2}(e_{k_2-\beta}, e_{k_2-n})$ are linearly independent.*

One possible approach is to set all terms $t_1^p t_3^q$ to zero except when $p-q$ equals to $m-\alpha$ or $n-\beta$. If we assume $n - \beta \neq \alpha - m$ or $k_1 - \alpha$ or $k_1 - m$, and $m - \alpha \neq k_2 - \beta$ or $k_2 - n$, then we get two polynomials $-(k_1 - \alpha)t_1^{m-\alpha}t_3^{m-k_1}$ and $-(k_2 - \beta)t_1^{n-\beta}t_3^{n-k_2}$ which are linearly dependent if and only if $m - \alpha = k_2 - n$ and $m - k_1 = \beta - n$. If $\alpha = \beta$, the above conditions imply that $k_1 = k_2$ and $m + n = k_1 + \alpha$. Similarly, if $k_1 = k_2$, then the above conditions imply that $\alpha = \beta$ and $m + n = k_1 + \alpha$.

We plan to return to this topic in the future.

Chapter 5

W_3 invariant for $\pi_0\mathrm{Diff}(\natural_m S^1 \times D^3)$

This chapter is motivated by and is part of an ongoing but unfinished project whose aim is to find isotopically non-trivial splitting 3-spheres of the 2-dimensional unlink in S^4. In this chapter, we give ideas for defining a version of the W_3 invariant for $\pi_0\mathrm{Diff}(\natural_m S^1 \times D^3)$ with $m \geq 2$ where $\natural_m S^1 \times D^3$ denotes the boundary connected sum of m copies of $S^1 \times D^3$. We will then focus on the $m = 2$ case, and study the mapping class group $\pi_0\mathrm{Diff}(\natural_2 S^1 \times D^3)$. Finally, in Section 5.4 we describe the unfinished part about how the above might be applied, potentially leading to an infinite sequence of knotted splitting 3-spheres of the unlink in S^4.

5.1 CAT(0)-cubical complexes

In this section, we review the notion of CAT(0)-cubical complexes that will be needed in later sections. Most of the material can be found in [23].

We start with a brief motivation. Recall from Lemma 4.15 that W_3 can be calculated using a special class of submanifolds of the universal cover of $C_3[S^1 \times D^3]$. In this chapter, we will calculate a version of W_3 for $\pi_0\mathrm{Diff}(\natural_m S^1 \times D^3)$, for $m \geq 2$, using a similar method and a special class of submanifolds of the universal cover of $C_3[\natural_m S^1 \times D^3]$, called the **co-geodesic submanifolds** (cf. Definition 5.12) whose definitions depend on the unique existence of geodesics. In particular, we need the fact that the universal cover of

$C_3[\natural_m S^1 \times D^3]$ is a uniquely geodesic space. We shall achieve this by giving it a CAT(0) cubical complex structure (cf. Theorem 5.6 and Lemma 5.8).

Let $C^n = [0,1]^n$ denote the n-dimensional cube. The (codimension 1) faces of C^n are given by $F_{i,\epsilon} = \{x = (x_1, \ldots, x_n) \in C^n \colon x_i = \epsilon\}$ for $\epsilon = 1$ or 0. Lower-dimensional faces are obtained by intersections of the codimension 1 faces. We equip cubes with the restricted Euclidean metric.

Definition 5.1. Let $\mathcal{C}$ be a set of cubes and $\mathcal{S}$ a set of isometries between faces of the cubes called gluing maps such that no cube is glued to itself, and there are at most two distinct gluings between any two distinct cubes. Then such a pair defines a space $\bigcup_{C\in\mathcal{C}} C/\sim$ where $\sim$ is the equivalence relation induced by the gluing maps. This is called a cubical complex.

Definition 5.2. Let X be a cubical complex and $x, y \in X$. A string Σ from x to y is a sequence of points $x = x_0, x_1, \ldots, x_m = y$ such that each pair of consecutive points x_i and x_{i+1} in the sequence is contained in a single cube C_i. The length $L(\Sigma)$ of a string Σ is given by the sum $\sum_i d_{C_i}(x_i, x_{i+1})$ where d_{C_i} is the Euclidean metric on C_i. If X is string connected, meaning that any two points are connected by a string of intervals, then we equip it with the polyhedric metric:

$$d(x,y) = \inf\{L(\Sigma) \colon \ \Sigma \text{ is a string from } x \text{ to } y\}.$$

The polyhedric metric can be equivalently defined as

$$d(x,y) = \inf\{l(\gamma) \colon \gamma \text{ is a rectifiable curve in } X \text{ from } x \text{ to } y\}.$$

where a rectifiable curve $\gamma \colon [0,1] \to X$ means a curve with finite length

$$l(\gamma) := \sup_{0=t_0\le\cdots\le t_n=1} \sum_{i=1}^{n-1} d(\gamma(t_i), \gamma(t_{i+1}))$$

Definition 5.3. A cubical complex is *finite dimensional* if there is an upper bound on the dimension of cubes.

Proposition 5.4. *Finite-dimensional cubical complexes are complete geodesic spaces.*

Definition 5.5. The link of a vertex v of a cubical complex X is the induced simplicial complex obtained from X by taking the space $S(v, \epsilon) = \{x \in X : d(x, v) = \epsilon\}$ for a small $\epsilon \geq 0$. A link is called *flag* if there are no empty simplices, i.e. whenever the 1-skeleton of a simplex exists, so does the entire simplex (i.e. the higher dimensional faces all exist).

The next theorem will be crucial for us:

Theorem 5.6. *A cubical complex X is CAT(0) if and only if it is simply-connected and all links are flag.*

This is called **Gromov's link condition** due to Gromov. In particular, this implies that such cubical complexes are uniquely geodesic spaces.

Both Proposition 5.4 and Theorem 5.6 can be found in Section 3 of [23].

5.2 Definitions and construction

In this section, we extend the construction in Section 4.2 to $\natural_m S^1 \times D^3$ for $m \geq 2$.

Let $n \geq 1$. Since the fibration

$$C_n(\natural_m S^1 \times D^3) \to C_{n-1}(\natural_m S^1 \times D^3)$$

admits a section (see for example Section 4 of [7]), we see that the homotopy groups of the ordered configuration space $C_n(\natural_m S^1 \times D^3)$ are isomorphic to the homotopy groups of the product $X_0 \times X_1 \times \cdots \times X_{n-1}$ with X_i being $\natural_m S^1 \times D^3$ with i punctures. In other words, we can understand the homotopy groups of $C_n(\natural_m S^1 \times D^3)$ by understanding the homotopy groups of

$$(\vee_m S^1) \times (\vee_m S^1 \vee S^3) \times (\vee_m S^1 \vee S^3 \vee S^3) \times \cdots \times (\vee_m S^1 \vee_{n-1} S^3).$$

The fundamental group $\pi_1 C_n(\natural_m S^1 \times D^3)$ is thus generated by nm generators $(t_1)_i, (t_2)_i, \ldots (t_n)_i$ for $i = 1, 2, \ldots, m$. The third rational homotopy group $\pi_3 C_n(\natural_m S^1 \times D^3) \otimes \mathbb{Q}$ is generated

by elements of the form of $(t_l)_i.\omega_{jk}$ where $i = 1, 2, \ldots, m$ and $l,\ j,\ k \in \{1, 2, \ldots, n\}$ with the following relations:

- $\omega_{ij} = \omega_{ji}$
- $\omega_{ii} = 0$
- $(t_l)_i.\omega_{jk} = \omega_{jk}$ if $l \notin \{j, k\}$
- $(t_j)_i.\omega_{jk} = (t_k)_i^{-1}.\omega_{jk}$.

Again, as in Chapter 4, ω_{ij} denotes the element with all points fixed except the j-th point orbiting around the i-th point. The fifth rational homotopy group $\pi_5 C_n(\natural_m S^1 \times D^3) \otimes \mathbb{Q}$ is generated by the Whitehead products of the above elements satisfying the following extra relations:

- $[\omega_{ij}, \omega_{lm}] = 0$ if $\{i, j\} \cap \{l, m\} = \emptyset$
- $[\omega_{ij}, \omega_{jl}] = [\omega_{jl}, \omega_{li}] = [\omega_{li}, \omega_{ij}]$
- $(t_l)_i.[f, g] = [(t_l)_i.f, (t_l)_i.g]$.

In the following, we set up preparations for the construction and definition of an invariant

$$(W_3)_m \colon \pi_0\mathrm{Diff}(\natural_m S^1 \times D^3, \partial) \to \pi_2\mathrm{Emb}(I, \natural_m S^1 \times D^3; I_0) \to \pi_5 C_3'[\natural_m S^1 \times D^3] \otimes \mathbb{Q}/R$$

where I_0 is a chosen properly embedded interval which we will elaborate on shortly, and R represents some relations that will be discovered in this section. As in Chapter 4, this will be defined as a composition of two maps, namely the scanning map s, which depends on a choice of a properly embedded 3-ball in $\natural_m S^1 \times D^3$, and a map defined on $\pi_2\mathrm{Emb}(I, \natural_m S^1 \times D^3; I_0)$ that relies on the mapping space model ([25]) as discussed in Section 4.1.

Opposite to what we did in Section 4.2, this time we start with the second map. For $f \in \pi_1\mathrm{Emb}(I, \natural_m S^1 \times D^3; I_0)$, following the same strategy as in Section 4.2, we first define

a map

$$(\overline{ev}_2)_m(f)\colon S^1 \times C_2[I] \to C'_2[\natural_m S^1 \times D^3].$$

whose domain can be closed into a 3-sphere. By applying D. Sinha's mapping space model [25] as discussed in the end of Section 4.1, in the same way as it was applied in Section 4.2, we have the second evaluation

$$ev_2(f)\colon S^1 \times C_2[I] \to C'_2[\natural_m S^1 \times D^3].$$

Its restriction to the three boundary facets of $C_2[I]$, which we denote by $x_1 = 0$, $x_2 = 1$ and $x_1 = x_2$, are null homotopic since the codomain for each of these sub-strata is homotopy equivalent to $(S^1 \vee S^1) \times S^3$ with

$$\pi_2(S^1 \vee S^1) \times S^3 = \pi_1\Omega((S^1 \vee S^1) \times S^3) = 0.$$

By attaching null homotopies along these boundary facets, one obtains a map

$$(\overline{ev}_2)_m(f)\colon S^3 \to C'_2[\natural_m S^1 \times D^3].$$

Lemma 5.7. *For $f \in \pi_1\mathrm{Emb}(I, \natural_m S^1 \times D^3; I_0)$, $(\overline{ev}_2)_m(f)$ defines an element in the homotopy group $\pi_3 C'_2[\natural_m S^1 \times D^3] \otimes \mathbb{Q} \cong \mathbb{Z}[t_1^{\pm}, t_2^{\pm} \ldots, t_m^{\pm}] \oplus \mathbb{Z}^2$ modulo the following relations:*

- *(0,1,0) for $x_1 = 0$ facet*
- *(1,1,1) for the $x_1 = x_2$ facet*
- *(0,0,1) for the $x_2 = 1$ facet,*

where the first coordinate represents the Laurent polynomials part and the remaining two coordinates represent the $\mathbb{Z}^2$ part, which represents the degrees of the two velocity vectors.

Proof. These relations are obtained from the inclusions of the edges. The first relation comes from the inclusion map $C'_1[I] \cong \{x_1 = 0\} \times S^3 \to C'_2[I]$ of the $x_1 = 0$ edge sending

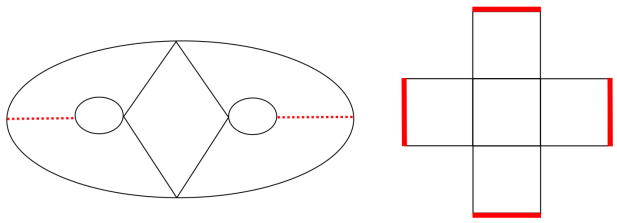

Figure 5.1: The fundamental domain of the universal cover of $S^1 \times D^3 \natural S^1 \times D^3$.

$((0, x_2), 1) \to (0, x_2, 1, 0)$. Therefore, the induced map

$$\pi_3 C_1'[\natural_m S^1 \times D^3] \cong \mathbb{Z} \to \pi_3 C_2'[\natural_m S^1 \times D^3] \cong \mathbb{Z}[t_1^{\pm}, t_2^{\pm} \ldots, t_m^{\pm}] \oplus \mathbb{Z}^2$$

is given by $1 \to (0, 1, 0)$. The third relation is obtained in exactly the same way, but with an induced map $1 \to (0, 0, 1)$. The second relation comes from the inclusion of the edge $x_1 = x_2$ sending $((x_1, x_1), 1)$ to $(x_1, t_1^0 t_2^0 . x_1, 1, 1)$. □

Therefore, we have defined a homomorphism

$$(\overline{ev}_2)_m \colon \pi_1 \mathrm{Emb}(I, \natural_m S^1 \times D^3) \to \mathbb{Z}[t_1^{\pm}, t_2^{\pm} \ldots, t_m^{\pm}]/\langle 1 \rangle.$$

This map will guide the way of our construction of $(W_3)_m$ below.

Next, to define the third stage map

$$(\overline{ev}_3)_m \colon \pi_2 \mathrm{Emb}(I, \natural_m S^1 \times D^3) \to \pi_5 C_3'[\natural_m S^1 \times D^3] \otimes \mathbb{Q}/R,$$

we first take a look at the universal cover of $\natural_m S^1 \times D^3$. This space can be described as follows. Take a 2-dimensional disk, remove m disjoint sub-disks from it and cut along a disjoint union of homotopically trivial (relative to the boundary) arcs connecting each of the sub-disks to the boundary of the big disk. See Figure 5.1 for the case $m = 2$. This gives us a fundamental domain. We then build a space T_m by gluing infinitely many fundamental domains together along their cut edges (drawn in red in Figure 5.1). The (4-dimensional) universal cover $T_m \times I \times I$ is obtained by taking product with I^2. We call the space $U_m \colon T_m \times I \subset T_m \times I^2$ the *universal tree*. We will focus on the case where

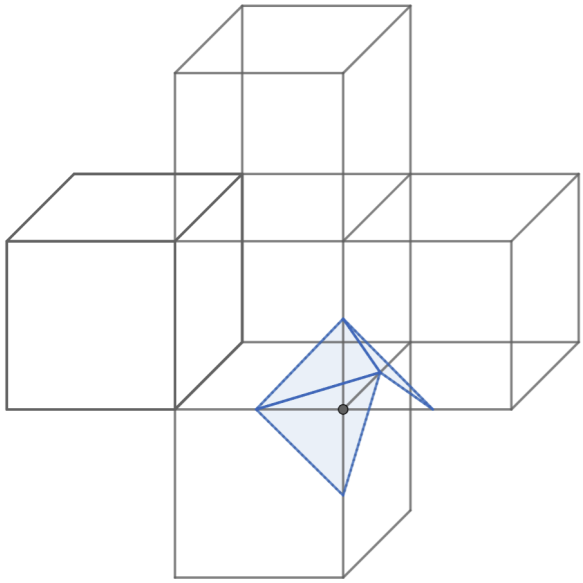

Figure 5.2: The links of the universal cover $T_2 \times I \times I$.

$m = 2$.

Lemma 5.8. *The space $T_2 \times I \times I$ admits a natural cubical complex structure (cf. Section 5.1) which contains 5 4-dimensional cubes in each fundamental domain. Furthermore, all links of this cubical complex are flag. Thus, it is a uniquely geodesic metric space whose geodesics are concatenations of straight intervals.*

Proof. One can verify that each link of $T_2 \times I \times I$ is a union of three ordered tetrahedrons, say $(\mathcal{T}_1, \mathcal{T}_2, \mathcal{T}_3)$ with $\mathcal{T}_i$ is being glued to $\mathcal{T}_{i+1}$ along a common face, for $i = 1, 2$. This space satisfies the condition of Definition 5.5. See Figure 5.2 for a 3-dimensional picture with a typical link drawn in blue. It is a union of three triangles with two consecutive triangles glued along a common edge. One can observe that the links of all the vertices in this picture are isomorphic.

The second paragraph follows from Proposition 5.4 and Theorem 5.6. □

Remark. In fact, one can go further and prove that Lemma 5.8 is true for all $m \geq 2$, meaning that the space $T_m \times I \times I$ admits a natural cubical complex structure (cf. Section 5.1), which contains $3m - 1$ 4-dimensional cubes in each fundamental domain, and the links of all vertices are isomorphic to a union of $m + 1$ tetrahedrons with consecutive ones being glued along a common face. These are all flag links.

We can also view $T_2 \times I \times I$ as a Riemannian manifold with corners. Locally, the Riemannian metric is given by the induced Euclidean metric in each fundamental domain.

Now we come back to our construction of $(\overline{ev}_3)_m$. Let $[f] \in \pi_2\mathrm{Emb}(I, \natural_m S^1 \times D^3; I_0)$, we need to define a map

$$(\overline{ev}_3)_m(f)\colon D^1 \times D^1 \times C'_3[I] \to C'_3[\natural_m S^1 \times D^3].$$

Lemma 5.9. *For $f\colon D^1 \times D^1 \times I \to \natural_m S^1 \times D^3$ representing $[f] \in \pi_2\mathrm{Emb}(I, \natural_m S^1 \times D^3; I_0)$, the restriction of the second evaluation*

$$ev_2(f)\colon D^1 \times D^1 \times C_2[I] \to C'_2[\natural_m S^1 \times D^3]$$

to the boundary facets of $C_2[I]$ is null homotopic.

Proof. We use the same ideas from the proof of Proposition 4.9. We describe a null-homotopy along the $x_1 = x_2$ facet, and the other two facets are similar.

As in the $S^1 \times D^3$ case, along the $x_1 = x_2$ facet, as x_1 approaches x_2, the velocity vectors agree with the direction of the collision. Along this facet of $C_2[I]$, we lift the restriction of f to it to the universal cover $\overline{C'_2[\natural_m S^1 \times D^3]}$ and observe that this map is given by the derivative on the facet $x_1 = x_2$ (cf. discussion in the end of Section 4.1). There is an extension of this derivative to the entire triangle as follows. For $p \in S^2$ and $x_1, x_2 \in C_2[I]$, we only need to specify one tangent vector. There is a unique geodesic connecting $q_1 = f_p(x_1)$ and $q_2 = f_p(x_2)$. This geodesic is given by a concatenation of intervals. Take the initial arc of the concatenation and define the direction vector (after scaling it a unit vector) determined by this arc to be our extension. In particular, such a map can be thought of as a map

$$S^2 \times C_2[I] \to C'_2[\natural_m S^1 \times D^3]\colon (p, x_1, x_2) \to (q_1, q_2, v)$$

where $p \in S^2$, $q_i = f(x_i)$ for $i = 1, 2$, and v is the tangent vector we just described. Now, the same argument applied in Proposition 4.9 works equally well here. Namely, if

we choose some $I_0 = \{pt\} \times I \times 0 \subset T_m \times I^2$, then the restriction of this extension to the other two edges $x_1 = 0$ and $x_2 = 1$ can be homotoped to I_0 since these vectors point to one side of a 3-sphere (one of the "vertical" directions I_0).

Similarly, one can construct null homotopies that can be attached along the other two facets $x_1 = 0$ and $x_2 = 1$ facets, just as in Proposition 4.9. □

Note that we could have used the argument in the proof above for defining $(\overline{ev}_2)$.

Now, we consider the third evaluation

$$(ev_3(f))_m \colon S^2 \times C_3[I] \to C_3'[\natural_m S^1 \times D^3].$$

By Lemma 5.9, the restriction to the four facets of $C_3[I]$ can be homotoped to elements in

$$\pi_4 C_3'[\natural_m S^1 \times D^3] \cong \pi_4(\vee_m S^1) \times (\vee_m S^1 \vee S^3) \times (\vee_m S^1 \vee S^3 \vee S^3) \times (S^3)^3.$$

Since $\pi_4 S^3 \cong \mathbb{Z}/2$, these restrictions are torsion. Therefore, following the same strategy of Section 4.2, we can perform the construction of $(\overline{ev}_3)_m$ rationally. If the order of the restriction to a boundary facet is o, then the restriction of the map $ev_3(of)$ to the boundary facets is null homotopic. So we define

$$\frac{1}{o}(\overline{ev}_3)_m(of) \coloneqq S^5 \to C_3'[\natural_m S^1 \times D^3].$$

by attaching null homotopies along the 4 boundary facets. It remains to argue that this is a rational homotopy invariant up to choices of these null homotopies. This is done by exploring inclusions of the boundary facets

$$C_2[I] \to C_3[I]$$

and the induced maps

$$\pi_5 C_2'[\natural_m S^1 \times D^3] \to \pi_5 C_3'[\natural_m S^1 \times D^3]$$

on π_5. This is summarized in the following lemma.

Lemma 5.10. *By analyzing the second homotopy groups of* $X_0 \times X_1 \times X_2 \sim (\vee_m S^1) \times (\vee_m S^1 \vee S^3) \times (\vee_m S^1 \vee S^3 \vee S^3)$*, we can deduce that the homotopy group* $\pi_5 C_3'(\natural_m S^1 \times D^3)$ *is isomorphic to the following quotient group of a free group*

$$\langle (t_1)_i^{\pm}, (t_2)_i^{\pm} \rangle / \langle \nu((t_1)_i) = \nu^{-1}((t_2)_i), (t_1)_i (t_2)_j = (t_1)_j (t_2)_i \ \forall i,j \text{ and } \forall \nu((t)_1, (t)_2, \ldots, (t)_m) \rangle$$

mod torsion where $i, j = 1, 2, \ldots, m$*. A polynomial* $(t_1)_i^{\alpha}(t_2)_j^{\beta}$ *represents the Whitehead bracket* $[(t_1)_i^{\alpha}(t_2)_j^{\beta}.\omega_{12}, \omega_{12}]$*. Here we will use the notation* $\langle (t)_i \rangle$ *to denote the free group with* m *generators*

$$\langle (t)_1, (t)_2, \ldots, (t)_m \rangle$$

and similarly the notations $\langle (t_1)_i \rangle$ *and* $\langle (t_2)_i \rangle$ *for the corresponding free groups with* m *generators. Also,* $\nu((t)_1, \ldots, (t)_m)$ *denotes an element in* $\langle (t)_1, (t)_2, \ldots, (t)_m \rangle$ *and similarly* $\nu((t_1)_1, \ldots, (t_1)_m)$ *and* $\nu((t_2)_1, \ldots, (t_2)_m)$ *denote elements in the groups* $\langle (t_1)_i \rangle$ *and* $\langle (t_2)_i \rangle$ *respectively.*

For each of the four facets $x_1 = 0$*,* $x_1 = x_2$*,* $x_2 = x_3$*,* $x_3 = 1$ *of the tetrahedron* $C_3[I]$*, attaching a null homotopy (modulo torsion)* $S^2 \times C_2[I] \times I \to C_2[\natural_m S^1 \times D^3]'$ *gives rise to the following relations, respectively.*

1. *For the* $x_1 = 0$ *facet, the generators* $(t_1)_i^{\alpha}.\omega_{12}$ *are mapped to* $(t_2)_i^{\alpha}.\omega_{23}$ *by the induced map on homotopy groups of the inclusion map, thus one obtains the relations* $[(t_2)_i^{\alpha}.\omega_{23}, (t_2)_j^{\beta}.\omega_{23}]$ *for all* $\alpha, \beta \in \mathbb{Z}$*. More generally, the elements* $\nu((t_1)_i).\omega_{12}$ *are mapped to* $\nu((t_2)_i).\omega_{23}$*, leading to the relations* $[\nu((t_2)_i).\omega_{23}, \mu((t_2)_i).\omega_{23}]$ *for* $\mu, \nu \in \langle (t_2)_i \rangle$*.*

2. *For the* $x_1 = x_2$ *facet, the inclusion doubles the first coordinate* $(x_1, x_2) \to (x_1, \delta x_1, x_2)$ *where* δx_1 *is a small perturbation in the direction of the corresponding velocity vector. The induced map on homotopy groups maps* ω_{12} *to* $\omega_{13} + \omega_{23}$*,* $(t_1)_i$ *to* $(t_1)_i(t_2)_i$ *and fixes* $(t_2)_i$ *leading to the relations* $[(t_1)_i^{\alpha}.\omega_{13} + (t_2)_i^{\alpha}.\omega_{23}, (t_1)_j^{\beta}.\omega_{13} + (t_2)_j^{\beta}\omega_{23}]$*. More generally,* $\nu((t_1)_i)$ *are mapped to* $\nu((t_1 t_2)_i)$*, leading to the relations* $[\nu((t_1 t_2)_i)(\omega_{13} +$

$\omega_{23}), \mu((t_1t_2)_i)(\omega_{13}+\omega_{23})]$ *for* $\mu, \nu \in \langle (t)_i \rangle$.

3. *For the* $x_2 = x_3$ *facet, the inclusion map doubles the second coordinate thus the induced map sends* ω_{12} *to* $\omega_{12}+\omega_{13}$, $(t_2)_i$ *to* $(t_2)_i(t_3)_i$ *and fixes* $(t_1)_i$ *leading to the relations* $[(t_1)_i^\alpha.\omega_{12} + (t_1)_i^\alpha\omega_{13}, (t_1)_j^\beta.\omega_{12} + (t_1)_j^\beta\omega_{13}]$. *More generally,* $\nu((t_1)_i)$ *are mapped to* $\nu((t_1)_i)$, *leading to the relations* $[\nu((t_1)_i)(\omega_{13}+\omega_{12}), \mu((t_1)_i)(\omega_{13}+\omega_{12})]$ *for* $\mu, \nu \in \langle (t_1)_i \rangle$.

4. *For the* $x_3 = 1$ *facet, the inclusion map fixes* x_1 *and* x_2 *and maps* x_3 *to* $(1,0)$. *Therefore, similarly to the* $x_1 = 0$ *facet, leading to the relations* $[(t_1)_i^\alpha.\omega_{12}, (t_1)_j^\beta.\omega_{12}]$. *More generally, the relations* $[\nu((t_1)_i).\omega_{12}, \mu((t_1)_i).\omega_{12}]$ *are satisfied for* $\mu, \nu \in \langle (t_1)_i \rangle$.

The relations 1 and 4 kill the relevant brackets that only involve ω_{23} and ω_{12} respectively. Thus the relations from 2 are simplified to

$$[\nu((t_1t_2)_i).\omega_{13}, \mu((t_1t_2)_i).\omega_{23}]+$$
$$[\nu((t_1t_2)_i).\omega_{23}, \mu((t_1t_2)_i).\omega_{13}]+$$
$$[\nu((t_1t_2)_i).\omega_{13}, \mu((t_1t_2)_i).\omega_{13}]$$

and relations from 3 are simplified to

$$[\nu((t_1)_i).\omega_{12}, \mu((t_1)_i).\omega_{13}]+$$
$$[\nu((t_1)_i).\omega_{13}, \mu((t_1)_i).\omega_{12}]+$$
$$[\nu((t_1)_i).\omega_{13}, \mu((t_1)_i).\omega_{13}].$$

Now, observe that $[\nu((t_1t_2)_i).\omega_{13}, \mu((t_1t_2)_i).\omega_{13}] = [\nu((t_1)_i).\omega_{13}, \mu((t_1)_i).\omega_{13}]$ since t_2 acts trivially on ω_{13}. Therefore, we can merge relations 2 and 3 into one relation in the following

way. Relations 2 give rise to

$$
\begin{aligned}
&[\nu((t_1t_2)_i).\omega_{13}, \mu((t_1t_2)_i).\omega_{23}]+\\
&[\nu((t_1t_2)_i).\omega_{23}, \mu((t_1t_2)_i).\omega_{13}] =\\
&\nu((t_1)_i)\mu^{-1}((t_1)_i)\mu^{-1}((t_3)_i).[\omega_{13},\omega_{23}] + \mu((t_1)_i)\nu^{-1}((t_1)_i)\nu^{-1}((t_3)_i).[\omega_{23},\omega_{13}] =\\
&(-\nu((t_1)_i)\mu^{-1}((t_1)_i)\mu^{-1}((t_3)_i) + \mu((t_1)_i)\nu^{-1}((t_1)_i)\nu^{-1}((t_3)_i)).[\omega_{12},\omega_{23}],
\end{aligned}
$$

and relations 3 give rise to

$$
\begin{aligned}
&[\nu((t_1)_i).\omega_{12}, \mu((t_1)_i).\omega_{13}]+\\
&[\nu((t_1)_i).\omega_{13}, \mu((t_1)_i).\omega_{12}] =\\
&\nu((t_1)_i)\nu((t_3)_i)\mu^{-1}((t_3)_i).[\omega_{12},\omega_{13}] + \mu((t_1)_i)\mu((t_3)_i)\nu^{-1}((t_3)_i)[\omega_{13},\omega_{12}] =\\
&(-\nu((t_1)_i)\nu((t_3)_i)\mu^{-1}((t_3)_i) + \mu((t_1)_i)\mu((t_3)_i)\nu^{-1}((t_3)_i))[\omega_{12},\omega_{23}].
\end{aligned}
$$

Therefore, we get the following relation as an analogue of Budney–Gabai's **Hexagon relation** as discussed in the end of Section 4.2.

Theorem 5.11. *The rational homotopy group $\pi_5 C_3'(\natural_m S^1 \times D^3) \otimes \mathbb{Q}$ is generated by $(t_1)_i, (t_3)_i$, $i = 1, 2, \ldots, m$ with the following relation satisfied.*

$$
\begin{aligned}
&-\nu((t_1)_i)\mu^{-1}((t_1)_i)\mu^{-1}((t_3)_i) + \mu((t_1)_i)\nu^{-1}((t_1)_i)\nu^{-1}((t_3)_i) =\\
&-\nu((t_1)_i)\nu((t_3)_i)\mu^{-1}((t_3)_i) + \mu((t_1)_i)\mu((t_3)_i)\nu^{-1}((t_3)_i).
\end{aligned}
$$

After a change of variable and rearrangements of the equation, we can write the relation in the following way:

$$\nu((t_1)_i)\mu((t_3)_i) + \mu^{-1}((t_1)_i)\nu^{-1}((t_3)_i) = \nu^{-1}((t_1)_i)\mu((t_3)_i)\nu^{-1}((t_3)_i) + \nu((t_1)_i)\mu^{-1}((t_1)_i)\nu((t_3)_i).$$

Therefore, we have now defined a map

$$(\overline{ev}_3)_m \colon \pi_2\mathrm{Emb}(I, \natural_m S^1 \times D^3) \to \Lambda_m = \pi_5 C'_3[\natural_m S^1 \times D^3] \otimes \mathbb{Q}/R$$

where R stands for the relations described in Lemma 5.10.

Recall that our mission is to define an invariant

$$(W_3)_m \colon \pi_0\mathrm{Diff}(\natural_m S^1 \times D^3, \partial) \to \pi_2\mathrm{Emb}(I, \natural_m S^1 \times D^3; I_0) \to \Lambda_m$$

as a composition of two maps. We have just finished defining the second map. We now turn to define the first map, namely the scanning map s. As in Section 4.2, it is only defined up to a choice of a properly embedded 3-ball in $\natural_m S^1 \times D^3$. In particular, let $D_s \subset \natural_m S^1 \times D^3$ be a properly embedded 3-disk called the *scanning disk*. We choose our base point interval $I_0 = 0 \times 0 \times [-1, 1] \subset D_s \cong [-1, 1] \times [-1, 1] \times [-1, 1]$. (In Section 5.3, we will discuss such choices for $m = 2$). An element $[\Phi] \in \pi_0\mathrm{Diff}(\natural_m S^1 \times D^3, \partial)$ represented by a diffeomorphism Φ maps the intervals $u, v \times [-1, 1] \subset D_s$, $u, v \in [-1, 1]$ to a two-parameter family of properly embedded intervals, leading to an element in $\pi_2\mathrm{Emb}(I, \natural_m S^1 \times D^3; I_0)$ in the same way as discussed in the beginning of Section 4.2.

Therefore, we have defined an invariant $(W_3)_m$. We remark that if we set $m = 1$ and choose D_s to be a disk $\{pt\} \times D^3 \subset S^1 \times D^3$, then the discussion so far in this section recovers the W_3 defined in Chapter 4.

We end this section with a discussion of ideas for calculation of $(W_3)_m$. One can refer to Section 4.4 for comparison. Fix a base point $(x_0, 0) \in U_m \times \mathbb{R} = T_m \times I \times \mathbb{R}$ where U_m is the universal tree. For a word ν in the free group generated by $(t_1)_i, (t_2)_i, (t_3)_i$ with $i = 1, 2 \ldots m$ (cf. the beginning of this section), we define the cohorizontal submanifold

$$\nu.\mathrm{Co}_1^2 = \{(p_1, p_2) \in \overline{C_2(\natural_m S^1 \times D^3)} \colon p_2 \text{ and } \nu.p_1 \text{ coincide on } T_m,$$

$$\text{and } p_2 - \nu.p_1 = \lambda(x_0, 0, 1) \text{ for some } \lambda > 0\}.$$

Note that the subtraction makes sense since it is only about the $I \times \mathbb{R}$ part. This submanifold $\nu.\mathrm{Co}_1^2$ detects the element $\nu.\omega_{12}$ as it intersects the image of $\nu.\omega_{12}$ at exactly one point, and does not intersect $\nu'.\omega_{12}$ if $\nu \neq \nu'$.

To detect elements in $\pi_5 C_3[\natural_m S^1 \times D^3] \otimes \mathbb{Q}$ as Whitehead products of elements in the form of $\nu.\omega_{12}$ and $\mu.\omega_{23}$ with ν and μ being words in the free group generated by the $3m$ generators $(t_1)_i$, $(t_2)_i$ and $(t_3)_i$ for $i = 1, 2, \ldots, m$, we make use of the language of **co-geodesic** submanifolds as a generalisation of Budney–Gabai's collinear submanifolds (cf. Section 4.4). In the universal cover $T_m \times I^2$ of $\natural_m S^1 \times D^3$, straight lines are not natural choices anymore as we are not working in a convex space. However, as discussed in Section 5.1, $T_m \times I^2$ is a simply-connected cubical complex with all links being flag, hence a uniquely geodesic space by Theorem 5.6, with geodesics given by concatenations of intervals (polylines). Thus, we can define submanifolds:

Definition 5.12. The co-geodesic submanifolds are defined as follows:

$$\mathrm{Cog}_{\nu,\mu}{}^1 = \{(p_1, p_2, p_3) \in T_m \times I^2 \colon \ \nu.p_1 \text{ lies on the geodesic determined by } \mu.p_3 \text{ and } p_2\}.$$

$$\mathrm{Cog}_{\nu,\mu}{}^3 = \{(p_1, p_2, p_3) \in T_m \times I^2 \colon \ \mu.p_3 \text{ lies on the geodesic determined by } \nu.p_1 \text{ and } p_2\}.$$

where ν and μ are words in the free group generated by the $3m$ generators $(t_1)_i$, $(t_2)_i$ and $(t_3)_i$ for $i = 1, 2, \ldots, m$.

The former submanifold intersects $\mu.\omega_{12}$ algebraically once, and the latter submanifold intersects $\nu.\omega_{23}$ once. Thus the pair $(\mathrm{Cog}_{\nu,\mu}{}^1, \mathrm{Cog}_{\nu,\mu}{}^3)$ detects the element $\mu\nu[\omega_{12}, \omega_{23}]$ in the sense that the preimage of this pair under $\mu\nu[\omega_{12}, \omega_{23}]$ is a standard linking pair in S^5 (cf. Section 4.4), and the preimage of the same pair under $\mu'\nu'[\omega_{12}, \omega_{23}]$ is empty if $\mu\nu[\omega_{12}, \omega_{23}] \neq \mu'\nu'[\omega_{12}, \omega_{23}]$. For any element in $\pi_5 C_3[\natural_m S^1 \times D^3] \otimes \mathbb{Q}$, we can write it as a linear combination of $[\omega_{12}, \omega_{23}]$ with coefficients given by words in the free group with $3m$ generators, and the linking number of the preimage of the pair

$$(\mathrm{Cog}_{\nu,\mu}{}^1, \mathrm{Cog}_{\nu,\mu}{}^3)$$

determines the coefficients.

To calculate these linking numbers, we use a trick similar to Budney–Gabai's argument as in Lemma 3.4 of [4] (see also Lemma 4.16). Recall that T_m is the universal cover of a regular neighbourhood of a wedge of m circles in $\mathbb{R}^2$. (cf. Figure 5.1 and the discussion around it.).

Embed $T_m \times I^2$ in $T_m \times I \times \mathbb{R}$ and consider the function $P_\lambda \colon T_m \times I \times \mathbb{R} \to T_m \times I \times \mathbb{R}$ defined by

$$P_\lambda(p_1, p_2, p_3, p_4) = (p_1, p_2, p_3, p_4 + \lambda d(p_1, p_2, p_3)^2)$$

where $\lambda > 0$ is positive and $d(p_1, p_2, p_3)$ is the distance from the point (p_1, p_2, p_3) to x_0. This 1-parameter family of diffeomorphisms sends polylines to parabolas that get steeper as λ increases. As λ goes to infinity, the polylines will be broken into steep segments of parabolas. It follows that the linking number of the preimage of $(\mathrm{Cog}_{\nu,\mu}{}^1, \mathrm{Cog}_{\nu,\mu}{}^3)$ can be calculated by the pair $(\mu\mathrm{Co}_2^1 - \mu\nu^{-1}\mathrm{Co}_3^1, \nu\mu^{-1}\mathrm{Co}_1^3 - \nu\mathrm{Co}_2^3)$(cf. Lemma 4.16). Here the cohorizontal submanifolds Co_i^j are defined in the same manner as before with point i and j being cohorizontal but the one remaining coordinate being allowed to change freely. This will allow us to calculate the W_3 invariant for embedded barbells in $\natural_m S^1 \times D^3$ for $m \geq 2$ using cohorizontal submanifolds.

5.3 The mapping class group of $S^1 \times D^3 \natural S^1 \times D^3$

In this section, we use the invariant

$$(W_3)_2 \colon \pi_0\mathrm{Diff}(S^1 \times D^3 \natural S^1 \times D^3, \partial) \to \Lambda_2$$

to study the mapping class group of $S^1 \times D^3 \natural S^1 \times D^3$ by looking at some embedded barbells. From now on, we fix $m = 2$. In this case, we simplify our notation and denote the generators of $\pi_1 C_3(S^1 \times D^3 \natural S^1 \times D^3)$ by t_1, t_2, t_3, u_1, u_2 and u_3. We consider embedded unknotted barbell in $S^1 \times D^3 \natural S^1 \times D^3$. For an unknotted barbell $\mathcal{B}$, without loss of generality, we may assume that both of the cuffs B and R (blue and red) are contained in

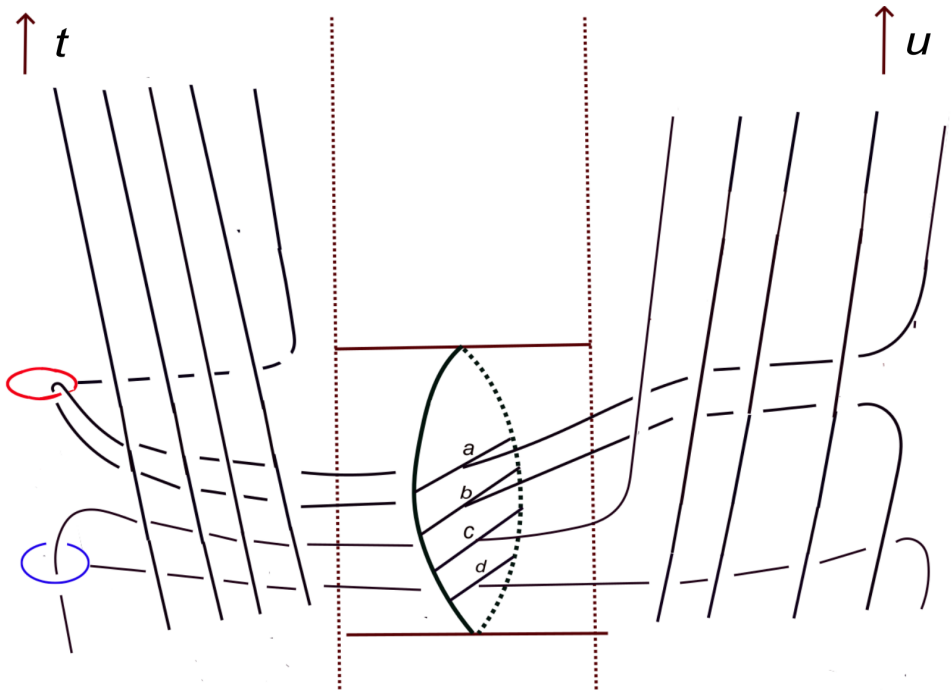

Figure 5.3: The barbell θ_{t^5,u^4,u^1}.

the first factor of our boundary sum.

We consider a barbell θ_{t^5,u^4,u^1} shown in Figure 5.3. It is specified by three words $(\nu, \mu, \gamma) = (t^5, u^4, u^1)$ in the free group of two generators t and u, representing the two circle factors of $S^1 \times D^3 \natural S^1 \times D^3$. We fix our convention that ν represents the path followed by the subarc of the bar that starts from the red cuff and ends just before intersecting the spanning disk of the blue cuff, μ represents the path followed by the subarc of the bar between the spanning disks of the blue cuff and the red cuff, and finally γ represents the path followed by the subarc from the spanning disk of the red cuff to the blue cuff. The cylinder in the middle of Figure 5.3 indicates the "neck" of the boundary connected-sum.

Recall from the last section that to define $(W_3)_2$, we need to choose a scanning disk properly embedded in $S^1 \times D^3 \natural S^1 \times D^3$. There is a natural choice Δ in the middle of the boundary connected sum neck, drawn in Figure 5.3. By assumption, the cuff spheres of θ_{t^5,u^4,u^1} is disjoint from Δ. The barbell diffeomorphism $\Phi_{\theta_{t^5,u^4,u^1}}$ makes $\Delta = I \times I \times I$ into an element in $\pi_2\mathrm{Emb}(I, S^1 \times D^3 \natural S^1 \times D^3)$ via the scanning map.

In Figure 5.3, there are four intersection points between the bar and Δ, denoted by a, b, c and d. Follwing the same strategy as in Chapter 4, we will analyze each of these

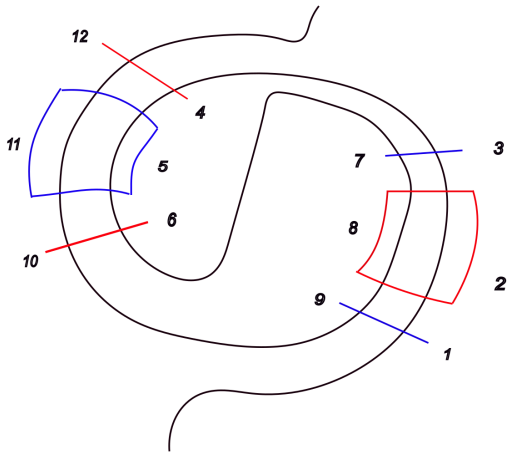

Figure 5.4: The type 2 intersection for b and c.

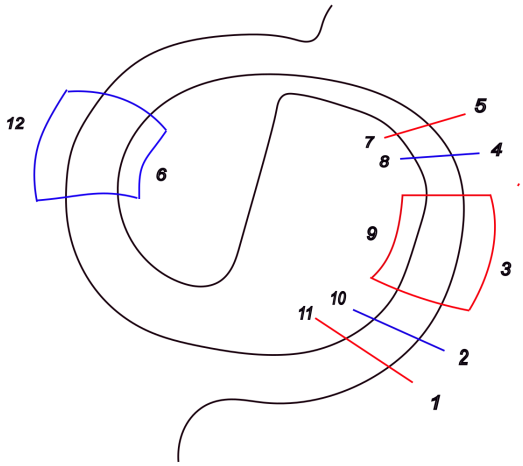

Figure 5.5: The type 3 intersection for a and d.

separately. In this case, these points are divided into two types, namely b and c are called type 2, and a and d are called type 3. These names come from the fact that they actually coincide with the definition of type 2 and type 3 intersections in Lemma 4.19. If we fix the direction pointing out of the page as our cohorizontal direction, then Figure 5.4 and Figure 5.5 illustrate the scanning pictures for the intersection points b, c and a, d respectively. In fact, they are just repetitions of Figures 4.9 and 4.10. It follows that the shapes of the triangle and tetrahedron pictures we get, which describe the preimage of the cohorizontal submanifolds $w.\mathrm{Co}_1^2$ for $w \in \langle t, u \rangle$, are identical to the previous cases for embedded barbells in $S^1 \times D^3$. Namely, Figures 16 and 17 in [4] can be used for our calculations. Notice that the point d actually produces a reflection of Figure 5.4 as d reaches the blue cuff by going left (unlike a which reaches the blue cuff by going left). The similar phenomenon is true for b and c. However, this does not affect the linking number calculations and does not introduce sign differences, since it changes the pullback orientations of all (preimage of) the cohorizontal submanifolds at once.

As before, we break up the calculation of the linking numbers of the preimage of

$$(\mu\mathrm{Co}_2^1 - \mu\nu^{-1}\mathrm{Co}_3^1, \nu\mu^{-1}\mathrm{Co}_1^3 - \nu\mathrm{Co}_2^3)$$

(cf. the end of Section 5.2) into the two colors, blue and red. Observe that the bar links

each cuff sphere only once. For the blue cuff sphere, the cohorizontal points occur when the bar goes through the blue cuff, and it takes u^5 to travel from this position back to the blue cuff. For the red cuff, this path is specified by $u^{-4}t^{-5}$.

For intersection points b and c, we calculate the linking numbers as follows:

1. $\mathrm{lk}(\mu\mathrm{Co}_2^1, \nu\mu^{-1}\mathrm{Co}_1^3) = -u_1^{-4}t_1^{-5}u_3^1t_3^{-5}$
2. $\mathrm{lk}(\mu\mathrm{Co}_2^1, \nu\mu^{-1}\mathrm{Co}_1^3) = u_1^{-5}t_3^5u_3^{-1}$
3. -$\mathrm{lk}(\mu\mathrm{Co}_2^1, \nu\mathrm{Co}_2^3) = 0$
4. -$\mathrm{lk}(\mu\mathrm{Co}_2^1, \nu\mathrm{Co}_2^3) = 0$
5. $\mathrm{lk}(\mu\nu^{-1}\mathrm{Co}_3^1, \nu\mathrm{Co}_2^3) = t_1^5u_1^{-1}u_3^{-5}$
6. $\mathrm{lk}(\mu\nu^{-1}\mathrm{Co}_3^1, \nu\mathrm{Co}_2^3) = -u_1^1t_1^{-5}u_3^{-4}t_3^{-5}$.

Similarly, for the intersection point a and d, the linking numbers are:

1. $\mathrm{lk}(\mu\mathrm{Co}_2^1, \nu\mu^{-1}\mathrm{Co}_1^3) = -u_1^{-4}t_1^{-5}u_3^1t_3^{-5}$
2. $\mathrm{lk}(\mu\mathrm{Co}_2^1, \nu\mu^{-1}\mathrm{Co}_1^3) = u_1^{-5}t_3^5u_3^{-1} + u_1^5u_3^{-4}t_3^{-5}u_3^5$
3. -$\mathrm{lk}(\mu\mathrm{Co}_2^1, \nu\mathrm{Co}_2^3) = -u_1^{-4}t_1^{-5}u_3^{-5}$
4. -$\mathrm{lk}(\mu\mathrm{Co}_2^1, \nu\mathrm{Co}_2^3) = -u_1^{-5}u_3^{-4}t_3^{-5}$
5. $\mathrm{lk}(\mu\nu^{-1}\mathrm{Co}_3^1, \nu\mathrm{Co}_2^3) = t_1^5u_1^{-1}u_3^{-5} + u_1^{-4}t_1^{-5}u_1^5u_3^5$
6. $\mathrm{lk}(\mu\nu^{-1}\mathrm{Co}_3^1, \nu\mathrm{Co}_2^3) = -u_1^1t_1^{-5}u_3^{-4}t_3^{-5}$.

Similarly to the calculations in Section 4.5, the powers of u_1, u_3, t_1 and t_3 are determined by how many times one needs to travel along each of the two circle factors to get from one point of a co-horizontal pair to the other. For example, $\mathrm{lk}(\mu\mathrm{Co}_2^1, \nu\mu^{-1}\mathrm{Co}_1^3)$ is obtained from the top left picture of Figure 16 of [4], where we have $\mu = u^{-4}t^{-5}$ and $\nu\mu^{-1} = u^5$, leading to $\nu = u^1t^{-5}$, thus we have $\mathrm{lk}(\mu\mathrm{Co}_2^1, \nu\mu^{-1}\mathrm{Co}_1^3) = -u_1^{-4}t_1^{-5}u_3^1t_3^{-5}$ where

the minus sign reflects that the linking pair in this case has a negative orientation with reference to the standard orientation of $D^1 \times D^1 \times C_3[I]$.

By taking the sum, we get the following theorem.

Theorem 5.13. *The $(W_3)_2$ invariant of the barbell θ_{t^5,u^4,u^1} is given by*

$$2(-u_1^{-4}t_1^{-5}u_3^1t_3^{-5} + u_1^{-5}t_3^5u_3^{-1} + t_1^5u_1^{-1}u_3^{-5} - u_1^1t_1^{-5}u_3^{-4}t_3^{-5}) + 2(-u_1^{-4}t_1^{-5}u_3^1t_3^{-5} + u_1^{-5}t_3^5u_3^{-1} + u_1^5u_3^{-4}t_3^{-5}u_3^5 - u_1^{-4}t_1^{-5}u_3^{-5} - u_1^{-5}u_3^{-4}t_3^{-5} + t_1^5u_1^{-1}u_3^{-5} + u_1^{-4}t_1^{-5}u_1^5u_3^5 - u_1^1t_1^{-5}u_3^{-4}t_3^{-5}).$$

Furthermore, by letting all terms be zero except the terms with the exponent of t_1 minus the exponent of u_3 being 10, we get

$$4t_1^5u_1^{-1}u_3^{-5} \neq 0$$

which survives from the Hexagon relations (cf. Theorem 5.11).

More generally, we can calculate the $(W_3)_2$ of barbells θ_{t^q,u^4,u^1} for $q = 5, 6, 7, \ldots$ in exactly the same way as above, getting

Theorem 5.14. *The $(W_3)_2$ invariant of the barbell θ_{t^q,u^4,u^1} for $q = 5, 6, 7, \ldots$ is given by*

$$\begin{aligned}
&2(-u_1^{-4}t_1^{-q}u_3^1t_3^{-q} + u_1^{-5}t_3^qu_3^{-1} + t_1^qu_1^{-1}u_3^{-5} - u_1^1t_1^{-q}u_3^{-4}t_3^{-q}) + \\
&2(-u_1^{-4}t_1^{-q}u_3^1t_3^{-q} + u_1^{-5}t_3^qu_3^{-1} + u_1^5u_3^{-4}t_3^{-q}u_3^5 \\
&- u_1^{-4}t_1^{-q}u_3^{-5} - u_1^{-5}u_3^{-4}t_3^{-q} + t_1^qu_1^{-1}u_3^{-5} + u_1^{-4}t_1^{-q}u_1^5u_3^5 - u_1^1t_1^{-q}u_3^{-4}t_3^{-q}).
\end{aligned}$$

Furthermore, these barbells are linearly independent.

Proof. The formula itself can be obtained in the same way we have outlined for θ_{t^5,u^4,u^1} above. The second statement follows by quotienting all terms except those with the property that the exponent of t_1 minus the exponent of u_3 being $q + 5$. Namely, for a linear combination

$$a_1\theta_{t^5,u^4,u^1} + a_2\theta_{t^6,u^4,u^1} + a_3\theta_{t^7,u^4,u^1} + \cdots + a_n\theta_{t^{n+4},u^4,u^1} = 0,$$

when all terms except those with the exponent of t_1 minus the power of u_3 being $n+9$ are declared to be zero, θ_{t^l,u^4,u^1} vanishes for $l \leq n+8$ which implies $a_n = 0$. Repeating this argument with n replaced by $1, 2, \ldots, n-1$ implies that all coefficients are zero. $\square$

Let $\Phi \in \mathrm{Diff}(S^1 \times D^3 \natural S^1 \times D^3, \partial)$ such that $\Phi(\Delta, \partial) = (\Delta, \partial)$. Then we can isotope Φ such that it fixes Δ pointwise which implies that $W_3([\Phi]) = 0$. Therefore, we have obtained an infinite sequence of knotted 3-balls $\Phi_{\theta_{t^l,u^4,u^1}}(\Delta)$ in $S^1 \times D^3 \natural S^1 \times D^3$ for $l \geq 5$. This also shows that the elements $[\Phi_{\theta_{t^l,u^4,u^1}}]$ do not come from $\pi_0\mathrm{Diff}(S^1 \times D^3, \partial) \times \pi_0\mathrm{Diff}(S^1 \times D^3, \partial)$ since the former group fixes Δ. So, combining with Theorem 5.14, we have the following theorem.

Theorem 5.15. *The group $\pi_0\mathrm{Diff}(S^1 \times D^3 \natural S^1 \times D^3, \partial)/\prod_2 \pi_0\mathrm{Diff}(S^1 \times D^3, \partial)$ has an infinitely generated subgroup. Moreover, there exist infinitely many properly embedded separating 3-balls in $S^1 \times D^3 \natural S^1 \times D^3$ with common boundary that are not isotopic relative to the boundary.*

5.4 Motivation and outlook

In this section, we describe a question that motivates the entire Chapter 5, and explain a possible approach to tackle it. The author plans to carry on the research described below during his time as a postdoc in the future.

Let $L = L_1 \cup L_2$ denote the standard 2-dimensional unlink in S^4. A **splitting sphere** for L is an embedded $S^3 \hookrightarrow S^4$ such that L_1 and L_2 lie in different components of $S^4 \setminus S^3$. Hughes-Kim-Miller ([15]) proposed the following question:

Question 5.16. *Do there exist non-isotopic splitting spheres of the unlink in the 4-sphere?*

The complement of a neighbourhood of the unlink in S^4 is diffeomorphic to the internal connected-sum $S^1 \times D^3 \# S^1 \times D^3$ which motivates us to study $\pi_0\mathrm{Diff}(S^1 \times D^3 \# S^1 \times D^3, \partial)$. In particular, the above question is equivalent to the existence of non-isotopic separating 3-spheres in $S^1 \times D^3 \# S^1 \times D^3$. In the remaining part of this section, we outline an approach to this question that utilizes the previous sections of this chapter.

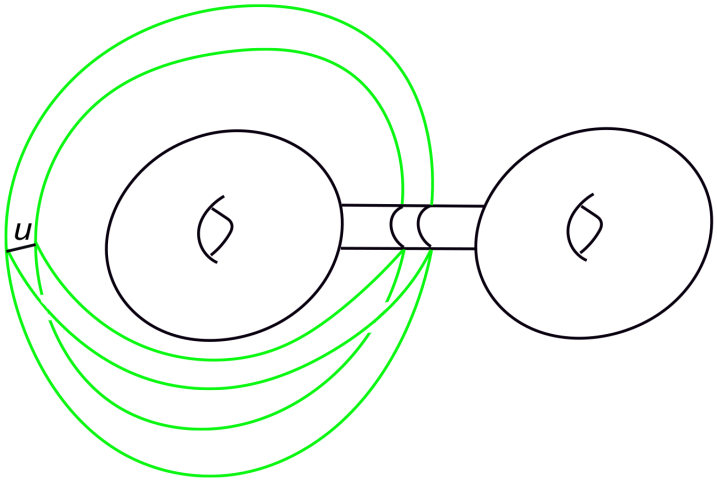

Figure 5.6: The relationship between $S^1 \times D^3 \natural S^1 \times D^3$ and $S^1 \times D^3 \# S^1 \times D^3$.

Let $X = S^1 \times D^3 \natural S^1 \times D^3$ and let $Y = S^1 \times D^3 \# S^1 \times D^3$. Figure 5.6 is meant to indicate their relationship (with a 3-dimensional picture). Let u be a properly embedded arc in Y as depicted in Figure 5.6. Then X is obtained from Y by drilling out a neighbourhood of u. Conversely, recall from the last section the scanning 3-ball Δ in the neck of the boundary connected sum of X. We observe that attaching a 3-handle along a neighbourhood of the boundary of Δ gives Y, and the union of Δ with the core of the 3-handle is a separating 3-sphere $\overline{\Delta}$. In Figure 5.6, the green part is meant to represented this attachment, but is drawn as a 3-dimensional 2-handle since it is one dimension lower.

We denote the component of the space of properly embedded arcs in $S^1 \times D^3 \# S^1 \times D^3$ that contains u by

$$\mathrm{Emb}(I, S^1 \times D^3 \# S^1 \times D^3; u).$$

We consider the following fibration

$$\mathrm{Diff}(S^1 \times D^3 \natural S^1 \times D^3, \partial) \to \mathrm{Diff}(S^1 \times D^3 \# S^1 \times D^3, \partial) \to \mathrm{Emb}(I \times D^3, S^1 \times D^3 \# S^1 \times D^3; u \times D^3).$$

The last few terms of the induced long exact sequence of homotopy groups are as follows:

$$\cdots \to \pi_1 \mathrm{Emb}(I \times D^3, Y) \to \pi_0 \mathrm{Diff}(X, \partial) \to \pi_0 \mathrm{Diff}(Y, \partial) \to \pi_0 \mathrm{Emb}(I \times D^3, Y; u \times D^3) \to 0,$$

where the first map is given by isotopy extension and the second map is given by extending

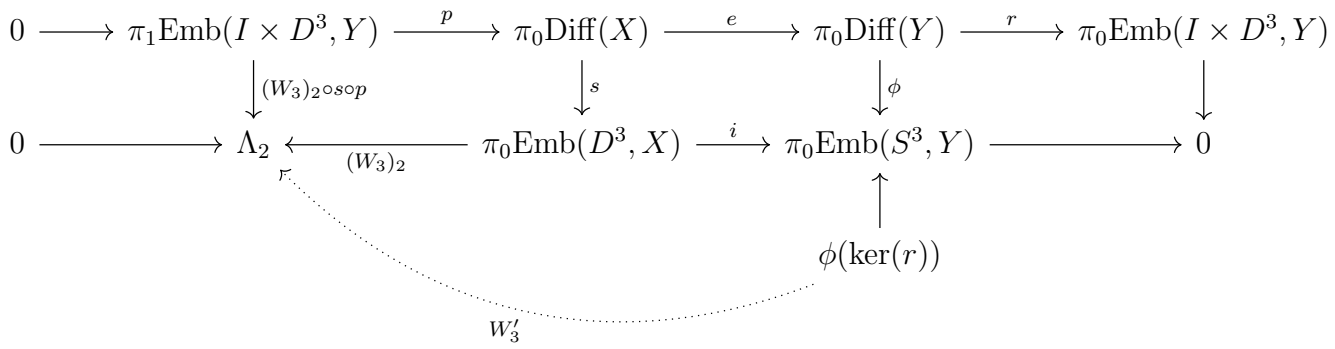

Figure 5.7: Definition of W_3'.

diffeomorphisms of X to Y using the identity map.

The situation is summarized in the above diagram. Here we view the $(W_3)_2$ invariant as an invariant defined on $\pi_0\mathrm{Emb}(D^3, X)$. We drop ∂ in the diagram to save space, but all mapping class groups in the diagram are boundary-fixing. The group Λ_2 in the left corner denotes the codomain of the $(W_3)_2$ invariant. The object $\pi_0\mathrm{Emb}(D^3, X)$ denotes isotopy classes of embedded separating 3-balls in X whose boundaries coincide with $\partial\Delta$. The group $\pi_0\mathrm{Emb}(S^3, Y)$ is the space of separating 3-spheres in Y and the map i is given by the 3-handle attachment, making a separating 3-ball into a separating 3-sphere. The maps s and ϕ are given by applying diffeomorphisms of X and Y respectively to Δ and the 3-sphere $\overline{\Delta} = (\Delta \cup \text{3-handle})$ in X and Y.

There is an induced W_3'-invariant defined on $\phi(\ker(r))$ as follows. For an embedded 3-sphere S in $\phi(\ker(r))$, we bring it back to $\pi_0\mathrm{Diff}(X, \partial)$ and follow $(W_3)_2 \circ s$. To see this is well-defined, suppose $S' \in \phi(\ker(r))$ is isotopic to S, then we have $\phi^{-1}(S), \phi^{-1}(S') \in \pi_0\mathrm{Diff}(Y, \partial)$ represented by two diffeomorphisms of Y that fix S and S' respectively. By the isotopy extension theorem, these two diffeomorphisms are isotopic, and in particular, they can be isotoped such that $\phi^{-1}(S)(\overline{\Delta}) = \phi^{-1}(S')(\overline{\Delta})$. So if we take their preimage along e, we get two diffeomorphisms that have the same impact on Δ, which implies that they get evaluated to the same element in Λ_2 by $(W_3)_2 \circ s$.

For $[\Phi] \in \pi_0\mathrm{Diff}(Y, \partial)$, if the composition $W_3' \circ \phi([\Phi]) \neq 0$, then Φ is not isotopic to the identity. If we can show that the composition

$$(W_3)_2 \circ s \circ p = 0,$$

then the non-trivial diffeomorphisms θ_{t^5,u^4,u^1}, θ_{t^6,u^4,u^1}, ... we constructed in the previous section would give rise to non-isotopic separating 3-spheres. The below is an outline of what we plan to do to prove this.

The map $\mathrm{Emb}(I \times D^3, Y) \to \mathrm{Emb}(I, Y)$ given by restricting to $I \times \{0\}$ is a fibration with fiber homotopy equivalent to the free loop space of $SO(3)$. Thus, it suffices to understand the space $\pi_1\mathrm{Emb}(I, X)$. To understand its image under p, we use the results in [16] which provide an isomorphism from $\mathbb{Z}[\pi_1 X \setminus 1]/\mathrm{dax}_u(\pi_3 X)$ to the group $\pi_1\mathrm{Emb}(I, X)$ which depends on the arc u. Here $\mathbb{Z}[\pi_1 X \setminus 1]$ is viewed as solely a group and we forget about the ring structure. In fact, for any oriented, smooth 4-manifold X, there is a central group extension

$$1 \to \mathrm{Z}[\pi_1 X \setminus 1]/\mathrm{dax}_u(\pi_3 X) \to \pi_1(\mathrm{Emb}(I, X), u) \to \pi_2 X \to 1$$

where dax_u denotes the **dax invariant**:

$$\mathrm{dax}_u \colon \pi_3 X \to \mathbb{Z}[\pi_1 X \setminus 1].$$

For $a \in \pi_3 X$, $\mathrm{dax}_u(a)$ is defined by picking a 2-parameter family of immersions representing a, which can be viewed as a self-homotopy of the constant loop at u, and analyze the double-points. In other words, choose a map $F \colon S^2 \to \mathrm{Imm}(I, X; u)$ such that the composition with the concatenation map with u^{-1} gives a. The latter space denotes the space of immersed intervals with the same endpoints as u. There is a natural inclusion map $\mathrm{Emb}(I, X; u) \hookrightarrow \mathrm{Imm}(I, X; u)$. The map $\overline{F} \colon I^2 \times I \to I^2 \times X$ defined by $(t, \theta) \to (t, F(t)(\theta))$ can be perturbed to an immersion with only (finitely many) isolated transverse double points. For each double point (t_i, x_i) with $x_i = F(t_i)(\theta_-) = F(t_i)(\theta_+)$ where $\theta_- < \theta_+$, define a double point loop g_{x_i} as the concatenation $F(t_i)|_{[-1,\theta_-]} \cdot F(t_i)^{-1}|_{[-1,\theta_+]}$. Then $\mathrm{dax}_u(a) \colon = \sum \epsilon_{x_i} g_{x_i} \in \mathbb{Z}[\pi_1 X]$ where ϵ_{x_i} is the local orientation of $\overline{F}$ obtained by comparing the orientations of tangent bundles to the image of the derivatives of $\overline{F}$ with the tangent space of $I^2 \times X$. See [16] for details.

Let $\pi_1(X, \partial X)$ be the set of homotopy classes of maps $k \colon I^1 \to X$ with endpoints $k(-1) = x_-$ and $k(1) \in \partial X$. The following theorem from [16] describes dax_u in terms of

the **equivariant intersection pairing**

$$\lambda\colon \pi_3 X \times \pi_1(X, \partial X) \to \mathbb{Z}[\pi_1 X \setminus 1].$$

Note that $\pi_1(X, \partial X)$ admits a $\pi_1 X$-action by precomposition.

Theorem 5.17. *(See Theorem A and Corollary B in [16]) For a fixed $u \in \pi_1(X, \partial X)$ and for $a \in \pi_3 X$ and $g \in \pi_1 X$, the following is true:*

- $\mathrm{dax}_u(a) = \mathrm{dax}_{u_-}(a) + \lambda(a, u)$
- $\mathrm{dax}_{u_-}(ga) = g\mathrm{dax}_{u_-}(a)\bar{g} - \lambda(ga, g) + \lambda(g, ga)$.

Here $u_-\colon I \to X$ is an embedding of an arc with endpoints $u_-(-1) = x_-$ and $u_-(1) = x'_-$ where x'_- is a point close to x_- such that u_- is isotopic relative to the endpoints into ∂X, and dax_{u_-} is defined in the same way as dax_u with a different base point.

We now briefly recall the definition of the equivariant intersection pairing λ and refer the readers to [16]. For $a \in \pi_3 X$ represented by $A\colon S^3 \to X$ and $k \in \pi_1(X, \partial X)$ represented by $k\colon (I, \partial I) \to (X, \partial X)$, we can assume that they intersect transversely in the interior of X. For each intersection point y, there is a double point loop $\lambda_y(A, k) = \lambda_y(A) \cdot \lambda_y(k)^{-1}$ where $\lambda_y(A)$ and $\lambda_y(k)^{-1}$ are paths from x_- to y along A and k respectively. Define

$$\lambda(a, k) = \sum_{y \in (A \cap X) \setminus \{x_-\}} \epsilon_y(A, k)[\lambda_y(A, k)]/[1],$$

where the sign $\epsilon_y(A, k)$ is given by the local orientation at y. One verifies that λ is linear in the first coordinate and $\lambda(a, gk) = \lambda(a, g) + \lambda(a, k)\bar{g}$ for $g \in \pi_1 X$, $k \in \pi_1(X, \partial X)$ and $a \in \pi_3 X$. Note that the quotient by [1] means that we forget the term at $1 \in \pi_1 X$.

However, for us, the situation is simplified when $X = S^1 \times D^3 \# S^1 \times D^3$. We have $\pi_3 X \cong \mathbb{Z}[t^{\pm}, v^{\pm}]$ that is generated by the action of $\pi_1 X \cong \mathbb{Z} * \mathbb{Z} = \langle v \rangle * \langle t \rangle$ on the connected-sum sphere S. Further, $\pi_2 X = 0$ thus we have an isomorphism $\mathbb{Z}[\pi_1 X \setminus 1]/\mathrm{dax}_u(\pi_3 X) \to \pi_1(\mathrm{Emb}(I, X), u)$. Figure 5.8 depicts the 3-dimensional analogous representation of the connected-sum 2-sphere by a loop of arcs. Note that here we use v rather than u to avoid confusions with the arcs u and u_-.

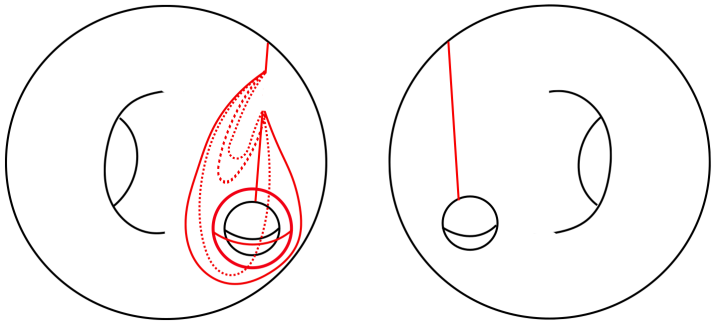

Figure 5.8: Representation of the connected-sum sphere S by a loop of embedded intervals.

Using Theorem 5.17, we can work out the image of λ which is given by $2\mathbb{Z}[t^{\pm 1}, v^{\pm 1} \setminus 1]$ as follows. For a representative of $1 \in \pi_3 X$, say the connected-sum sphere, there is no intersection between it and u (see Figure 5.6. For a representative a of a polynomial, for example $t^i v^j t^k \in \pi_3 X$, $\lambda(a, u)$ gives back $t^i v^j t^k$. Further, if we choose u_- to be an arc with both endpoints in the same boundary component of $X = S^1 \times D^3 \# S^1 \times D^3$, then $\mathrm{dax}_{u_-}(t^i v^j t^k) = t^i v^j t^k$, since we can choose a representative with a single double point that produces the same polynomial. It follows that $\pi_1\mathrm{Emb}(I, X)$ is isomorphic to

$$\mathbb{Z}[t^{\pm 1}, v^{\pm 1} \setminus 1]/2\mathbb{Z}[t^{\pm 1}, v^{\pm 1} \setminus 1] \cong (2\mathbb{N} + 1)[t^{\pm 1}, v^{\pm 1} \setminus 1].$$

An element here is described by picking a small sub-arc of the base point (see Figure 5.6) for the base point arc u, pushing it along a path which corresponds to this element, and spinning around the base point arc, and finally coming back. This process is defined as **spinning** in Definition 4.1 of [3]. It is also described in [16].

The image $p(\pi_1\mathrm{Emb}(I, X))$ can be described by barbell diffeomorphisms specified by words in the free group of two generators together with a positive integer that records the number of times the bar of the barbell goes through the neck of the boundary connected sum. Figure 5.9 is an example of an element in $\pi_1\mathrm{Emb}(I, X)$ that corresponds to $t^3 v^3 t^2$ (see also Figure 2.15 as an example of a corresponding twin twist represented in this manner), where a subarc of u spins around the loop $t^3 v^3 t^2$ and links itself. This creates a double-point whose resolution gives rise to a 1-parameter family of embedded arcs. It folows that the isotopy extension leads to a diffeomorphism supported in a neighbourhood

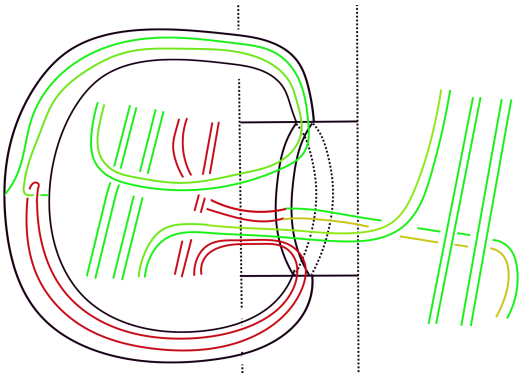

Figure 5.9: The element $t^3v^3t^2$ in $\pi_1\mathrm{Emb}(I, X)$.

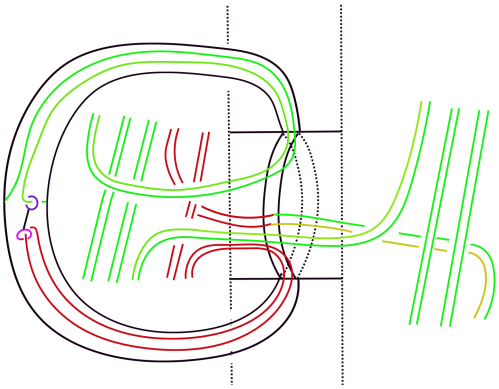

Figure 5.10: The embedded barbell induced by $t^3v^3t^2$ in $\pi_1\mathrm{Emb}(I, X)$.

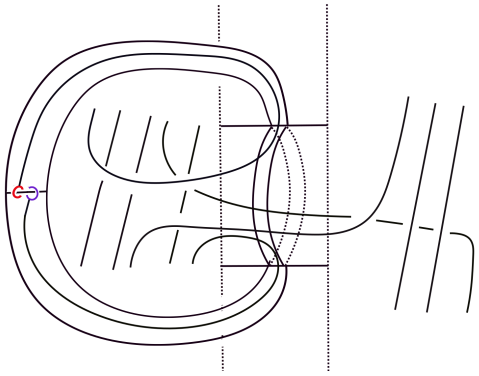

Figure 5.11: The induced barbell by $t^3v^3t^2$ dragged to a standard position.

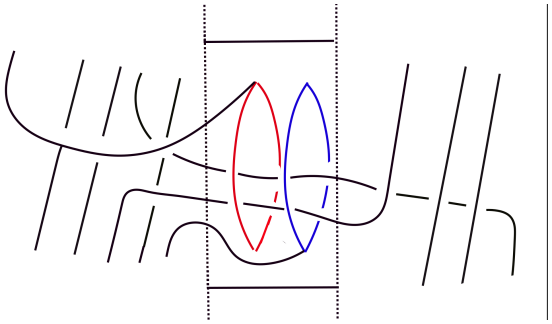

Figure 5.12: The barbell $\mathcal{B}(t^3u^3t^2)$ induced by $t^3v^3t^2$ in standard position in Y.

diffeomorphic to a model barbell manifold. Figure 5.10 depicts this initial barbell manifold induced from the double point resolution. Figure 5.11 is the result of an isotopy that puts both cuff spheres in a standard position and Figure 5.12 is obtained by drilling out a neighbourhood of u to get back to Y.

The image $p(\pi_1\mathrm{Emb}(I, X))$ is generated by such barbells. Here we do not need to specify the meridians of the cuff spheres, because every horizontal strand (as a sub-arc of the bar) that passes through the entire boundary connected sum neck is required to pass through both cuff spheres as well.

The $(W_3)_2$ invariant of $\mathcal{B}(t^3v^3t^2)$ can be calculated with the same strategy as in Section 5.3. We scan through Δ which is in the neck of the boundary sum on the right-hand side of the blue cuff. By the same argument used in the proof of Lemma 4.25, we can argue

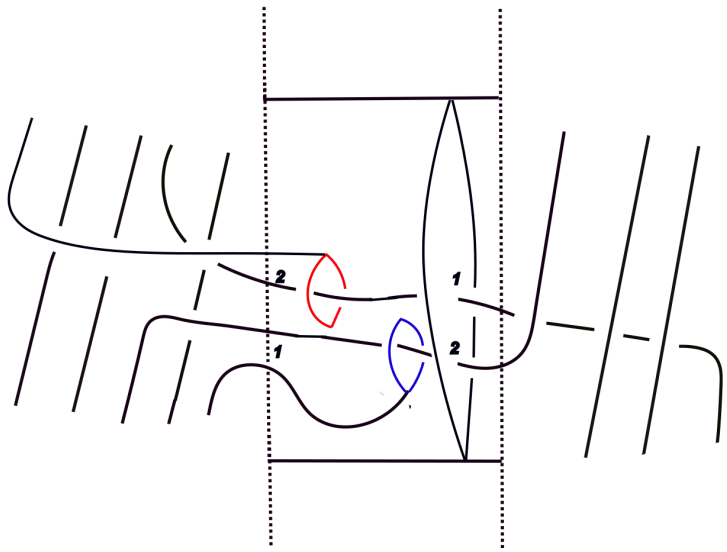

Figure 5.13: The barbell $\mathcal{B}(e_2, e_2)$.

that

$$W_3(\mathcal{B}(t^3v^3t^2)) = \sum_{i,j}^{2} W_3(\mathcal{B}_2(e_i, e_j))$$

where $\mathcal{B}_2(e_i, e_j)$ denotes the barbell such that the red cuff loops around the i-th strand counting from the bottom to the top on the left-hand side and the blue cuff loops around the j-th strand counting from the top to the bottom on the right-hand side. Here the subscript 2 indicates the number of changes from a t power to an u power or from an u power to a t power. Figure 5.13 shows the barbell $\mathcal{B}_2(e_2, e_2)$.

The next step would be trying to prove the following conjecture, which is a generalisation of Lemma 4.24.

Conjecture 5.18. *Let $w \in \langle t, v\rangle$, and let $\#(w)$ be the number of changes from a t- power to an u-power and vice versa. Then the the bar of the barbell $\mathcal{B}((w))(e_i, e_j)$ has $\#(w)$ intersections with Δ, and we have*

$$(W_3)_2(\mathcal{B}(w)(e_i, e_j)) = -(W_3)_2(\mathcal{B}(w)(e_j, e_i)).$$

If this conjecture is true, then it would imply that for a barbell in the image $p(\pi_1\mathrm{Emb}(I, X))$ that is represented by a word w, the $(W_3)_2$ invariant of it vanishes since the "sub-barbells" $B(w)(e_i, e_j)$ come in pairs with their $(W_3)_2$ cancel each other. In particular, this conjec-

ture would imply that $(W_3)_2(p(\pi_1\mathrm{Emb}(I, X))) = 0$, which will then imply that the barbells θ_{t^5,v^4,v^1}, θ_{t^6,v^4,v^1}, ... in $S^1 \times D^3 \natural S^1 \times D^3$ (viewing as embedded in $S^1 \times D^3 \# S^1 \times D^3$) we discussed in the last section do not lie in the image $p(\pi_1\mathrm{Emb}(I, X))$, therefore lead to non-trivial diffeomorphisms of $S^1 \times D^3 \# S^1 \times D^3$ and knotted separating 3-spheres.

Conjecture 5.19. *The mapping class group of $S^1 \times D^3 \# S^1 \times D^3$ has an infinitely generated subgroup generated by the induced barbell diffeomorphisms from θ_{t^5,v^4,v^1}, θ_{t^6,v^4,v^1}, ...*
Further, there exist infinitely many non-isotopic separating 3-spheres in $S^1 \times D^3 \# S^1 \times D^3$.

Bibliography

[1] T. Brendle, N. Broaddus, and A. Putman. The mapping class group of connect sums of $S^2 \times S^1$. *Transactions of the American Mathematical Society*, Jan. 2023.

[2] R. Budney. Diffeomorphism groups of small high-dimensional manifolds. with more computations, 2021. Glasgow seminar talk.

[3] R. Budney and D. Gabai. Knotted 3-balls in S^4, 2021. arXiv preprint: 1912.09029.

[4] R. Budney and D. Gabai. On the automorphism groups of hyperbolic manifolds, 2023. arXiv preprint: 2303.05010.

[5] J. Cerf. *Sur les difféomorphismes de la sphère de dimension trois ($\Gamma_4 = 0$)*. Lecture Notes in Mathematics. Springer-Verlag, 1968.

[6] J. Cerf. La stratification naturelle des espaces de fonctions différentiables réelles et le théorème de la pseudo-isotopie. *Publications Mathématiques de l'IHÉS*, 39:5–173, 1970.

[7] F. R. Cohen. Introduction to configuration spaces and their applications. In *Braids*, pages 183–261. World Scientific Publisher Hackensack, NJ, 2010.

[8] B. Farb and D. Margalit. *A Primer on Mapping Class Groups (PMS-49)*. Princeton Mathematical Series. Princeton University Press, 2011.

[9] D. T. Gay. Diffeomorphisms of the 4-sphere, Cerf theory and Montesinos twins, 2021. arXiv preprint: 2102.12890.

[10] D. T. Gay. Personal communication, 2023.

[11] D. T. Gay and D. Hartman. Relations amongst twists along Montesinos twins in the 4-sphere, 2022. arXiv preprint: 2206.02265.

[12] R. Gompf and A. Stipsicz. *4-Manifolds and Kirby Calculus*. Graduate studies in mathematics. American Mathematical Society, 1999.

[13] A. Hatcher. On the diffeomorphism group of $S^1 \times S^2$. *Proceedings of the American Mathematical Society*, 83(2):427–430, 1981.

[14] A. E. Hatcher. A proof of the Smale conjecture, $\mathrm{Diff}(S^3) \simeq O(4)$. *Annals of Mathematics*, 117(3):553–607, 1983.

[15] M. Hughes, S. Kim, and M. Miller. Non-isotopic splitting spheres for a split link in S^4, 2023. arXiv preprint: 2307.12140.

[16] D. Kosanović. On homotopy groups of spaces of embeddings of an arc or a circle: the Dax invariant, 2022. arXiv preprint: 2111.03041.

[17] F. Laudenbach. Sur les 2-sphères d'une variété de dimension 3. *Annals of Mathematics*, 97(1):57–81, 1973.

[18] F. Laudenbach. *Topologie de la dimension trois homotopie et isotopie*. Number 12 in Astérisque. Société mathématique de France, 1974.

[19] F. Laudenbach and V. Poénaru. A note on 4-dimensional handlebodies. *Bulletin de la Société Mathématique de France*, 100:337–344, 1972.

[20] R. Lipshitz, P. S. Ozsváth, and D. P. Thurston. Computing $\widehat{HF}$ by factoring mapping classes. *Geometry and Topology*, 18(5):2547 – 2681, 2014.

[21] Y. Matsumoto. *An Introduction to Morse Theory*. American Mathematical Society, 2002.

[22] J. Montesinos. On twins in the four-sphere I. *The Quarterly Journal of Mathematics*, 34(2):171–199, 1983.

[23] P. Schwer. Lecture notes on CAT(0) cube complexes, 2019. arXiv preprint: 1910.06815.

[24] D. Sinha. Manifold theoretic compactifications of configuration spaces, 2004. arXiv preprint: math/0306385.

[25] D. P. Sinha. The topology of spaces of knots: Cosimplicial models. *American Journal of Mathematics*, 131(4):945–980, 2009.

[26] C. T. C. Wall. *Differential Topology*. Cambridge Studies in Advanced Mathematics. Cambridge University Press, 2016.

[27] M. Weiss. Embeddings from the point of view of immersion theory : Part I. *Geometry and Topology*, 3(1):67 – 101, 1999.